Lawrence Berkeley Laboratory
UNIVERSITY OF CALIFORNIA

Physics Division

Presented at the 3rd Theoretical Advanced Study Institute, Santa Cruz, CA, July–August 1986

COLLIDER PHYSICS FOR THE LATE 1980'S

I. Hinchliffe

February 1987

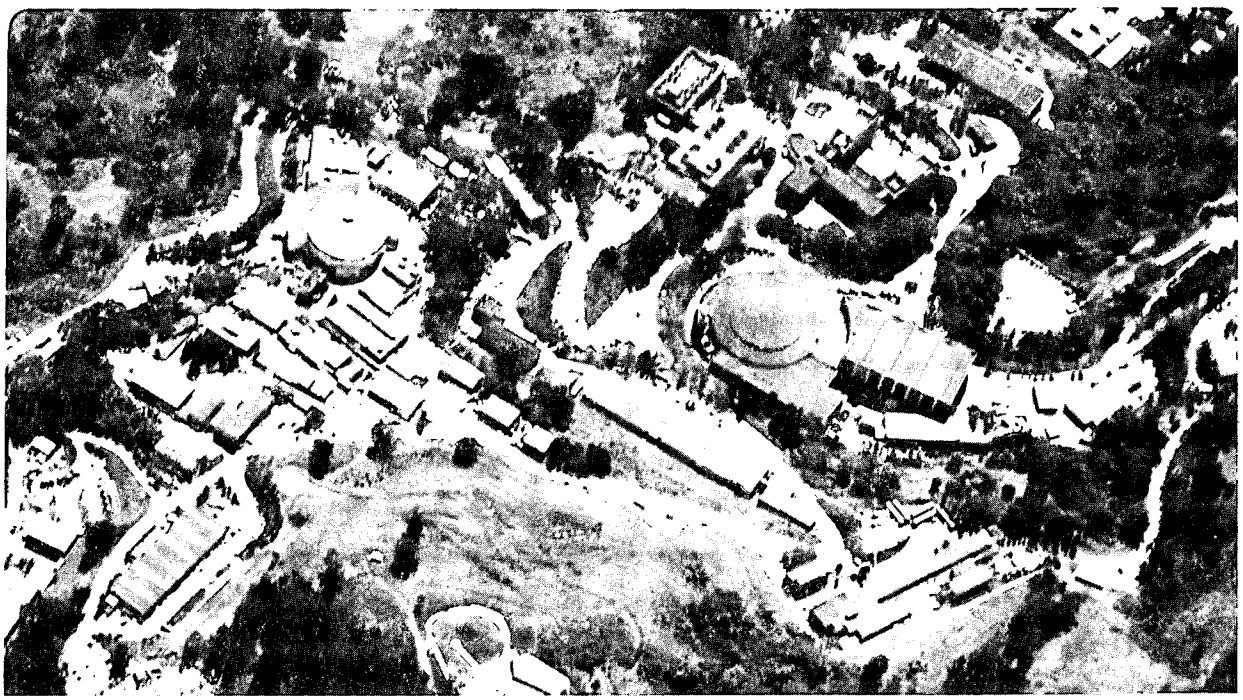

Prepared for the U.S. Department of Energy under Contract DE-AC03-76SF00098

DISCLAIMER

February 27, 1987 LBL-22404

Collider Physics for the Late 1980's *

Ian Hinchliffe

Lawrence Berkeley Laboratory
University of California
Berkeley, California 94720

Lectures presented at the 3rd Theoretical Advanced Study Institute, Santa Cruz, California, July – August 1986.

*This work was supported by the Director, Office of Energy Research, Office of High Energy and Nuclear Physics, Division of High Energy Physics of the U.S. Department of Energy under Contract DE-AC03-76SF00098.

COLLIDER PHYSICS FOR THE LATE 1980'S

I. Hinchliffe

Lawrence Berkeley Laboratory
University of California
Berkeley, California 94720

Introduction

In these lectures, I shall discuss some topics in the standard model of strong and electroweak interactions and how these topics are relevant for the high energy colliders which will become operational in the next few years. Table 1 shows the characteristics of the colliders that I shall discuss. Of the three e^+e^- colliders, LEP and the SLC will spend most of their operation in studying the physics of the Z and in making detailed tests of the Weinberg-Salam model. After its upgrade to LEPII in the early 1990's, LEP will be able to study the physics of e^+e^- collisions above the W pair threshold. Tristan will study QCD physics including the formation of resonances in the collisions of two photons and, hopefully, toponium if the top quark is within its energy range. The Tevatron collider will continue the type of physics done at the $Sp\bar{p}S$ collider, and with its increased energy will be able to extend the mass range over which we can search for new particles.

I shall begin with a discussion of radiative corrections in the Glashow-Weinberg-Salam model,[1] stressing how these corrections may be measured at LEP and the SLC. A brief discussion of CP violation will follow. This will be followed by a discussion of the Higgs boson and the searches which can be carried out for it. I shall then discuss some features of QCD which are relevant to hadron colliders. This discussion will complement the lectures of Luigi DiLella,[2] who has shown impressive evidence from the CERN Sp$\bar{p}$S collider for the correctness of QCD. Finally I shall discuss some of the problems which the standard model does not solve. I shall indicate the energy ranges which are accessible at these new colliders for the quest for new physics. More details of the searches for new physics can be found in the lectures of E. Eichten at last year's school.[3]

1. Testing the Weinberg-Salam model.

The Lagrangian describing the weak and electromagnetic interactions of the quarks and leptons is given by[1]

$$\mathcal{L} = -\frac{1}{4} F^a_{\mu\nu} F_a^{\mu\nu} - \frac{1}{4} G_{\mu\nu} G^{\mu\nu} + i\bar{\psi}_{Li}\gamma^\mu D_\mu \psi_{Li} \qquad (1.1)$$

$$+ \mu^2(\Phi^+\Phi) - \lambda(\Phi^+\Phi)^2$$
$$+ \lambda_{ek}\bar{\ell}_{L,k}\Phi e_{R,k} + \lambda_{ukl}\bar{q}_{L,k}\Phi^+ u_{R,l} + \lambda_{dkl}\bar{q}_{L,k}\Phi d_{R,l}$$

where

$$F^a_{\mu\nu} = \partial_\mu W^a_\nu - \partial_\nu W^a_\mu + g_2 \epsilon^{abc} W^b_\mu W^c_\nu$$

and

$$G_{\mu\nu} = \partial_\mu B_\nu - \partial_\nu B_\mu$$

are the field strength tensors for the three gauge bosons of $SU(2)_L$ (W^a_μ) and $U(1)$ (B_μ), which have coupling constants g_2 and g_1. The indices on the fermion fields are generation indices which take values in the range (1,2,3).

The left-handed fermions appear in $SU(2)_L$ doublets

$$\psi_{iL}: \quad \ell_L = \frac{1}{2}(1-\gamma_5)\begin{pmatrix} \nu \\ e \end{pmatrix}, \quad q_L = \frac{1}{2}(1-\gamma_5)\begin{pmatrix} u \\ d \end{pmatrix}$$

which have $U(1)$ charges -1, and 1/3. The right-handed fermions appear as $SU(2)_L$ singlets

$$\psi_{iR}: \quad e_R = \frac{1}{2}(1+\gamma_5)e, \quad u_R = \frac{1}{2}(1+\gamma_5)u, \quad d_R = \frac{1}{2}(1+\gamma_5)d$$

with $U(1)$ charges -2, 4/3 and $-2/3$, respectively. This pattern is, of course, replicated for the second and third generations which contain the μ and τ leptons and the strange, charm, top and bottom quarks. The Higgs doublet Φ has $U(1)$ charge -1. The covariant derivatives D_μ are given by

$$D_\mu = (\partial_\mu - ig_2 T^a W^a_\mu - ig_1 \frac{y}{2} B_\mu).$$

Here y is the $U(1)$ charge of the representation on which D_μ acts. For an $SU(2)$ doublet $T^a = \tau^a/2$, where τ^a is a Pauli matrix, while for an $SU(2)$ singlet, $T = 0$.

This Lagrangian contains seventeen parameters. There are two gauge coupling constants g_2 and g_1 describing the interactions of the $SU(2)$ and $U(1)$ gauge theories. Two parameters μ and λ determine the Higgs mass and the interactions of the Higgs field with itself. The remaining parameters are the quark and lepton Yukawa couplings λ_i. Let us examine the spectrum of physical states in the model.

For $\mu^2 > 0$ the ground state of the theory is given when the Higgs field ϕ has a non-zero vacuum expectation value (VEV):

$$\langle \Phi \rangle = \begin{pmatrix} 0 \\ \frac{v}{\sqrt{2}} \end{pmatrix} \tag{1.2}$$

with $v = (\mu^2/\lambda)^{1/2}$. This non-zero VEV results in a mass for three of the four gauge bosons. The charged gauge bosons of $SU(2)_L$ have mass

$$M_W^2 = g_2^2 \frac{v^2}{4}. \tag{1.3}$$

There is a massless neutral gauge boson, the photon,

$$A_\mu = \sin\theta_W W_\mu^3 - \sin\theta_W B_\mu$$

and a massive boson

$$Z_\mu = \cos\theta_W W_\mu^3 + \cos\theta_W B_\mu$$

with mass $M_Z^2 = v^2(g_1^2 + g_2^2)/4$. Here the weak mixing angle θ_W is given by

$$\tan\theta_W = \frac{g_1}{g_2}. \tag{1.4}$$

The electric charge of the electron is given by $e = g_2 \sin\theta_W$. The non-zero value of v results in lepton masses

$$m_e = \lambda_e \frac{v}{\sqrt{2}}. \tag{1.5}$$

The quark masses are more complicated since weak interactions allow transitions between different generations, i.e., $s \to u + W^-$. The Yukawa interactions of the up quarks can be chosen to be diagonal, i.e.,

$$\lambda_{u_{ij}} = \lambda_{u_i} \delta_{i,j}.$$

The masses of the charge 2/3 quarks are then given by

$$m_{u_i} = \lambda_{u_i} \frac{v}{\sqrt{2}}. \tag{1.6}$$

The down quark mass matrix contains seven parameters which are the masses of the d, s and b quarks and the four angles of the Kobayashi-Maskawa mixing matrix. The final parameter is the Higgs mass $m_H = \sqrt{2\lambda}\, m_W/g_2$. The theory has a large number of parameters but is able to describe a wealth of experimental data. The most important parameters are v, g_1 and g_2 which control the strength of weak and electromagnetic interactions. Most experimental tests of the model do not depend upon quark or lepton masses (or alternatively, on the quark and lepton Yukawa couplings) so that experimental success is more remarkable.

The W and Z bosons couple to quarks, leptons and the remaining physical Higgs boson H with interactions shown in Table 2.

I have so far discussed the model at the tree level, i.e., to lowest order in the coupling constants g_1 and g_2. Before discussing tests of the theory, it is worth noting

the approximate size of the radiative corrections which can be expected. These corrections will depend upon the fine coupling constant $\alpha = e^2/(4\pi)$. In addition, tests will be made over a large range of momenta. Momentum transfers can be very small (for example, in Thompson scattering) or very high (for example, the production of a Z or W boson). The gauge interactions produce effects which depend logarithmically on these scales. Hence an order of magnitude estimate of radiative corrections will give $\alpha/\pi \log(M_W^2/m_e^2)$. This is of order 5%. Some experiments are already sensitive to corrections of this size; experiments at the Z^0 resonance performed at LEP[4] or the SLC[5] will be more sensitive so it is important to discuss radiative corrections in some detail.

I will begin with the radiative corrections in Quantum Electrodynamics. Consider the scattering of two charged particles of mass M, at momentum transfer Q. To lowest order in α, this scattering is described by the exchange of a single photon (Fig. 1a). If the theory contains a particle of mass m_e, the effect of this particle can appear at next order in perturbation theory via the graph of Fig. 1b. The relevant Feynman diagram is the one-loop correction to the photon self energy shown in Fig. 2. This graph is given by

$$\Pi_{\mu\nu}(Q^2) = -e^2 \int \frac{d^4k}{(2\pi)^4} \frac{\mathrm{Tr}[\gamma^\mu(k+m_e)\gamma^\nu(k-Q+m_e)]}{(k^2-m_e^2)((k-Q)^2-m_e^2)}. \tag{1.7}$$

This integral is divergent; we can regulate it by performing the loop integral in n dimensions, i.e. by making the replacement[6]

$$\frac{d^4k}{(2\pi)^4} \to \frac{d^nk}{(2\pi)^n}.$$

We then have

$$\begin{aligned}\Pi_{\mu\nu}(Q^2) &= (Q_\mu Q_\nu - Q^2 g_{\mu\nu})\Pi(Q^2) \\ &= (Q_\mu Q_\nu - Q^2 g_{\mu\nu})\frac{2i\alpha}{\pi}\left[\frac{2}{4-n} + \log(4\pi) - \gamma_E\right. \\ &\left. - \int_0^1 z(1-z)\log\left(\frac{Q^2 z(1-z) - m_e^2}{\mu^2}\right)dz + O(n-4)\right].\end{aligned} \tag{1.8}$$

Here γ_E is the Euler-Mascheroni constant ($\gamma_E = 0.577$) and $\alpha = e^2/4\pi$. I have expanded the result around $n = 4$ and not written the terms which vanish as $n \to 4$. The scale μ has been introduced since, in n dimensions, the interaction of an electron with a photon has the following form

$$e\mu^{(n-4)/2}\bar{\psi}\gamma^\mu\psi A_\mu. \tag{1.9}$$

The coupling constant e (or α) then remains dimensionless in n dimensions. μ is an arbitrary constant — physics cannot depend upon it.

The scattering of the heavy particles then has an amplitude of the following form

$$\frac{e^2}{Q^2}[1 + i\Pi(Q^2)]. \tag{1.10}$$

In order to make contact with physics, the divergence at $n = 4$ must be removed, i.e., the theory must be renormalized. Two renormalization schemes are often used:

(a) Minimal subtraction.[7] Here the term $\frac{2}{n-4}$ and the attendant constants γ_E and $\log 4\pi$ are thrown out. This amounts to defining a renormalized charge

$$e_R^2 = e^2 + \frac{e^2}{4\pi^2}\left[\frac{1}{(4-n)} + \frac{1}{2}log4\pi - \frac{\gamma_E}{2}\right]. \tag{1.11}$$

This scheme is very easy to use but it is unphysical; the resulting renormalized coupling constant is not directly related to any physical quantity. This definition is the one normally used in QCD.

(b) Define the renormalized charge so that as $Q^2 \to 0$, the scattering amplitude is e_R^2/Q^2.[8] Hence, $e_R^2 = e^2[1 + i\Pi(0)]$. This definition has the advantage that it can be related directly to a physical quantity, the scattering rate at small momentum transfer. It is the definition used in Quantum Electrodynamics; it corresponds to the value of $\alpha = 1/137$ measured from Thompson scattering.* This definition cannot be used in QCD since perturbation theory is not reliable as $Q^2 \to 0$.

In the limit of large Q^2, the scattering amplitude has the following form

$$\frac{\alpha_R}{Q^2}\left[1 + \frac{\alpha_R}{3\pi}\log(Q^2/m_e^2)\right]. \tag{1.12}$$

I have retained terms of order $\log Q^2/m_e^2$ only and have used the definition (b) of α. We can introduce a running coupling constant $\alpha(Q^2)$ by

$$\alpha(Q^2) = \alpha\left[1 + \frac{\alpha}{3\pi}\log(Q^2/m_e^2)\right]. \tag{1.13}$$

The scattering amplitude is then proportional to $\alpha(Q^2)/Q^2$.

In the standard model there are contributions to $\alpha(Q^2)$ from all charged particles. The only one whose mass is not known is the top quark. Each charged particle begins to contribute when $Q^2 > m_i^2$. The evolution of $\alpha(Q^2)$ is shown in Fig. 3. At $Q^2 = M_W^2$ [10]

$$\alpha_{em}(M_W^2) \sim 1/128. \tag{1.14}$$

*The most accurate measurements of α come from the Josephson Junction.[9] Since the momentum transfers in this case are extremely small, the value obtained corresponds to the definition discussed here.

Having defined the electromagnetic coupling α_{em}, it now remains to specify the other parameters of the Weinberg-Salam model. Apart from the fermion masses and the Kobayashi-Maskawa angles there are three parameters. In the Lagrangian these are μ, λ and one of g_1 and g_2. (The other is fixed by α). At lowest order these parameters can be taken to be M_W, M_H and g_2. A renormalized mass is easy to define; it is simply the position of the pole in the particle's propagator which corresponds to its physical mass. g_2 remains to be defined.

At present the W mass is not well measured. Consequently, we shall not take it to be one of the fundamental parameters. The Higgs mass must be taken as one parameter. The two remaining ones will be directly related to two accurately measured physical quantities. The muon lifetime is extremely well measured. This can be used to extract the Fermi constant G_F.[11] We need one other quantity. I will take this to be the mass of the Z boson which will be well measured at the SLC or LEP in the near future. The fundamental parameters are therefore: α_{em}, obtained from the Josephson Junction; G_F, obtained from the muon lifetime; M_Z and the Higgs mass M_H which does not play a crucial role in the subsequent discussion. This procedure eliminates the need to define the coupling constant g_2.

In lowest order the Fermi constant G_F is related to the muon lifetime (τ_μ) by

$$\frac{1}{\tau_\mu} = \frac{G_F^2 m_\mu^3}{192\pi^3}\left[1 - \frac{8m_e^2}{m_\mu^2}\right]. \tag{1.15}$$

It is traditional to include higher order QED corrections from the graphs of the type shown in Fig. 4. The right-hand side of Eq. (1.15) is modified by a factor[11]

$$1 + \frac{\alpha}{2\pi}\left[\frac{25}{4} - \pi^2\right]\left[1 + \frac{2\alpha}{3\pi}\log(m_e/m_\mu)\right]. \tag{1.16}$$

Since α is known, the muon lifetime can be used to extract G_F. †

Once the Z mass is determined the W mass is predicted[12] to be

$$M_W = \frac{M_Z}{\sqrt{2}}\left[1 + \left[1 - \frac{4\pi\alpha}{\sqrt{2}M_Z^2 G_F(1-\Delta r)}\right]^{1/2}\right]^{1/2}. \tag{1.17}$$

---

†Strictly speaking, a factor of $1 + \frac{3m_\mu^2}{5M_W^2}$ should also be included. This arises since the Fermi interaction is due to the exchange of a W boson which has a propagator of the form

$$\frac{\left(-g^{\mu\nu} + \frac{q^\mu q^\nu}{M_W^2}\right)}{(q^2 - M_W^2)}.$$

If this is expanded as a power series in q^2/M_W^2, the leading term is $1/M_W^2$. The next order term gives rise to a term proportional to m_μ^2/M_W^4. In practice this correction is irrelevant since its effect is less than the error on τ_μ.

Δr includes the effect of radiative corrections, for a top quark mass of 35 GeV and a Higgs mass of 100 GeV

$$\Delta r = 0.0696 \pm 0.0020. \tag{1.18}$$

There is some uncertainty in Δr. Apart from the unknown top and Higgs masses, the contribution of light quarks in the loops of Fig. 2 is uncertain. This contribution must be gotten from measurements of the cross-section for the process $e^+e^- \rightarrow$ hadrons since QCD corrections are not small and cannot be calculated when $Q^2 \leq 1\ GeV^2$.

What has happened to the weak mixing angle θ_W? In the approach that I have used it is not a fundamental parameter. It can be defined by $\cos\theta_W \equiv M_W/M_Z$. The coupling constant g_2 can now be defined by $g_2 \equiv e/\tan\theta_W$. In lowest order when Δr is zero, g_2 is related to G_F in the usual way

$$G_F = \frac{g_2^2}{4\sqrt{2}M_W^2}. \tag{1.19}$$

There is an alternative renormalization scheme to the one I have described. e and g_2 can be defined by minimal subtraction[13] (call these $\bar{e}$ and $\bar{g}_2$). The weak mixing angle is now defined by

$$\tan\overline{\theta_W} = \bar{e}/\bar{g}_2. \tag{1.20}$$

$\bar{\theta}_W$ and θ_W are related by $\sin\bar{\theta}_W = \sin\theta_W + 0.006$.[13] In view of the possible confusion I shall not use $\sin\theta_W$ in the subsequent discussion.

The present measurements of M_Z from UA1 and UA2 has a large error.[14] Table 3 shows the value of M_Z extracted from the analysis of a large set of low energy experiments. For example, the ratio of cross-sections

$$\frac{\sigma(\nu_\mu e \rightarrow \nu_\mu e)}{\sigma(\nu_\mu e \rightarrow \nu_e \mu)} = \frac{7M_Z^4 - 20M_Z^2M_W^2 + 16M_W^4}{13M_Z^4 - 28M_Z^2M_W^2 + 16M_W^4} \tag{1.21}$$

can be used to extract M_Z using the formula of Eq. (1.17) for M_W. This expression for the ratio of cross-sections is given in lowest order. The errors are too large for radiative corrections to be relevant.

The two types of experiments which have the smallest quoted errors are deep inelastic neutrino scattering[21] and the asymmetry in polarized electron deuterium scattering.[18] The ratio of the cross-sections for neutral and charged current deep inelastic neutrino scattering from a nucleon [‡] is given by

$$\frac{\sigma(\nu_\mu N \rightarrow \nu_\mu X)}{\sigma(\nu_\mu N \rightarrow \mu X)} = \frac{\frac{1}{2} - x + \frac{20x^2}{27} + \epsilon\left(\frac{1}{6} - \frac{x}{3} + \frac{20x^2}{27}\right)}{1 + \epsilon/3}. \tag{1.22}$$

[‡] N here refers to a target which consists of an equal mixture of protons and neutrons.

In lowest order $x = 1 - M_W^2/M_Z^2$. ϵ is the ratio of the fraction of nucleon's momentum carried by antiquarks to that carried by quarks. Radiative corrections cause a small shift in x.[22] This shift depends upon the kinematics of the experiment and is of order 0.005. The value of $x = 0.226 \pm 0.004$ which is quoted has an error which is smaller than this higher order correction.

There are a number of uncertainties in the value of x extracted from deep inelastic scattering. Firstly, there are QCD corrections to the structure functions. A more important source of uncertainty is that due to the charm quark. There is a contribution to the charged current cross-section from the reaction $\nu + s \rightarrow \mu^- + c$. This rate is affected by a threshold factor which depends on the charm quark mass. The neutral current cross-section is affected to a lesser degree since the process $\nu + c \rightarrow \nu + c$ is inhibited due to the small number of charm quarks in the nucleon. If the charm quark mass is allowed to vary from 1.2 to 1.8 GeV, there is an uncertainty of order $\pm$ 0.005 in x.[21] Since the charm quark mass is not determined within this range, I am forced to conclude that this measurement is not sensitive to radiative corrections.

In the case of the scattering of a polarized electron from a deuteron,[18] one observes the interference between Z and photon exchange (see Fig. 5). The following asymmetry is predicted

$$\frac{\sigma_L - \sigma_R}{\sigma_L + \sigma_R} = Q^2 \left[a_1 + a_2 \left(\frac{1-(1-y)^2}{1+(1-y)^2} \right) \right], \tag{1.23}$$

where $\sigma_L(\sigma_R)$ is the cross-section for a left (right) handed electron and

$$\begin{aligned} a_1 &= \frac{-G_F}{2\sqrt{2}\pi\alpha} \frac{9}{10} \left[1 - \frac{20x}{9} \right], \\ a_2 &= \frac{-G_F}{2\sqrt{2}\pi\alpha} \frac{9}{10} [1 - 4x]. \end{aligned} \tag{1.24}$$

The kinematical variable y is the fractional energy loss of the electron: $y = \frac{E_1 - E_2}{E_1}$ where E_1 (E_2) is the incoming (outgoing) electron energy. In this case the higher order corrections computed for the kinematics of the SLAC *ed* scattering experiment are $\delta x = 0.005$.[13] Again this is comparable to the experimental error. It appears, therefore, that only the next generation of experiments will be able to see higher order corrections.

Table 4 shows the values of M_W and M_Z found by the UA1 and UA2 collaborations.[14] The predicted value of M_Z and M_W inferred from the results in Table 3 are shown for comparison. The agreement is remarkable.

As I have stressed, most of the radiative corrections are due to known quantities in the standard model such as the coupling of the electron to the gauge bosons. In

principle, the accurate measurement of such radiative corrections can give information on the two main unknown parameters, namely the top quark and Higgs masses. In order to illustrate this, consider the effect of these particles upon the relationship between the W and Z masses (see Eq. (1.17)).

There are contributions to the W and Z self energies from the t and b quarks which are shown in Fig. 6. The evaluation of these graphs at zero external momentum gives[23]

$$\begin{aligned}\Pi_W^{\mu\nu} &= -\frac{3ig^{\mu\nu}g_2^2}{32\pi^2}\left[m_t^2\log m_t^2/\mu^2 + m_b^2\log m_b^2/\mu^2\right.\\ &\left. + \frac{m_t^2m_b^2}{m_t^2-m_b^2}\log m_t^2/m_b^2 - \frac{1}{2}(m_t^2+m_b^2)\right],\\ \Pi_Z^{\mu\nu} &= \frac{3ig^{\mu\nu}g_2^2}{32\pi^2}\frac{M_{Z_{LO}}^2}{M_{W_{LO}}^2}(m_t^2\log m_t^2/\mu^2 + m_b^2\log m_b^2/\mu^2).\end{aligned} \tag{1.25}$$

I have used dimensional regularization and dropped the terms proportional to $\frac{1}{n-4}$, γ_E and $\log 4\pi$. The quantities $M_{W_{LO}}$ and $M_{Z_{LO}}$ are the lowest order values for the W and Z masses. These contributions cause shifts in the W and Z masses

$$M_{W,Z}^Z = M_{W,Z,LO}^Z\left[1 + \frac{\Pi_{W,Z}^{\mu\nu}}{g^{\mu\nu}M_{W,Z,LO}^2}\right]. \tag{1.26}$$

These contributions then modify the relationship between the W and Z masses

$$M_W^2 = M_{W_{LO}}^2\left[1 + \frac{3G_F}{8\sqrt{2}\pi^2}\left[\frac{2m_t^2m_b^2}{m_t^2-m_b^2}\log\left(\frac{m_t^2}{m_b^2}\right) + m_t^2 + m_b^2\right]\right]. \tag{1.27}$$

Notice that the μ dependence (and the terms proportional to $1/(n-4)$ had I written them) have canceled, i.e., this correction is finite and independent of the renormalization scheme. Notice that the effect of these corrections is to increase M_W as the t quark mass rises. Current constraints from low energy experiments and from the measured value the W mass imply $m_t \leq 320GeV$.

There are also shifts in the W and Z masses which arise from radiative corrections involving the Higgs.[24] The Feynman diagrams are shown in Fig. 7. The graphs of Fig. 7c do not contribute to the Δr of Eq. (1.17), since these graphs correspond to a renormalization of the Higgs VEV, whose value does not affect M_W/M_Z. In the limit of large Higgs mass we have

$$M_W^2 = M_{W_{LO}}^2\left(1 - \frac{3G_F}{8\sqrt{2}}M_Z^2\left(1 - \frac{M_W^2}{M_Z^2}\right)\log(m_H^2/M_W^2)\right). \tag{1.28}$$

The dependence upon M_H is rather weak; M_W falls slowly as m_H is increased. Figure 8 shows the relationship between the W and Z masses for different values of top quark and Higgs masses.

The result that as m_t or m_H increases the radiative corrections increase, may seem to be contrary to intuition. Consider a theory with a particle of mass M. If this theory is probed with energies much less than M, then there is a general result known as the decoupling theorem which states that the effect of the heavy particle is proportional to $1/M^p$, where p is some positive number. As $M \to \infty$, the particle decouples from low energy physics.[25] Thus, for example, the effects of the τ lepton on $(g-2)$ of the muon are very small. This theorem is proved under the assumption that the coupling of the particle does not vary with M. This is the case for a heavy lepton in QED whose coupling to the photon, α_{em}, is independent of M.

In the case of the electroweak theory, the couplings cannot be held fixed as M is increased. Recall that the top quark mass is related to the W mass via

$$m_t = \sqrt{2}\frac{\lambda_t}{g_2} M_W \tag{1.29}$$

where λ_t is the Yukawa coupling of the t quark to the Higgs boson. If M_W is held fixed and m_t is increased, then λ_t must increase; the top quark interacts more strongly with the Higgs. Clearly, for a sufficiently large m_t, λ_t will be so large that perturbation theory ceases to be reliable. I shall return to this point later. Recall also that the Higgs mass is related to the W mass and the Higgs self interaction (λ) by

$$m_H^2 = 2\lambda M_W^2/g_2^2. \tag{1.30}$$

Again, if M_W is held fixed then a large m_H implies a large λ.

The graphs of Figs. 6 and 7 appear to depend only upon the gauge couplings g_1 and g_2 and not upon λ_t and λ. This is illusory as the following argument will demonstrate. Before the $SU(2) \times U(1)$ symmetry is broken, the theory contains four massless gauge bosons and four scalars (the components of the complex Higgs doublet Φ). After symmetry breaking, three of the gauge bosons acquire mass. In order to do so they must each gain an additional degree of freedom, their longitudinal polarization states. Three of the scalars supply those degrees of freedom. Hence, "the physical W and Z bosons have some Higgs in them". Couplings of physical W's and Z's are therefore sensitive to the Higgs Yukawa coupling.[§] Hence fermions and Higgs bosons of large mass in the standard model do not decouple and can affect the relationship between the W and Z masses.

At lowest order, there is a relationship (cf. Eqs. (1.3) and (1.4)) between g_1, g_2, M_W and M_Z, viz.,

$$\frac{M_W^2}{M_Z^2} = \frac{g_2^2}{g_1^2 + g_2^2}. \tag{1.31}$$

The form of this relationship is due to the breaking of $SU(2) \times U(1)$ via a Higgs doublet. In models with more complicated Higgs sectors (for example Higgs triplets)

[§]This argument can be seen clearly by writing the theory in 't Hooft-Feynman gauge.

this relationship is lost. We can introduce an additional parameter ρ to take account of this possibility

$$\rho \equiv \frac{\sqrt{2}M_W}{M_Z\left(1+\left(1-\frac{4\pi\alpha}{\sqrt{2}G_F M_Z^2(1-\Delta r)}\right)^{1/2}\right)^{1/2}} \tag{1.32}$$

so that $\rho \equiv 1$ in the standard model. (Note that $\Delta r = 0$ in lowest order; in higher orders it should take the value predicted in the minimal model.) If the low energy data listed in Table 3 is analyzed with the parameter ρ, one gets[15]

$$\rho = 1.006 \pm 0.008. \tag{1.33}$$

Since ρ is consistent with 1 it is reasonable to ask if this implies that the Higgs sector of the $SU(2)_L \times U(1)$ model is severely constrained.

The part of the $SU(2)_L \times U(1)$ Lagrangian describing the self interaction of the Higgs fields, namely

$$\mu^2(\Phi^+\Phi) + \lambda(\Phi^+\Phi)^4 \tag{1.34}$$

has a larger symmetry than $SU(2)_L \times U(1)$. One can consider the complex Higgs doublet as having four real components. The interactions of Eq. (1.34) are invariant with respect to rotations among these components, i.e., there is an $O(4) = SU(2) \times SU(2)$ symmetry. When the $SU(2)_L$ symmetry is broken as one component of the Higgs doublet gets a non-zero VEV, the $O(4)$ symmetry is broken to $O(3) = SU(2)$. It is this $SU(2)$, known as custodial $SU(2)$,[26] which insures that $\rho = 1$. It does this because the resulting mass for the three components W_μ^1, W_μ^2 and W_μ^3 of the gauge boson multiplet of $SU(2)_L$ has the form

$$M_W^2(W_\mu^1 W_\mu^1 + W_\mu^2 W_\mu^2 + W_\mu^3 W_\mu^3). \tag{1.35}$$

The mixing of W_μ^3 with B_μ then produces the Z_μ and photon. Any variant of the standard $SU(2) \times U(1)$ model which has a custodial $SU(2)$ symmetry (e.g., a model with an arbitrary number of Higgs doublets) will predict $\rho = 1$. As an example of a model without such a symmetry, suppose that we try to break the $SU(2)_L \times U(1)$ symmetry with a mixture of doublets and triplets. The self interaction of the triplet has an $O(3)$ symmetry which breaks to $O(2)$ when one component acquires a VEV. The residual symmetry of the Higgs sector is then no larger than $O(2)$. There is no custodial $SU(2)$ and ρ is not equal to one. In the case of a model with only triplets $\rho = 3/2$.

How well can we expect to be able to measure the radiative corrections in the near future? At LEP and the SLC the Z mass can be measured directly. The error on M_Z is controlled by the accuracy with which the beam energy can be measured. An error $\delta M_Z = 50\ MeV$ would seem to be reasonable.[4,5] The W mass can be

measured at LEP from the reaction $e^+e^- \rightarrow W^+W^-$. The shape of the cross-section and energy distribution of leptons from the decays $W \rightarrow e\nu$ can be used. Studies[27] indicate that an error $\delta M_W \simeq 100\ MeV$ should be achievable.

Since it will be several years before the W mass can be measured at LEP, it is reasonable to ask how well one can measure the W mass at hadron colliders. The W mass must be inferred from the transverse momentum distribution of the leptons from the decay $W \rightarrow e\nu$. As can be seen from Table 4, the current errors on the W and Z mass are large. Part of the error on the W mass is a systematic error arising from calibration. This error can largely be eliminated once the Z mass has been measured in e^+e^- annihilation since leptons from Z decay have known transverse momentum and can be used as a calibration. The remaining error is a statistical one which can be reduced as more W's and Z's are produced. The proposal[28] for the $D0$ detector at the Tevatron claims that an error $\delta M_W \approx 100\ MeV$ can be obtained. A value of $\delta M_W \approx 300\ MeV$ appears to be achievable in the near future. Such an error implies a sensitivity to t quark masses greater than 90 GeV (see Fig. 8).

Other tests of the electroweak theory can arise from measurements of asymmetries at LEP of the SLC.[29] I shall concentrate my discussion on those asymmetries measured at the Z^0 resonance where the event rates are large and a good statistical sample can be obtained. The total cross-section for $e^+e^- \rightarrow Z \rightarrow all$ is approximately 40 nb.

Measurements of asymmetries can have much smaller errors than measurements of rates themselves. This is because certain systematic errors, for example in the luminosity measurement, will cancel out. The first asymmetry that I will discuss is the forward-backward asymmetry for the process $e^+e^- \rightarrow Z \rightarrow f\bar{f}$, where f is a fermion

$$A_{FB} = \frac{\int(\sigma(f,\theta) - \sigma(\bar{f},\theta))d(\cos\theta)}{\int(\sigma(f,\theta) + \sigma(\bar{f},\theta))d(\cos\theta)}. \tag{1.36}$$

Here $\sigma(f,\theta)$ $(\sigma(\bar{f},\theta))$ is the cross-section for the production of $f(\bar{f})$ at angle θ to the e^- beam. In lowest order this asymmetry is given by

$$A_{FB} = 3\frac{v_e v_f a_e a_f}{(v_e^2 + a_e^2)(v_f^2 + a_f^2)}. \tag{1.37}$$

The quantities v_i and a_i are given in Table 2. In order to measure this asymmetry it is necessary to distinguish the f from the $\bar{f}$. This is not possible if f is an up, down or strange quark. It may be possible for c and b quarks where the semileptonic decay produces a lepton whose charge is correlated with that of the quark. Clearly, the cleanest final state occurs if f is a muon. I will specialize my discussion to this case. Figure 9[29] shows A_{FB} as a function of the Z mass. Three curves are shown: the lowest order prediction and the value radiatively corrected for $m_t = 30\ GeV$ with $m_H = 10\ GeV$ and $m_H = 1\ TeV$.

How well can A_{FB} be measured? At an e^+e^- luminosity of $10^{31} cm^{-2} sec^{-1}$, there are approximately 1000 $\mu^+\mu^-$ events per day. If we neglect systematic errors, a LEP experiment with an exposure of 200 days can achieve $\delta A_{FB} \approx 0.002$. An experiment at SLC, with its expected lower luminosity, is likely to have an error which is at least three times larger.

It is clear that, with an accuracy of this order, an experiment can detect the difference between a calculation in lowest order and one including radiative corrections. Most of these radiative corrections arise from known physics, such as the coupling of the electron to the W, Z and photon. Figure 10 shows the contribution to A_{FB} from an additional quark doublet. As in the case of corrections to the W mass, the correction becomes large in the region of large quark masses. The curves are shown as a function of the mass of the charge 2/3 quark for a fixed value of the ratio of the quark masses in the doublet. I have indicated regions on the figure which can be excluded by other measurements. If the charge 1/3 quark has mass less than $M_Z/2$ it will be observed directly in Z decay so that the region above the dot-dashed line is probed. If the W mass is within 300 MeV of its predicted value, the region above the dotted line will be excluded; an error of 100 MeV rules out the region above the dashed line. I have indicated a $\pm 2\sigma$ error bar for the LEP scenario discussed above. I am forced to conclude that A_{FB} is not a sufficiently sensitive quantity to be used as a probe of new physics.

Figure 11 shows the contribution to A_{FB} from a doublet of squarks such as will occur in a supersymmetric version of the standard model. Notice that if the up and down squarks are degenerate the contribution to A_{FB} is zero at large squark masses. This is an example of decoupling since the squarks can have equal, non-zero, masses even if the $SU(2) \times U(1)$ symmetry is unbroken and a large degenerate mass does not imply a large Yukawa coupling. If the ratio of the squark masses is large, then there is no decoupling since the splitting violates SU(2) symmetry and must arise from the vacuum expectation value of Higgs fields.

If the polarization of the outgoing fermion f can be measured, then a polarization asymmetry A_{pol} can be determined

$$A_{pol} = \frac{\sigma(h=1) - \sigma(h=-1)}{\sigma(h=1) + \sigma(h=-1)}, \tag{1.38}$$

where $\sigma(h)$ is the cross-section for the production of f with helicity h. In lowest order A_{pol} is given by

$$A_{pol} = \frac{2 v_f a_f}{(v_f^2 + a_f^2)}. \tag{1.39}$$

The only particle whose polarization can be measured is the tau lepton. In the decay $\tau \rightarrow \pi\nu$, the momentum spectrum of the π is sensitive to the tau helicity

$$\frac{dW}{dX_\pi} = 1 - h(2X_\pi - 1) \tag{1.40}$$

where $X_\pi = 2E_\pi/\sqrt{s}$. The branching ratio $\tau \to \pi\nu$ is only 10% or so. The error on A_{pol} from such a measurement is unlikely to be small enough for one to be sensitive to new physics.

If the electron or positron beam can be polarized then one can measure

$$A_{LR} = \frac{\sigma(L) - \sigma(R)}{\sigma(L) + \sigma(R)}. \tag{1.41}$$

Here $\sigma(L)$ $(\sigma(R))$ is the cross-section for producing a Z from a left (right) polarized electron and an unpolarized positron. A_{LR} is given by

$$A_{LR} = \frac{2v_e a_e}{(v_e^2 + a_e^2)}. \tag{1.42}$$

Since there are no plans for polarization at LEP, I will discuss the SLC where a polarized electron source is under construction.[30] Since the total Z production rate is used in the measurement of A_{LR}, the statistical errors are smaller. There is a systematic error due to the measurement error on the polarization of the electron beam $(\Delta p/p)$. Table 5, extracted from the proposal to measure A_{LR}, shows the error on A_{LR} as a function of $\Delta p/p$ and of the number of produced Z^0's. For orientation, at a luminosity of $10^{30} cm^{-2} sec^{-1}$ it takes approximately one year of running to produce 10^6 Z^0's. The value of A_{LR} is shown in Fig. 12 as a function of M_Z in three different scenarios, all of which are consistent with current data. In order to establish a 3σ effect which discriminates between $m_t = 30\ GeV$ and $m_t = 180\ GeV$, it will be necessary to measure the polarization to better than 2% and have more than 10^5 produced Z^0's. Figure 10 shows δA_{LR} due to a new quark doublet. I have indicated a $\pm 2\sigma$ error bar corresponding to $\Delta p/p = 1\%$ and to 10^6 produced Z^0's. It may be somewhat easier to establish an effect than in the case of the forward-backward asymmetry.

Before leaving this subject, I would like to comment briefly upon the effect of a more radical modification of the standard model.[31] The recent upsurge in string theory has provided a motivation for considering models where the gauge group is extended. I shall discuss one particular example where the low energy group is $SU(3) \times SU(2)_L \times U(1)_y \times U(1)_{y'}$. In this model the charged current structure is unaffected but there are changes in the neutral current due to the presence of an additional neutral gauge boson associated with the group $U(1)_{y'}$. I shall assume that the coupling constant g' of this group is equal to g_1, a choice supported by these string motivations. If the electric charge operator Q has the same value as in the standard model, viz., $Q = T_3 + y/2$, then the photon will be the same linear combination of B and W_3 as in the standard model. The two massive neutral gauge bosons will be linear combinations of the standard model Z and B', the gauge boson of the $U(1)_{y'}$ group.

The mass matrix of the neutral bosons will depend upon the structure of the Higgs sector and will have the following form

$$|M|^2 = \begin{vmatrix} (g_2^2+g_1^2)\ A & (g_2^2+g_1^2)^{1/2} g_1\ B \\ (g_1^2+g_2^2)^{1/2} g_1\ B & g\ C \end{vmatrix} \tag{1.43}$$

where

$$A = \sum_i \left\langle \phi_i T_3^2 \phi_i \right\rangle ,$$

$$B = \sum_i \left\langle \phi_i \frac{T_3}{2} y_i' \phi_i \right\rangle ,$$

$$C = \sum_i \left\langle \phi_i \frac{y_i'^2}{4} \phi_i \right\rangle .$$

Here the sum i runs over Higgs representations ϕ_i with $U(1)_{y'}$ charge y_i'. T^3 is the neutral generator of $SU(2)_L$. In the case of the standard model $y^i = 0$ and $A = v^2/4$. The eigenvalues are M_{Z_1} and M_{Z_2}. If we assume that there are only doublets under $SU(2)_L$ and singlets under $SU(2)_L \times U(1)_y$, then in the limit $y' = 0$ we will recover the standard model with $\rho = 1$ and a non-minimal Higgs sector.

The model now has five parameters. The three of the standard model, α, G_F and M_{Z_1} together with M_{Z_2} and a parameter describing the Higgs structure analogous to ρ, $\rho' = B/A$. The W mass is predicted in terms of these parameters; it is shown in Fig. 13. A measurement of M_W to an accuracy of 300 MeV is sensitive to the mass of the second massive neutral gauge boson provided that it is lighter than 300 GeV.

The left-right asymmetry measured on the Z_1 resonance is shown in Figure 14. Again it would appear that the best experiments are sensitive to $M_{Z_2} \lesssim 300$ GeV. This value is close to that which can be observed directly at the Tevatron collider from the production of the Z_2 boson followed by its decay into e^+e^- or $\mu^+\mu^-$.

What can we conclude about the potential of measurements of radiative corrections? As we have seen it will be very difficult for an experiment to be sensitive to new physics; the best hopes seem to lie with a precise determination of the W and Z masses and with the left-right asymmetry. It is very important to emphasize that if an effect is seen in measurements of radiative corrections it may be very difficult to discern its origin. Only the direct observation of new particles can resolve ambiguities.

I would like to conclude this section of the weak and electromagnetic interactions of the standard model by discussing CP violation. There are two potential sources of CP violation within the standard model: that arising from a phase in the Kobayashi–Maskawa mixing matrix and that arising from strong interactions. The latter can

arise from a term $\tilde{\theta}F_{\mu\nu}F_{\alpha\beta}\epsilon^{\mu\nu\alpha\beta}$ which can be present in the QCD Lagrangian (Here $F_{\mu\nu}$ is the field strength tensor of the gluon field). $\tilde{\theta}$ is an arbitrary parameter whose value is not predicted by QCD. For a more detailed review see ref. 32. This CP violation is potentially disastrous. Such a term can give rise to a neutron electric dipole moment. The requirement that this moment be below the experimental limit gives the constraint $\tilde{\theta}\lesssim 10^{-16}$, an unnaturally small number. Faced with such a small number, theorists are tempted to find a reason for $\tilde{\theta} = 0$. Two mechanisms are known whereby $\tilde{\theta}$ may be set to zero.

Through the Adler–Bell–Jackiw anomaly $\tilde{\theta}$ is related to quark masses, if one of the quark masses is zero, $\tilde{\theta}$ can be rotated to zero; it is an unphysical parameter in this case. The current quark masses, i.e. those given by $< H > \neq 0$, are determined using current algebra from the π and K masses. These analyses show that the up quark mass is lightest and has a mass of about 4 MeV.[33] It has recently been claimed that terms which are higher order a chiral perturbation theory may modify these values and allow solution where the up quark mass is zero.[34] If this were the case, this would provide the simplest solution to the strong CP problem. An alternative solution to the strong CP problem involves the existence of an additional symmetry called a Peccei–Quinn[35] symmetry which can be used to remove $\tilde{\theta}$. The symmetry is broken spontaneously and a light pseudo–scalar particle, the axion, is produced. The simplest variant of this model are ruled out by the failure to find an axion. More details of these issues can be found in recent reviews.[32,36] In the rest of the discussion I will issue assume that $\tilde{\theta} = 0$ by one of the above mechanisms and will concentrate on CP violation in the quark mixing matrix.

The interactions of the W^+_μ with the quark currents J^u_μ for the left–handed up quarks) and J^d_μ (for the left handed down quarks), a total of nine terms.

These interactions can be parameterized by a 3×3 matrix which contains 3 angles and six phases. Five of these phases can be absorbed into redefinitions of quark fields (only the relative phases of the quark fields can be used, hence only 5 can be removed). The matrix is then parameterized by 3 angles and one phase. Various parameterizations exist in the literature, physics is independent of the choice), I shall use the following one.[37]

$$\begin{pmatrix} V_{ud} & V_{us} & V_{ub} \\ V_{cd} & V_{cs} & V_{cb} \\ V_{td} & V_{ts} & V_{tb} \end{pmatrix} = \begin{pmatrix} c_\beta c_\theta & c_\beta s_\theta & s_\beta \\ -s_\gamma c_\theta s_\beta e^{i\delta'} & c_\gamma c_\theta - s_\gamma s_\beta s_\theta e^{i\delta'} & s_\gamma c_\beta e^{i\delta'} \\ -s_\beta c_\gamma c_\theta + s_\gamma s_\theta e^{-i\delta'} & -c_\gamma s_\beta s_\theta - s_\gamma c_\theta c^{-i\delta'} & c_\gamma c_\beta \end{pmatrix} \tag{1.44}$$

Here V_{ij} is such that the coupling of a W^+ is $g_2 V_{ij}\bar{q}_i q_j W^+$, and $c_\alpha = \cos\alpha, s_\alpha = \sin\alpha$ etc.

CP violation is seen at present, only in the $K_L - K_S$ system. Consider the mixing between the K_0 and $\bar{K}_0$ states which can occur through the second order

weak process shown in figure 15. This mixing will occur if these are only two generations of quarks. However, in this case this is no phase in V_{ij} so that CP will not be violated in this mixing. In the case of three or more generations CP is violated. We can write the mass eigenstates of the $K\bar{K}$ system as

$$\begin{aligned} |K_L> &= \frac{1}{\sqrt{2}(1+|\epsilon|^2)}[(1+\epsilon)|K_0> -(1-\epsilon)|\bar{K}_0>] \\ |K_S> &= \frac{1}{\sqrt{2}(1+|\epsilon|^2)}[(1+\epsilon)|K_0> +(1-\epsilon)|\bar{K}_0>] \end{aligned} \tag{1.45}$$

These states are so defined that if CP is conserved, $\epsilon = 0$ and $|K_L>$ ($|K_S>$) is CP odd (even), can only decay into 3 (2) pions and has a longer (shorter) lifetime. ϵ is related to the off diagonal part of $\bar{K}_0 - K_0$ mass matrix (M_{12}) given by figure 15.

$$\epsilon = \frac{ImM_{12}}{2ReM_{12}} \tag{1.46}$$

In addition to this CP violation in the eigenstates K_L and K_S, there is the possibility of CP violation in the decays. In the decay $K \to 2\pi$, the final state can have Isospin 2 or 0. If CP is a good symmetry the decay $K_L \to 2\pi$ cannot occur. These are two CP violating parameters

$$\begin{aligned} \epsilon_0 &= <2\pi, I=0|K_L> / <2\pi, I=0|K_S> \\ \epsilon_2 &= <2\pi, I=2|K_L> / <2\pi, I=2|K_S> \end{aligned} \tag{1.47}$$

Choosing the phase convention $<2\pi, I=0|K^0> =$ real, we have $\epsilon_0 = \epsilon$ and

$$\epsilon_2 \alpha \frac{Im <2\pi, I=2|K^0>}{<2\pi, I=0|K^0>} \equiv \epsilon' \tag{1.48}$$

Experimentally we have $|\epsilon| = 2 \times 10^{-3}$ and $\epsilon'/\epsilon = 0.003 \pm 0.003$.[38,39] Since we have only one CP violation parameter, we should be able to fix it using ϵ and then predict ϵ'/ϵ. The current uncertainties arise from our inadequate knowledge of QCD at low momentum transfers. We need to know the hadronic wave functions of the K_0 and $\bar{K}_0$ states, so that the matrix elements of the operators obtained from figure 15 can be evaluated and ϵ calculated. In principle these calculations could be done without approximation using QCD on a lattice and Monte–Carlo techniques. Such calculations are underway but, at present, the errors are large. In the absence of such exact calculation we must rely upon models of the hadronic wave–functions, such as the MIT bag model.

Another QCD problem is also present is estimating the real part of M_{12}. The intermediate states of figure 15, can consist of light quarks with low momenta flowing around the loop. It is not clear how well one can trust a quark calculation of figure

15 if these intermediate states such as $\pi\pi$ or η are important, since we should expect substantial QCD corrections in this case. This problem is not so severe as it might appear. If two of the charge 2/3 quark masses become degenerate the CP violation in the $K_0 - \bar{K}_0$ system disappears. Since all three of the charge 2/3 quarks must contribute to generate a non–zero value of ϵ, the dominant range of internal loop momenta which contribute are of order $(m_t - m_c)$, too large for QCD corrections to be important.

Consider the decay $K \to 2\pi$ shown in figure 16. This graph shows the spectator decay diagram where its strange quark decays while the anti–down quark is a spectator. CP violation will occur at a higher order in weak interactions hence we should expect that ϵ' would be very small. However, the graph predicts that the final states with I =2 and I = 0, corresponding to weak transition with $\Delta I = 3/2$ and 1/2, should be of approximately equal strength. This is far from the truth, the $\Delta I = 1/2$ transition is favored experimentally by a factor of order 200. This $\Delta I = 1/2$ rule is difficult to explain in the context of the spectator diagrams. Strong interaction effects do enhance the $\Delta I = 1/2$ amplitude but calculations, although uncertain since they rely on perturbative QCD in a region of doubtful validity, do not give a large enough enhancement.[40] There could also be effect from the overlap of final state wave–functions. In the absence of reliable (lattice) QCD calculations, the situation is unclear.

The penguin diagram of figure 17 has been suggested as a possible solution to the $\Delta I = 1/2$ problem.[41] Notice that the effect of this operator is to change an s quark into a d quark, and is therefore a pure $\Delta I = 1/2$ operator. Although it is higher order in strong interactions than the spectator diagram, calculations using model hadronic wavefunctions indicate that it may be dominant. Notice that CP violation can occur in the penguin at the same order as the decay itself; the u quark can be replaced by c or t. Hence if penguins are important we expect ϵ' will not be too small. Calculations[42] give $\epsilon'/\epsilon \sim 0.02$, the precise value depends on the top quark mass and upon uncertain hadronic wavefunctions. Such a large value is inconsistent with the most recent data. These are two ways out. Firstly, penguins are unimportant and we do not understand the origin of the $\Delta I = 1/2$ rule. More speculative is the possibility that the penguins are correct but that these are additional CP violating effects which can effect the prediction of ϵ'/ϵ. Contributions from supersymmetry[43] or an extended Higgs sector[44] have been discussed. If direct evidence for supersymmetry or such Higgs particles were found, these possibilities would have to be included. In the absence of such evidence, caution should be exercised.

The situation could be clarified in two ways. Better theoretical calculations of the $K - K_0$ system and $K \to 2\pi$ decays using lattice QCD[45] would enable one to tell whether penguins are relevant or whether the $\Delta I = 1/2$ rule can be

understood without them. Data in CP violations from another process could be vitally important. The standard model would predict a neutron dipole moment of order $10^{-33} e-cm$, far below the current limit. CP violation is predicted in the decay $K_S \to 3\pi$, but this is extraordinarily difficult to measure. The mesons made of $b\bar{d}$ and $\bar{b}d$, as well as those made of $b\bar{s}$ and $\bar{b}s$, may give us a system similar to that of $K_L - K_S$. There is some evidence that mixing similar to that in the kaon system has been observed.[46] In order to observe a CP violating effect a very large number of B mesons must be produced. One possibility is to look at the semi-leptonic decays arising from the production of pairs of $B\bar{B}$ mesons. The ratio of branching rations

$$\frac{BR(B\bar{B} \to \mu^+\mu^+ + X) - BR(B\bar{B} \to \mu^-\mu^- + X)}{BR(B\bar{B} \to \mu^+\mu^+ + X) + BR(B\bar{B} \to \mu^+\mu^- + X)} \tag{1.49}$$

is expected to be about 10^{-5} in the standard model. There has been some discussion about the feasibility of detecting this at the SSC where the production rate of B bosons is expected to very large.[47] The process does not require one to reconstruct the decay of the B meson. The experiment is clearly very hard.

There is one other possibility for investigating CP violation. If the phase on the quark mixing matrix is the only source of CP violation, then it must be related to the net baryon number[48] in the universe, if the universe evolved from a state with no net baryon number. Unfortunately there are so many other ingredients such as the nature of the baryon number violation and the thermal evolution of the universe, we cannot use the cosmology as a useful constraint. Nevertheless a better undertaking of CP violation would help a better understanding of the cosmological problem.

2. Where is the Higgs?

There is very little experimental information about the Higgs sector of the $SU(2) \times U(1)$ model other than that it must have a custodial $SU(2)$ symmetry so that ρ is equal to one at tree level. Do we know anything from theoretical studies?

Since $m_H^2 = \frac{2\lambda}{g_2^2} M_W^2$, it would appear that m_H could be made arbitrarily small by reducing λ. This is not the case since for very small λ one must consider the effect of gauge interactions which induce Higgs self interactions at higher order. The Higgs self interactions are described by the effective potential¶

$$V_{eff}(\Phi) = -\mu^2 \Phi^+\Phi + \lambda(\Phi^+\Phi)^2. \tag{2.1}$$

Radiative corrections from Feynman diagrams of the type indicated in Fig. 18 modify this potential. At one loop $V_{eff}(\Phi)$ becomes[49]

$$V(\Phi) = -\mu^2(\Phi^+\Phi) + \lambda(\Phi^+\Phi)^2 + c(\Phi^+\Phi)^2 \log((\Phi^+\Phi)/M^2) \tag{2.2}$$

¶Although the effective potential is not gauge invariant, its minimum is. Consequently the subsequent discussion which relates only to the minimum is physically meaningful.

where

$$c = \frac{1}{16\pi^2 v^4}(3(2M_W^2 + M_Z^2) + m_H^4 - 4\sum_j m_f^4)$$

and M is a renormalization scale. The Higgs mass m_H is given by

$$m_H^2 = \frac{\partial^2 V}{\partial \Phi^2}\Big|_{\Phi=\langle\Phi\rangle} . \tag{2.3}$$

In general V_{eff} will have more than one minimum. If we require that the minimum with $\langle\Phi\rangle \neq 0$ is lower than that with $\langle\Phi\rangle = 0$ (the phase in which the W boson remains massless), so that this phase will be the true ground state, then a bound on λ, and hence m_H, can be obtained since all the other quantities in Eq. (2.2) are known. We have[50]

$$m_H \gtrsim 7\ GeV.$$

A more detailed study which requires that the universe not be trapped at $\langle\Phi\rangle = 0$ for too long[51] gives $m_H \gtrsim 10\ GeV$. This bound is extremely model dependent. A similar bound will exist in models with different Higgs sectors.[52] In models with an arbitrary number of Higgs doublets there must be at least one physical Higgs boson with a mass greater than this bound.

As λ is increased m_H increases. Eventually λ will become too large for the perturbative formula for the Higgs mass to be valid. We can estimate this value naively by requiring that $\lambda^2/4\pi$ be less than one. This implies $m_H \lesssim 600\ GeV$. In order to be more precise it is necessary to consider the effects of the constraints imposed by partial wave unitarity.[53]

Consider the S matrix for a two-particle scattering process $a + b \rightarrow c + d$. Unitarity requires that

$$S^+ S = 1. \tag{2.4}$$

Writing $S = 1 + iT$, we have

$$-ImT = T^+ T. \tag{2.5}$$

The scattering matrix T is given by

$$T = (2\pi)^4 \delta^4(p_a + p_b - p_c - p_d)\frac{1}{(2\pi)^6}\frac{1}{s}|M_{ab\rightarrow cd}|^2 . \tag{2.6}$$

Here p_i is the momentum of particle i and M_i the invariant matrix element obtained, for example, by calculating a set of Feynman diagrams. M may be decomposed as follows:

$$M(s, \cos\theta) = 16\pi \sum_{J=0}^{\infty}(2J+1)A_J(s)P_J(\cos\theta). \tag{2.7}$$

θ is the center-of-mass scattering angle between particles a and c, $P_J(\cos\theta)$ is a Legendre polynomial and $A_J(s)$ is some function. Equation 2.5 implies that

$$Im\ A_0 \geq |A_0|^2 . \tag{2.8}$$

We can expand A_0 as a perturbation series in some coupling constant g

$$A_0(s) = a_1(s)g^2 + a_2(s)g^4 + \ldots \tag{2.9}$$

If the perturbation expression is reliable then

$$g^2 < a_1/a_2. \tag{2.10}$$

The Born term a_1g^2 is real, hence Eq. 2.8 implies that

$$-Im(a_2g^4) > (a_1g^2). \tag{2.11}$$

But $|A| > |ImA|$ for any A, so that the requirement that perturbation theory be reliable implies that

$$\left|a_1g^2\right| < 1. \tag{2.12}$$

Now this result can be applied to the process $H + H \rightarrow H + H$. If we assume that $m_H >> M_W$, the relevant Feynman diagrams are shown in Fig. 19 and give

$$A_0(HH \rightarrow HH) = -\frac{G_F m_H^3}{8\pi\sqrt{2}}\left[3 + \frac{9m_H^2}{s - m_H^2} - \frac{2m_H^2}{s - m_H^2}\log(s/m_H^2 - 3)\right]. \tag{2.13}$$

Requiring $|A_0| < 1$ (see Eq. (2.12)) in the limit $s \rightarrow \infty$ implies that

$$m_H < 1.7\ TeV.$$

A stronger bound is obtained by considering the coupled channel problem: $HH \rightarrow ZZ, HH \rightarrow WW, WW \rightarrow ZZ, HZ \rightarrow HZ, HW \rightarrow HW$. In this case one has[54]

$$m_H < \sqrt{\frac{8\pi\sqrt{2}}{3G_F}} = .98\ TeV. \tag{2.14}$$

This bound indicates that there must be a scalar particle of mass less than 1 TeV or the Weinberg-Salam model will contain a strong, non-perturbative coupling. The presence of such a coupling implies that there must be non-perturbative structure in the WW or ZZ channel for WW or ZZ invariant masses of order 1 TeV. (Recall that the longitudinal components of the W and Z come from the Higgs fields.) General arguments which apply to strongly coupled systems can be used to predict these effects.

The basic argument that I have just outlined contains the essential features which justify the choices of energy and luminosity for the SSC. In order to probe the nature of the interactions responsible for the breakdown of the $SU(2) \times U(1)$ symmetry it is necessary to probe the WW and ZZ system with invariant masses of order 1 TeV.

A similar argument can be used to constrain the masses of heavy quarks or leptons which are proportional to Yukawa couplings.[23,54] Consider the scattering of a quark or lepton F_i of mass m_i: $F_i\bar{F}_i \to F_j\bar{F}_j$. There are contributions to the scattering amplitude from exchanges of Z and Higgs bosons in the s and t channels. In the limit $s \to \infty$ with $m_i >> m_H, M_Z$, M has the following form

$$M = \sqrt{2} G_F m_i m_j \delta_{\lambda\bar{\lambda}} \delta_{\lambda'\bar{\lambda}'} [1 - \lambda\lambda' - 2\delta_{ij}]. \tag{2.15}$$

Here $\lambda(\lambda')$ labels the helicity of the fermion $i(j)$ and $\bar{\lambda}$ labels the helicity of the anti-fermions. The constraint of partial wave unitarity implies that

$$m_i^2 + m_j^2 < \frac{8\sqrt{2}\pi}{G_F}. \tag{2.16}$$

If $m_1 = m_2$ this implies that $m_1 \lesssim 530\ GeV$. In the case of a heavy lepton of mass m_L in a doublet with a massless neutrino: $m_L \lesssim 1.2\ TeV$. Quarks of masses larger than this cannot be discussed within the context of perturbation theory.‖

Let us now turn to the possible experimental signatures for Higgs bosons. The Higgs can decay to fermion anti-fermion WW and ZZ final states with the following partial widths:

$$\begin{aligned}
\Gamma(H \to f\bar{f}) &= \frac{G_F m_f^2 m_H}{4\pi\sqrt{2}} (3)(1 - 4m_f^2/m_H^2)^{3/2}, \\
\Gamma(H \to W^+W^-) &= \frac{G_F m_H^3}{32\pi\sqrt{2}} (4 - 4\epsilon + 3\epsilon^2)(1 - \epsilon)^{1/2}, \\
\Gamma(H \to ZZ) &= \frac{G_F m_H^3}{64\pi\sqrt{2}} (4 - 4\epsilon' + 3\epsilon'^2)(1 - \epsilon')^{1/2}.
\end{aligned} \tag{2.17}$$

with $\epsilon' = 4M_Z^2/m_H^2$ and $\epsilon = 4M_W^2/m_H^2$. The factor of 3 is included in the first expression only if f is a quark. The implications of these formulae are easy to see. If $m_H < 2M_W$, the Higgs will decay dominantly into the heaviest fermion channel which is open. Once m_H is greater than $2M_W$, the decay into two gauge bosons will dominate. This effect is shown in Fig. 20. Notice that the width grows rapidly as m_H is increased. Eventually $\Gamma/m_H \sim 0(1)$: this is another manifestation of the breakdown of perturbation theory at large values of m_H.

The Higgs can be produced in e^+e^- annihilation from the decay of a Z through the graph shown in Fig. 21, with a rate shown in Fig. 22. The rate is given by[55]

$$\frac{1}{\Gamma(Z \to \mu^+\mu^-)} \frac{d\Gamma(Z \to H + \mu^+\mu^-)}{dx} = \frac{\alpha}{4 sin^2\theta_W cos^2\theta_W}$$

‖An exception to this can occur in modifications of the standard model which contain fermions whose mass is not controlled by $\langle\Phi\rangle$. For example, a right-handed neutrino can have an arbitrarily large Majorana mass.

$$\times \frac{(1-x+\frac{x^2}{12}+\frac{2m_H^2}{3M_Z^2})(x^2-\frac{4m_H^2}{M_Z^2})^{1/2}}{(x-\frac{m_H^2}{M_Z^2})^2} \tag{2.18}$$

Here $x = 2E_H/M_Z$ where E_H is the energy of the Higgs boson. The rate is rather small, but the signature is very clean. It is not necessary to reconstruct the Higgs from its decay products; one searches for a peak in the mass recoiling against the lepton pair. Backgrounds arise from the production of a heavy quark pair if both of the quarks decay semileptonically. If we require that the leptons be isolated this background is not important. If one looks in the e^+e^- decay channel, then there is a background from the two photon process $e^+e^- \to e^+e^- +$ hadrons which produces a serious problem for Higgs masses below about 8 GeV. A Higgs of mass less than 40 GeV should be discovered at LEP/SLC using this process. If the Higgs mass exceeds 0.6 M_Z, then this rate is exceeded by that from $Z \to H + \gamma$.[56] Again the signal is very clean, but the small rate makes it unlikely that this process will be observed.

The Higgs boson can also be produced at higher energies in e^+e^- annihilation via the process $e^+e^- \to Z + H$,[57] with the rate shown in Fig. 23. The production cross-section at center-of-mass energy $\sqrt{s}$ is given by

$$\frac{d\sigma(e^+e^- \to Z+H)}{d(\cos\theta)} = \frac{\pi\alpha^2(1+8sin^4\theta_W-4sin^2\theta_W)}{16sin^4\theta_W cos^4\theta_W(s-M_Z^2)^2}\frac{2\kappa}{\sqrt{s}}(M_Z^2+\frac{\kappa^2 sin^2\theta}{2}). \tag{2.19}$$

Here θ is the angle between the Higgs and the beam and κ is the Higgs momentum. Again it is not necessary to reconstruct the final state arising from the Higgs decay. The cross section is not large, particularly if the Z can only be detected via its decay to $\mu^+\mu^-$ or e^+e^-. Nevertheless LEP should be able to probe Higgs masses up to $0.9(\sqrt{s}-M_Z)$ using this mechanism.

Another potentially important process is the decay of the toponium bound state (θ) into $H+\gamma$,[58] the rate for which is shown in Fig. 24. Since coupling of a Higgs to a quark is proportional to the quark mass, the rate will be largest if the top quark mass (m_t) is large. The rate is given by

$$\frac{\Gamma(\theta \to H\gamma)}{\Gamma(\theta \to \mu^+\mu^-)} = \frac{G_F m_t^2}{\sqrt{2}\pi\alpha}(1-\frac{m_H^2}{m_\theta^2})^{1/2}. \tag{2.20}$$

This process has a rather large QCD correction.[59] If this is included, the right-hand side of Eq. (2.20) is multiplied by

$$\left(1-\frac{4\alpha_s}{3\pi}a(m_H^2/m_\theta^2)\right)$$

Here, $a(x) \sim 10$ for $x \leq 0.8$, so that the correction reduces the naive rate. The branching ratio is reasonably large, but it is important to recall that the production

rate for toponium in e^+e^- annihilation is not large. A 80 GeV toponium state has a production cross section of order 0.1 nb.

The product of a Higgs in hadron-hadron collisions occurs via several mechanisms. Since the Higgs coupling to light quarks is very small, the production of Higgs bosons from the annihilation of light quark-antiquark pairs strongly suppressed. There are too few heavy quarks inside the proton for their annihilation to generate a reasonable rate. There are two important mechanisms. Firstly, the Higgs can be produced via gluon-gluon fusion according to the Feynman diagram shown in Fig. 25.[60] This graph contains a vertex coupling the Higgs to a quark-antiquark pair, which is proportional to the quark mass. Consequently, the rate from this process depends sensitively upon the mass of the top quark. The production rate at center-of-mass energy $\sqrt{s}$ is a proton-proton collision is given by

$$\sigma(pp \to H + X) = \frac{G_F \pi}{32\sqrt{2}} \left(\frac{\alpha_s}{\pi}\right)^2 \eta^2 \int_{M_H^2/s}^1 \frac{M_H^2}{s} g(x) g(m_H^2/sx) dx. \qquad (2.21)$$

$g(x)$ is the gluon distribution of a proton (see Sec. 3). Defining $\epsilon_i = 4m_i^2/m_H^2$ for a quark of mass m_i, η is given by

$$\eta = \sum_i \frac{\epsilon_i}{2}(1 + (\epsilon_i - 1)\phi(\epsilon_i))$$

with

$$\phi(\epsilon) = \begin{cases} -[\sin^{-1}(1/\sqrt{\epsilon})]^2 & \epsilon > 1 \\ \frac{1}{4}(\log(\eta_+/\eta_-) + i\pi)^2 & \epsilon < 1 \end{cases}$$

where $\eta_\pm = 1 \pm \sqrt{1-\epsilon}$.

An alternative mechanism is shown in Fig. 26.[61] At large values of m_H, the rate from this mechanism becomes large due to the large width for $H \to WW$. The exact formula for this rate is complicated; it simplifies drastically in the so-called effective W approximation. This approximation assumes that the W's are emitted parallel to the incoming quarks and they are treated as if they are on mass-shell. It is similar to the effective photon approximation used to describe two-photon reactions in e^+e^- annihilation where the electron beams are treated as sources of on-shell photons. In this approximation the cross-section for $q + q \to H + qq$ via intermediate W's is given by[62]

$$\sigma\,(q_i + q_j \to H + q_j + q_i) = \frac{1}{16M_W^2} \left(\frac{\alpha}{\sin^2\theta_W}\right)^3$$
$$\times [(1 + m_H^2/\hat{s}) \log(\hat{s}/m_H^2) - 2 + 2m_H^2/\hat{s}]\theta(-e_i e_j) \qquad (2.22)$$

where $\sqrt{\hat{s}}$ is the center-of-mass energy of the qq system and e_i is the charge of quark of type i. This may be converted into a hadronic cross-section via the parton model

(see Sec. 3). In the case of intermediate Z bosons the factor $\theta(-e_i e_j)$ is replaced by $\frac{1}{\cos\theta_W^6}(v_i^2+a_i^2)(v_j^2+a_j^2)$ where v_i and a_i were defined in Section 1.

This mechanism will only be important at the SSC; cross-sections evaluated at Tevatron and Sp$\bar{\text{p}}$S energies are dominated by the gluon fusion process. The rates for Higgs production are shown in Fig. 27. There are other mechanisms leading to final states with $H+Z, W+Z$ and $H+t\bar{t}$.[63] The rates for Higgs production via these mechanisms are smaller than those discussed above and will be useful only if the additional particles can be used as a tag in order to improve the signal-to-noise ratio.[64]

The signals for Higgs bosons at the SSC are discussed extensively elsewhere.[65,66] At the Tevatron the rates are reasonable only for Higgs masses less than 150 GeV or so. In this mass region the Higgs will decay dominantly to $t\bar{t}$ if the t quark is light enough. There is a large background from the QCD production of $t\bar{t}$ pairs (this will be discussed in the next section) which will make detection difficult even if the t quark can be identified efficiently.

If the $t\bar{t}$ channel is not open, the Higgs will decay to $\tau^+\tau^-$ with a branching ratio of $m_\tau^2/3m_b^2 \sim 4.5\%$. The only background source of τ pairs is Drell-Yan production $p\bar{p} \to \tau^+\tau^- + X$, via a virtual Z or photon. Figure 28 shows the signal and background in the τ pair channel. I have assumed a resolution of 10 GeV in the $\tau^+\tau^-$ invariant mass. It can be seen that the signal to background ratio is rather poor. This figure assumes a top quark mass of 150 GeV. The tau final state can be identified from the one-prong tau decays ($\tau \to e\nu\nu$, $\mu\nu\nu$, $\pi\nu$, etc.). Energy is lost into neutrinos so that the resolution in the $\tau^+\tau^-$ invariant mass will be poor. The experiment is clearly very difficult.

There is one other possibility. The Higgs can decay to two photons (see Fig. 29) with the branching ratio[67]

$$BR(H \to \gamma\gamma) \sim \frac{m_H^2 |A| \alpha^2}{6\pi^2 m_b^2}. \tag{2.23}$$

I have assumed that $m_t > m_H/2$. Here A is a number arising from the W, quark and lepton loop diagram. Its value depends upon the masses of the particles involved but it is of order four for Higgs masses around 100 GeV. The background arises from the production of photon pairs via quark-antiquark collisions and is not too large. Unfortunately the branching ratio is so small that there are insufficient events for this decay mode to be useful. It has been suggested[68] as a possible mode at the SSC where the event rates are much larger.

What can we conclude about the prospects for finding the Higgs in the near future? If its mass is less than 40 GeV or so, it should be found in the decay of the Z either at the SLC or at LEP. Masses larger than this can be probed in the decay of toponium, if toponium exists in an accessible mass range. Notice that if

$m_t > m_b + M_W$, the top quark will decay too quickly for narrow toponium bound states to exist. Higgs masses up to 100 GeV can be probed in the early 1990's at LEP when the energy is increased to 100 GeV per beam. Higgs bosons of mass greater than this will have to wait for the SSC.

Another outstanding problem in the standard model concerns the number of generations which is not constrained by the model itself. The number of generations can be constrained, if we assume that the neutrinos are massless, by counting their number. There is an astro-physical argument based upon the abundance of the light elements which suggests that the total number of neutrinos is less than four. Direct searches can be made in e^-e^+ annihilation or from measurements of the Z width. The current limit and the prospects are discussed by Dave Burke[69] in his lectures at this school.

It is also possible to constrain the number of neutrinos from the measured production rates of W and Z bosons in hadron colliders. The quantity

$$\frac{\sigma(p\bar{p} \to W + anything)}{\sigma(p\bar{p} \to Z + anything)} \frac{BR(W \to e\nu)}{BR(Z \to e^+e^-)}$$

can be measured. Using a theoretical calculation of the ratio of cross-sections (see next section), the ratio of branching ratios can be inferred. From this it is possible to extract the number of neutrinos.[70] There is some uncertainty due to the unknown t quark mass which enters into the calculation of $BR(W \to e^+e^-)$. This dependence is not strong and a useful limit can be derived from this technique. However measurements at the SLC will have greater precision.

3. QCD

In this chapter, I shall provide an introduction to perturbative QCD. I shall emphasize the uses of QCD in calculating rates at hadron-hadron colliders. Since QCD processes account for most of the background for new physics at such colliders, it is important to understand the uncertainties in these predicted rates. Given the limited time available I have had to be selective in the topics discussed.** I will begin with a discussion of the one parameter of QCD, namely, its coupling constant. I shall then discuss the parton model in some detail. I will conclude with a discussion of the production of new quarks at hadron-hadron colliders. This discussion will serve as a framework for an analysis of some of the uncertainties in such calculations.

The QCD Lagrangian may be written as follows:

$$-\frac{1}{4}F^i_{\mu\nu}F^i_{\mu\nu} + \sum_j \bar{\psi}_j(i\not{\partial} - m_j)\psi_j \qquad (3.1)$$

**For a more detailed discussion see refs. 71,72

The sum on j runs over quark flavors and,

$$F^i_{\mu\nu} = \partial_\mu G^i_\mu - \partial_\nu G^i_\mu - igf_{ijk}G^i_\mu G^i_\mu$$

and

$$D_\mu = \partial_\mu - ig\, t^i\, G^i_\mu$$

Here t^i are the 3×3 representation matrices and the structure constant f_{ijk} are given by $[t_i, t_j] = if_{ijk}t_k$.

Apart from the quark masses, which have their origin in the Weinberg-Salam model, the theory has only one fundamental parameter, the coupling constant g. As in the case of the electroweak theory, beyond tree level it is necessary to define a renormalized coupling constant $g(\mu)$. In the case of QED this could be done in terms of the static potential between two electrons. The analogous definition in QCD would be in terms of the inter-quark potential. In the case of light quarks such a definition is impossible in the context of a perturbative theory since QCD is strongly coupled at such low momentum scales. A definition in terms of the potential between two heavy quarks is possible but not particularly convenient. I shall therefore use the modified minimal subtraction scheme discussed in Sect. 1 (see Eq. (1.11)).

Let us calculate a physical process $P(Q^2)$, which depends on some energy scale Q; P could, for example, represent a cross-section. If we neglect quark masses, calculate in n dimensions then

$$P(Q^2) \sim \left[\frac{2A}{4-n} - A\gamma_E + A\log 4\pi - F(\mu, Q^2, g)\right] \tag{3.2}$$

Recall that the scale μ is introduced so that the coupling constant g remains dimensionless in n dimensions, *viz.*,

$$g \to g\mu^{(4-n)/2} \tag{3.3}$$

It is convenient to choose the quantity P to be dimensionless; this can always be done by multiplying it by an appropriate power of Q. Then P must have the form, after subtraction of the $1/(n-4)$, γ_E and $\log 4\pi$ terms

$$P(Q^2) = F(Q^2/\mu^2, \alpha) \tag{3.4}$$

I have replaced g by α: $\alpha \equiv g^2/4\pi$. Now, the scale μ is arbitrary so that a physical quantity cannot depend upon its value

$$\frac{dP}{d\mu} = 0 \tag{3.5}$$

which implies

$$\left(\mu^2\frac{\partial F}{\partial \mu^2} + \beta(\alpha)\frac{\partial F}{\partial \alpha}\right) = 0 \tag{3.6}$$

Here $\beta(\alpha)$ is defined by

$$\beta(\alpha) \equiv \mu^2 \frac{\partial \alpha}{\partial \mu^2} \tag{3.7}$$

(Recall that the bare coupling α depends on μ (see Eq. (1.11).) We can introduce a momentum-dependent coupling $\alpha(t)$ via

$$t \equiv \int_{\alpha}^{\alpha(t)} \frac{dp}{\beta(p)} \tag{3.8}$$

where $t = \log(Q^2/\mu^2)$ Then Eq. (3.6) has the solution

$$F(t, \alpha) = F(1, \alpha(t)) \tag{3.9}$$

Hence the only dependence on the scale Q or t is carried by $\alpha(t)$. We can expand β as a power series in α.

$$\beta = -b\frac{\alpha}{4\pi} - b'(\frac{\alpha}{4\pi})^2 + \ldots \tag{3.10}$$

Hence $\alpha(\mu^2)$ has the following form:

$$\alpha(\mu^2) = \frac{4\pi}{b\log(\mu^2/\Lambda^2)} + \ldots \tag{3.11}$$

Here $b = 11 - 2n_f/3$ where n_f is the number of quark flavors with mass less than μ. We can regard the fundamental parameter of QCD either as $\alpha(Q_0^2)$ or as the scale Λ. Notice that as μ becomes small, α becomes large. Therefore, perturbation theory cannot be used to discuss processes which involve momentum flows as small as a few times Λ.

The value of Λ or $\alpha(Q_0^2)$ which has been obtained is dependent upon the renormalization scheme used. For example, I could have used minimal subtraction, in which case the $\log(4\pi)$ and γ_E would not have been removed. The expression for P written in terms of the new coupling constant $\bar{\alpha}$ can be used to express $\bar{\alpha}$ in terms of α, since the value of a physical quantity cannot depend on the scheme

$$\begin{aligned} P(\bar{\alpha}) = P(\alpha) \Rightarrow \bar{\alpha} &= f(\alpha) \\ &= \alpha + c\alpha^2 + \ldots \end{aligned} \tag{3.12}$$

which corresponds to a new value of Λ

$$\bar{\Lambda} = \Lambda e^{c/2b} \tag{3.13}$$

A physical quantity is, of course, independent of the renormalization scheme. However, if the series is terminated at some finite order in the coupling constant, the values of P (P_N) calculated to this order will differ

$$P_N(\bar{\alpha}) \neq P_N(\alpha) = P_N(\bar{\alpha}) + 0(\alpha^{N+1}) \tag{3.14}$$

Since the coupling constant of QCD is not very small and most processes are not known to a very high order, these differences can be significant.

As a specific example of QCD process, consider the total cross-section for $e^+e^- \rightarrow$ hadrons at center-of-mass energy $\sqrt{s}$. In the one photon approximation (see Fig. 30) this is given by

$$\sigma_{had} = \frac{8\pi\alpha_{em}^2}{3s^2} \sum_n (2\pi)^4 \delta(q - q_n) \langle 0|j_\mu|n\rangle \langle n|j_\mu|0\rangle \tag{3.15}$$

where j_μ is the electromagnetic current of the quarks

$$j_\mu = \sum_i e_i \bar{\psi}_i \gamma_\mu \psi_i \tag{3.16}$$

If we introduce the photon self-energy function $\Pi^{\mu\nu}$

$$\Pi_{\mu\nu}(q) = i \int d^4x e^{iqx} \langle |T(j_\mu(x) j_\nu(0))| 0\rangle \tag{3.17}$$

Defining $\Pi_{\mu,\nu}(q) = (g_{\mu,\nu}q^2 - q_\mu q_\nu) = \Pi(Q^2)$ then

$$\sigma_{had} = \frac{16\pi^2\alpha_{em}^2}{s} \, Im \, \Pi(s) \tag{3.18}$$

A dimensionless quantity is $R(s)$ defined by

$$R(s) = \frac{\sigma_{had}}{\sigma(e^-e^+ \rightarrow \mu^+\mu^-)} \quad . \tag{3.19}$$

Apart from the scale $\sqrt{s}$, R could also depend upon m_i^2/s, where m_i is the mass of a quark of type i. The dependence of R upon m_i can be seen by analyzing the Feynman diagram of Fig. 30. The graph is not singular as m_i tends to zero,

$$R_{m_i \rightarrow 0} = \text{const} + \frac{m_i^2}{s} \log m_i^2 \tag{3.20}$$

We can therefore neglect all light quark masses, R is then a function only of s/μ^2, and the previous argument implies that $R = R(\alpha(s))$. If we calculate R using perturbation theory we get

$$R = \sum e_i^2 \left(1 + \frac{\alpha_s}{\pi} + B\left(\frac{\alpha_s}{\pi}\right)^2 \ldots\right) \tag{3.21}$$

where B is a scheme-dependent constant which is small[73] in the $\overline{MS}$ scheme.

Why are the non-perturbative effects irrelevant? After all, the final state consists of hadrons rather than free quarks which are used in the perturbative calculation. This can be understood by considering the time evolution of the final state. At

very early times (equivalently large momenta) QCD is a weakly coupled theory so perturbation theory should be reliable. At large q the exponential in Eq. (3.17) is rapidly oscillating so only small values of x_μ contribute to $\Pi(q)$. Hence we are dominated by short distances (times). The hadronization of the final state takes place at later times (or order $1/\Lambda$) and although it can affect detailed properties of the final state, it is incapable of modifying the total cross-section.

A measurement of the total cross section in e^+e^- annihilation is in principle one of the best ways to determine the strong coupling constant. Unfortunately, its measurement has large systematic errors. At LEP or the SLC the same QCD corrections apply to the width of the Z. Thus it may be possible to determine α_s from a precise measurement of the hadronic width of the Z. In order to get a 10% error on α_s it will be necessary to measure the width of the Z to about 15 MeV.

Other tests of QCD in e^+e^- annihilation depend upon the study of the jets of particles produced in the final state from the hadronization of the produced quarks and gluons. At lowest order in α_s, the final state consists of a quark-antiquark pair; at next order we can get a state with an additional gluon (terms of this type contribute to the order α_s terms in eqn. 3.21). Since the quarks and gluons hadronize into jets of particles, this would seem to imply that the ratio #(3jets)/#(2jets) should be of order α_s. This is only partially true since it is necessary to define what is meant by a jet. Consider the final state of two quarks and a gluon illustrated by figure 31. The Feynman graph contains an internal propagator which gives rise to a factor of $1/(p_2+p_3)^2$; this factor becomes singular when either the gluon becomes very soft, i.e. $p_3 \to 0$, or when it moves parallel to the outgoing quark p_2. In the calculation of the inclusive cross-section, these singularities are cancelled by the divergences also present in the radiative corrections to the final state of quark and antiquark (see figure 32).

These soft and collinear divergences correspond precisely to those parts of phase space where a detector would only detect two jets. Consider an idealised detector consisting of a set of elements each of which covers an angular cone of opening angle δ and has an energy threshold ϵ. This detector will incapable of resolving two jets if one of them is very soft (energy ϵ or less), or if the two jets have an angular separation which is less than δ. We can define the f to be the fraction of total cross-section in which all but a fraction ϵ of the total energy is deposited into two cones of opening angle δ. Then to order α_s,

$$(1-f) = \frac{\sigma_{3-jet}}{\sigma_{total}} \tag{3.22}$$

provides a definition of the three jet fraction.

We can calculate this fraction as follows. Working in the center of mass of the e^+e^- system and defining $x_i = 2E_i/\sqrt{s}$, where E_i is the energy of the outgoing quark or antiquark (see figure 31), the differential cross section for the three parton final

state can be written as

$$\frac{1}{\sigma_{total}}\frac{d\sigma}{dx_1 dx_2} = \frac{2\alpha_s}{3\pi}\frac{x_1^2+x_2^2}{(1-x_1)(1-x_2)} \tag{3.23}$$

Notice that this is singular when either x_1 or x_2 is zero which corresponds to the configuration where the gluon is soft ($x_1 \sim x_2 \sim 1$) or hard and parallel to one of the quarks (either $x_1 \sim 1$ or $x_2 \sim 1$). Hence[74]

$$\begin{aligned}(1-f) &= \int_{\epsilon,\delta}\frac{1}{\sigma_{total}}\frac{d\sigma}{dx_1 dx_2} \\ &= \frac{4\alpha_s}{3\pi}(4log(1/\delta)log(1/2\epsilon) - 3log(1/\delta) + \pi^2/3 - 7/4). \end{aligned} \tag{3.24}$$

Notice that as ϵ and δ become very small the logarithms in this expression can become very large. Ultimately the perturbation expansion in α_s breaks down since there are terms in next order which are of order $\alpha_s^2 log^2(1/\delta)$. Since this is not small compared with $\alpha_s log(1/\delta)$, the expansion is not reliable. The situation can be improved by resumming these large logarithms to all orders. I will give an example of such a resummation later when I discuss multiplicity growth.

Can we use eqn. 3.24 in order to determine the strong coupling constant from data? A lower bound on δ is placed by hadronization effects. These non-perturbative effects will cause a spread in the size of a jet of order

$$\delta_{min} \sim \frac{\langle p_t \rangle}{\langle p_p \rangle} \sim \frac{p_t n}{E_{jet}} \tag{3.25}$$

where $\langle p_t \rangle$ is the mean value of transverse momentum imparted to a hadron in the hadronization process and n is the multiplicity of the jet, defined as the number of hadrons within it which are stable with respect to strong interactions ($\pi's$, $K's$, etc.). $\langle p_t \rangle$ is of order 300 MeV, so for jets at PEP or PETRA where the multiplicity is of order eight,[75] $\delta_{min} \sim 0.1$, a rather large value. The formula of equation 3.24 cannot be used at values of δ below this. Hence the problem of very large logarithms does not arise at current energies. The details of the hadronization can also affect the determination of α_s as the following argument shows. If we have a detector which is insensitive to hadrons of momentum less than p_{min}, then if a jet fragments into a set of slow hadrons, it may be that the jet is not detected because all the hadrons are below p_{min}. The details of hadronization can affect the number of jets observed by such a detector. Of course, the hadronization algorithm can be tested by direct comparison with the data. Such Monte Carlo algorithms are a vital part of all QCD tests involving jets; I refer the reader to one of the recent reviews for more information concerning them.[76]

In the formulae given above, I have not specified the scale at which α_s is evaluated. In the case of the total cross section this scale is unambiguous, it must be

$\sqrt{s}$. In the three jet case it may be more appropriate to use the average invariant mass of a jet pair in the event since the internal quark propogator is off-shell by approximately this amount. As discussed above, this question cannot really be answered without a calculation of the order α_s^2 terms. These have been computed[77] and would indicate the a scale of order $\sqrt{s}(1-T)$ should be used. Here T is the thrust defined by

$$T = max \frac{\sum_i p_{i,l}}{\sum_i |p_i|}. \tag{3.26}$$

Here the sum runs over all particles in the event and the maximisation takes place with respect to the direction of an axis. The component of the particle's momentum p_i along this axis is $p_{i,l}$. For a two jet event $T = 1$ if we neglect the effects of hadronization. This choice of scale for the argument of α_s therefore reflects to some extent the off-shellness of the internal quark propagator.

There are two contributions to the multiplicity of hadrons within a jet. A jet is initiated by a quark or gluon which is produced in a hard scattering. This parton is off mass-shell by an amount of order the energy involved in the hard scattering. This parton can produce a shower of other partons via a branching process controlled by perturbative QCD; the invariant mass of each parton being degraded at each branching. Eventually the invariant mass becomes of order 1 GeV and perturbative QCD ceases to be reliable. The final hadronization takes place via a non-perturbative process. The multiplicity of the partonic shower can be calculated in perturbative QCD. Since the hadronization is characterised by a mass scale of order 1GeV which does increase with the jet energy, the growth of multiplicity is controlled by the growth of the parton shower and is therefore calculable.

In order to discuss the growth of the partonic shower,[78] consider figure 33 which shows the production of a pair of gluons from a stationary source, followed by the emission of one gluon from one of the outgoing gluon lines. We can define a fragmentation function $D(z, q^2)$ to be the probability that there is an outgoing gluon with momentum $zq/2$ produced in the shower. At lowest order in α_s where the source simply produces two gluons of energy $q/2$

$$D(z, q^2) \propto \delta(1-z). \tag{3.27}$$

The graph of figure 33 gives a contribution to $D(z, q^2)$ at order α_s. Here $z = 2p/q$, where p is the momentum of the "observed" gluon.

$$zD(z, q^2) = C_A \frac{\alpha_s}{\pi} \int d^3k \frac{F(k,p)}{(k+p)^4} \tag{3.28}$$

The complicated factor $F(k,p)$ can be simplified if we work in the limit of small z,

$$zD(z, q^2) = C_A \frac{\alpha_s}{\pi} \int_0^2 \frac{d\rho}{\rho + \rho_0} \tag{3.29}$$

where $\rho = 1 - cos\theta$, where θ is the angle between k and p, and

$$\rho_0 = \frac{2p^2}{z^2q^2} \tag{3.30}$$

So that we have

$$zD(z,q^2) = \frac{\alpha_s C_A}{\pi} log(1/\rho_0) \tag{3.31}$$

At next order in α_s, the relevant Feynman graphs are shown in figure 34. Again making the approximation that z is small we get

$$zD(z,q^2) = (\frac{\alpha_s C_A}{\pi})^2 \int_z^1 \frac{dz_1}{z_1} \int_{\rho_0}^2 \frac{d\rho_{1p}}{\rho_{1p}} \int_{\rho_{1p}}^2 \frac{d\rho_{12}}{\rho_{12}} \tag{3.32}$$

where $z_1 = k_1/p$ and $\rho_{ij} = 1 - cos\theta_{ij}$. Notice that in this result the integrals over the angles between the pairs of gluons are ordered. Performing the integrals in eqn (3.32) gives

$$zD(z,q^2) = \frac{1}{2}(\frac{\alpha_s C_A}{\pi})^2 log^2(1/\rho_0) log(1/z) \tag{3.33}$$

A similar calculation can be used to show that one can write an integral equation for $D(z,q^2)$ which gives the degradation in z and Q^2 which occurs as a result of multiple gluon emission.

$$zD(z,\rho) = \delta(1-z) + \frac{\alpha_s C_A}{\pi} \int_\rho^2 \frac{d\rho'}{\rho'} \int_z^1 \frac{dz_1}{z_1} z_1 D(z_1,\rho') \tag{3.34}$$

with $\rho = 2p^2/q^2z^2$.

The multiplicity of the partonic shower is given by

$$\langle n \rangle = \int_0^1 dz D(z,Q^2) \tag{3.35}$$

Equation (3.34) can be solved by taking moments with respect to z.

$$D_n(\rho) = \int_0^1 dz z^{n-1} D(z,\rho) \tag{3.36}$$

The solution is

$$D_n(\rho) = exp(\frac{\alpha_s C_A}{\pi(n-1)}). \tag{3.37}$$

In order to calculate the multiplicity we need a moment at fixed q^2 rather than one at fixed ρ. Defining

$$D_n(q^2) = \int_0^1 x^{n-1} D(z,q^2) \tag{3.38}$$

we have

$$D_n(q^2) = C_n exp(\gamma_n log(q^2/p^2)) \tag{3.39}$$

with

$$C_n = \frac{1}{2}\frac{n-1+\sqrt{(n-1)^2+\frac{8\alpha_s C_A}{\pi}}}{\sqrt{(n-1)^2+\frac{8\alpha_s C_A}{\pi}}} \tag{3.40}$$

and

$$\gamma_n = \frac{1}{4}(-n+1+\sqrt{(n-1)^2+\frac{8\alpha_s C_A}{\pi}}) \tag{3.41}$$

We can now include the effect of the running coupling constant, which yields the result

$$D_n(q^2) = C_n(\alpha_s(q^2))exp(\int_{p^2}^{q^2}\gamma_n(\alpha_s(t^2))\frac{dt^2}{t^2}) \tag{3.42}$$

Hence the multiplicity is given by

$$\langle n\rangle \sim \frac{1}{2}exp(\sqrt{\frac{2C_A}{\pi b}(log(q^2/\Lambda^2)-log(p^2/\Lambda^2))}) \tag{3.43}$$

The previous computation will overestimate the multiplicity. Consider the production of a quark-antiquark pair in e^+e^- annihilation. As these quarks begin to separate and emit gluons the parton multiplicity will rise. However if one of the quarks attempts to emit a very soft gluon (of momentum p), the emission will be suppressed if the distance of order $1/p$ is greater than the separation of the quark-antiquark pair since the gluon will see the total color charge of the pair, which is zero. This coherence effect causes the emission of soft gluons and hence the multiplicity to be suppressed and is not included in the above calculation. A calculation including these effects lowers the multiplicity.[79]

In order to discuss processes which involve hadrons in the initial state, we must discuss the parton model.[80] Consider the case of electron-proton scattering, where the cross-section can be written as

$$\frac{d\sigma}{dxdy} = \frac{4\pi\alpha_{em}^2 s}{Q^4}\left[\frac{1+(1-y)^2}{2}2xF_1(x,Q^2)+(1-y)(F_2(x,Q^2)-2xF_1(x,Q^2))\right] \tag{3.44}$$

The variables are defined as follows (see Fig. 35): q is the momentum of the exchanged photon and P is not momentum of the target proton and k is that of the incoming electron

$$\begin{aligned} Q^2 &= -q^2 \\ \nu &= \frac{q\cdot P}{M_p} \\ x &= \frac{Q^2}{2m_p\nu} \end{aligned} \tag{3.45}$$

$$y = \frac{q \cdot p}{k \cdot p}$$

$$s = 2p \cdot k + m_p^2$$

where m_p is the proton mass. I have neglected parity violating effects which arise from the exchange of a Z boson instead of a photon.

In the naive parton model the proton is viewed as being made up of a set of non-interacting partons. The structure functions F_1 and F_2 are related to the probability distribution $q_i(x)$ which represents the probability of finding a parton of type i (quark or gluon) inside the proton with fraction x of the proton's momentum, and the scattering cross-section for such a virtual photon from a parton.

$$F_1 = \frac{F_2}{2x} = \sum_i \int_x^1 \frac{dy}{y} q_i(y)[e_i^2 \delta(x/y - 1)] \tag{3.46}$$

where e_i is the charge of parton of type i. The δ-function appears from the cross-section for $q + \gamma \to q$. Let us consider QCD corrections to this scattering. At next order in α_s, there are contributions from gluon emission which lead to the final state $q + g$ and also from virtual gluons (see Fig. 36). To order α_s (3.46) is replaced by

$$F_1 = \sum_i \frac{dy}{y} q_i(y) \left[e_i^2 \delta\left(\frac{x}{y} - 1\right) + \sigma_i\left(\frac{x}{y}, Q^2\right)\right] \tag{3.47}$$

with

$$\sigma_i(z, Q^2) = \frac{\alpha_s}{2\pi} e_i^2 \left[t P_{qq}(z) + f(z) + 0\left(\frac{1}{Q^2}\right)\right] \tag{3.48}$$

with

$$P_{qq}(z) = \frac{4}{3} \frac{(1 + z^2)}{1 - z}$$

for $z \neq 1$. Here $t = \log(Q^2/\mu^2)$ and the scale μ has appeared from dimensional regularization (I have dropped terms $1/(n-4)$). The μ dependence arises because σ_i is not finite in four dimensions. In the cases discussed previously, the divergences arise from large momentum flows inside loop diagrams (ultra-violet divergences). In this case these divergences cancel. Individual Feynman diagrams can also have divergences when momentum flows become very small or particles are collinear. The former (soft) divergences cancel between the real and the virtual diagrams but the collinear ones do not. In order to see the origin of the problem consider the graph of Fig. 36 and work in a frame where $k_\mu = (k, k, 0, 0)$.

If the transverse momentum of the gluon(p) relative to k is small then we can take $p = (\eta k + k_\perp^2/2\eta k,\ \eta k,\ k_\perp\ 0)$. (Terms of order $k_\perp^2$ are neglected.) The internal quark line now has invariant mass squared $r^2 = (k - p)^2 = k_\perp^2/\eta$, so that the squared amplitude from the graph will contain $1/k_\perp^4$. Now at very small $k_\perp$ helicity

conservation forbids the emission of a real gluon from a quark line, so that one factor of $k_\perp^2$ appears in the numerator. We now have for the total cross-section $q + \gamma \to q +$ anything, a contribution

$$\sigma \sim \frac{\alpha_s}{2\pi} \int \frac{dk_\perp^2}{k_\perp^2} \tag{3.49}$$

which gives rise to a logarithmic singularity. Notice that for a massive quark the singularity becomes $\log(Q^2/m_q^2)$.

We have obtained a result which depends on μ (or contains the large log (Q^2/m_i^2) if quark masses are retained). This is not physically meaningful. But Eq. (3.47) contains the unknown quantity $q_i(y)$. We can define[80]

$$q_i(x,t) = q_i(x) + \frac{\alpha_s t}{2\pi} \int_x^1 \frac{dy}{y} q(y) P_{qq}\left(\frac{x}{y}\right) \tag{3.50}$$

Hence

$$F_1 = \sum_i \int_x^1 e_i^2 \frac{dy}{y} q_i(y) \left[\delta\left(\frac{x}{y} - 1\right) + \frac{\alpha_s}{2\pi} f\left(\frac{x}{y}\right)\right] + 0(\alpha^2) \tag{3.51}$$

The t dependence can be eliminated at the cost of introducing a t-dependent structure function

$$\frac{d}{dt} q(x,t) = \frac{\alpha_s}{2\pi} \int_x^1 \frac{dy}{y} q(y,t) P_{qq}\left(\frac{x}{y}\right) + 0(\alpha_s^2) \tag{3.52}$$

I have so far considered an oversimplification of the true problem. To order α_s there is an additional partonic process, namely $gluon + \gamma \to q + \bar{q}$ (see Fig. 37). This process also contains a log (Q^2/μ) arising from the propagation of the internal quark close to its mass shell. This singularity results in the replacement of Eq. (3.47) and (3.48) by

$$\begin{aligned} F_1(x,t) \; = & \int_x^1 \frac{dy}{y} \left[\sum_i e_i^2 q_i(y) \left[\delta(\frac{x}{y}) + \frac{\alpha_s}{2\pi} \left[t P_{qq}(\frac{x}{y}) + f_q(\frac{x}{y})\right]\right.\right. \\ & \left.\left. + (\sum_i e_i^2) g(y) \frac{\alpha_s}{2\pi} \left[t P_{qg}(\frac{x}{y}) + f_g(\frac{x}{y})\right]\right] \end{aligned} \tag{3.53}$$

with $P_{qg}(x) = 1/2(x^2 + (1-x)^2)$. The t dependence can be absorbed by defining

$$q_i(x,t) = q_i(x) + \frac{\alpha_s}{2\pi} t \int_x^1 (q_i(y) P_{qq}(\frac{x}{y}) + g(y) P_{qg}(\frac{x}{y})) \frac{dy}{y} \tag{3.54}$$

so that the quark and gluon distributions ($q_i(x)$ and $g(x)$) are now coupled.

Given data from which $q_i(x,t_0)$ and $g(x,t_0)$ can be obtained as functions of x for a fixed t_0, the equations for the evolution of $q(x,t)$ and $g(x,t)$ with t can be solved to obtain them for all t.

Before leaving the Altarelli-Parisi equations, I would like to discuss the behaviour of the structure functions at very small values of x.[81] As the energy available increases it becomes possible to reach smaller and smaller values of x at fixed Q^2. The solution of equation 3.54 for some value of $x = x_0$ requires data at one value of Q^2 for all $x > x_0$.

Consider the behaviour of the gluon distribution at small x, We can neglect the generation of gluons from quarks since the gluon density is larger at small x (see figure 38). The Altarelli-Parisi equation simplifies to

$$\frac{d}{dt}g(x,t) = \frac{\alpha_s}{2\pi}\int_x^1 \frac{dy}{y} g(y,t) P_{gg}\left(\frac{x}{y}\right). \tag{3.55}$$

Furthermore $P_{gg}(x)$ may be approximated by

$$P_{gg}(x) = \frac{6}{x} \tag{3.56}$$

Eqn. (3.55) can be recast as

$$-x\frac{d^2(xg(x,t))}{dxdlogt} = \frac{12}{b} xg(x,t) \tag{3.57}$$

Here I have eliminated $\alpha_s(q^2)$ using eqn (3.11). Eqn (3.57) can be solved to give

$$xg(x,Q^2) \propto exp\left(\sqrt{\frac{48}{b} log(1/x) loglog(Q^2)}\right) \tag{3.58}$$

The growth of this at small x is very rapid. It is eventually cut off when the Altarelli-Parisi equations break down. We can estimate the position of this breakdown as follows. The Altarelli Parisi equations describe the growth of incoherent parton showers: the shower initiated by one parton is independent of that of the other partons. This assumption must eventually break down. Let us view the proton in a frame where is moving extremely fast, the appropriate frame for the parton picture. The proton looks like a pancake with area $1/m_\pi^2$. Viewed on a scale Q^2 it contains a set of partons each of size $1/Q$. The fractional area occupied by partons is[82]

$$\frac{xg(x,Q^2)m_\pi^2}{Q^2}. \tag{3.59}$$

Provided this fraction is small the partons are not densely packed and the incoherent approximation is correct. If the fraction is of order one, the incoherent approximation breaks down and the growth of $g(x,Q^2)$ is cut off. The growth of $g(x,Q^2)$ has some important implications which I will discuss below.

A vital property of QCD is that the distribution functions defined by (3.54) are universal. In order to illustrate this, consider the Drell-Yan process in proton-proton collisions. In the naive parton model, the cross-section for the production of a

$\mu^+\mu^-$ pair of invariant mass M in a proton-proton collision with total center-of-mass energy $\sqrt{s}$ is given by

$$\frac{d\sigma}{dM^2} = \frac{4\pi\alpha_{em}^2}{9M^2 s}\int dx_1 dx_2 [\sum_i q_i(x_1)\bar{q}_i(x_2)e_i^2\delta(x_1x_2 - M^2/s) + (1 \Leftrightarrow 2)] \qquad (3.60)$$

Here $\bar{q}$ is an antiquark distribution. The fundamental process is quark-antiquark annihilation into $\mu^+\mu^-$. Consider the corrections to this at order α_s. As in the case of ep scattering these can involve either virtual or real gluons (see Fig. 39). These corrections modify Eq. (3.60), *viz.*,

$$\begin{aligned}\frac{d\sigma}{dM^2} &= \frac{4\pi\alpha_{em}^2}{9M^2 s}\int \frac{dx_1}{x_1}\frac{dx_2}{x_2}\Big[[e_i^2 q_i(x_1)\bar{q}_i(x_2) + (1 \Leftrightarrow 2)] \\ &\Big[\delta(1-z) + \theta(1-z)\frac{\alpha_s}{2\pi}[2P_{qq}(z)t + f'(z)]\Big] \\ &+ [\sum_i e_i^2(q_i(x_1) + \bar{q}_i(x_1))G(x_2) + (1 \Leftrightarrow 2)] \\ &[\theta(1-z)\frac{\alpha_s}{2\pi}[P_{qg}(z) + f''(z)] \qquad (3.61)\end{aligned}$$

where $z = M^2/(sx_1x_2)$.[83] The last part of the expression arises from the process $g + q \rightarrow \mu^+\mu^- + q$.

If we replace $q(x)$ by $q(x,t)$ defined by Eq. (3.54) then the resulting expression will have no t's appearing explicitly, *viz.*,

$$\frac{d\sigma}{dM^2} = \frac{4\pi\alpha_{em}^2}{9M^2 s}\int dx_1 dx_2 [e_i^2 q_i(x_1,t)\bar{q}_i(x_2,t)\delta(x_1x_2 - M^2/s) + (1 \Leftrightarrow 2) + \mathcal{O}(\alpha_s(Q^2))] \qquad (3.62)$$

where the order $\alpha_s(Q^2)$ terms contain no powers of t. This absorption of the singular terms into $q(x,t)$ is known as factorization; it is a universal property which guarantees that hard processes can be reliably calculated in perturbative QCD and that the same set of structure functions should be used for all processes.[84]

I would now like to discuss some of the characteristics of W and Z production at hadron colliders. The total cross-section is given by the annihilation of quark-antiquark pairs. (c.f. eqn. 3.60)

$$\sigma_{W^+} = \frac{G_F\pi\sqrt{2}M_W^2}{3s}\int_\tau^1 \frac{dx}{x}[f_u(x,M_W^2)f_{\bar{d}}(\tau/x,M_W^2) + f_{\bar{d}}(x,M_W^2)f_u(\tau/x,M_W^2] \qquad (3.63)$$

with $\tau = M_W^2/s$; I have set the Cabbibo angle to zero and only included the up and down quarks. The complete formula is a trivial extension of that given. This process has higher order QCD corrections identical to those discussed above in the case of the Drell-Yan production of μ pairs (see eqn 3.61). One has so far not been able to

detect the W or Z via its decay into quark antiquark pairs, and hence hadronic jets, because of the large background from the production of jets via the QCD processes discussed above. This issue is discussed in some detail by Di Lella.[2] Hence the data give us the product of the production cross-section and the branching ratio into e^+e^- for the Z and $e\nu$ for the W. These measurements are consistent with those expected from eqn. 3.63 particularly when the order α_s corrections are included.[85]

In the process of eqn. 3.63 the W is produced with no transverse momentum. At next order in α_s the W can be produced in association with a gluon. This will produce a W with transverse momentum which is balanced by a gluon jet. The cross-section for such production can be written as[86]

$$\frac{d\sigma}{dp_t dy} = 2p_t \int_{x_{min}}^{1} dx \frac{u(x, M_W^2)\bar{d}(x_1, M_W^2)\sigma(\hat{s}, \hat{t}, \hat{u})}{xs + u - M_W^2} \tag{3.64}$$

with

$$\begin{aligned} x_1 &= \frac{-xt - (1-x)M_W^2}{xs + u - M_W^2} \\ x_{min} &= -u/(s + t - M_W^2) \\ \sigma(s,t,u) &= \frac{2\pi\alpha_{em}\alpha_s}{9sin^2\theta_W} \frac{s^2 + u^2 + 2M_W^2 t}{-s^2 u} + (t \leftrightarrow u). \end{aligned} \tag{3.65}$$

Here the hatted variables apply to the partons and the unhatted to the hadrons. The W is produced with transverse momentum p_t and rapidity y.

If we integrate over y the formula of eqn 3.64 will contain a term proportional to $log(p_t/M_W)$. It is possible for this logarithm to become large at reasonable values of p_t. Since the next order in α_s will contain $log^2(p_t/M_W)$, it is possible for $\alpha_s log(p_t/M_W)$ to be of order one. In this case we must resum these multiple gluon emissions to all orders in α_s.[87] If we consider the partonic process $q + overline eq \rightarrow W + g$ and compare it with the lowest order process $q + \bar{q} \rightarrow W$ we must integrate over the three momentum of the gluon. Writing the three momentum of the gluon $p_{gluon} = (p_t, xp_w)$, where p_w is the momentum of the W at lowest order and p_t is the transverse momentum of the gluon (or W) with respect to the $q\bar{q}$ direction, we have a contribution proportional to

$$\int \frac{dp_{p_t}^2}{p_t^2} \frac{2\alpha_s}{3\pi} \int dx \frac{1 + x^2}{1 - x}. \tag{3.66}$$

At small p_t we can integrate over x and obtain

$$\frac{d\sigma}{dp_t^2} = \sigma_{LO}(\delta(p_t^2) + \frac{2\alpha_s log(M_W^2/p_t^2)}{3\pi p_t^2}). \tag{3.67}$$

Here σ_{LO} is the cross-section for $q = \bar{q} \rightarrow W$. Similarly the contribution from the n gluon state is given by

$$\frac{1}{n!}\prod_{i=1}^{n}\int \frac{d^2p_{t_i}}{p_{t_i}^2}\frac{4\alpha_s}{3\pi} log(M_W^2/p_{t_i}^2)\delta(p_{t_W} - \sum_1^n p_{t_i}) \tag{3.68}$$

The sum over n is complicated by the presence of the δ-function. This can be solved by performing a fourier transform into impact parameter space.

$$\delta(p_{t_W} - \sum_1^n p_{t_i}) = \frac{1}{2\pi^2}\int d^2b e^{ib(p_{t_W} - \sum_1^n p_{t_i})}. \tag{3.69}$$

The summation on n is now straightforward and equation 3.63 becomes

$$\begin{aligned}\frac{d\sigma_{W+}}{dp_{t_W}^2} = \frac{G_F\pi\sqrt{2}M_W^2}{3s}\int_\tau^1 \frac{dx}{x} \\ \int \frac{bdb}{2\pi}e^{-ibp_{t_W}} exp(\int dk^2(J_0(bk)-1)\frac{2\alpha_s(k^2)}{3\pi}\frac{log(M_W^2/k^2)}{k^2}) \\ [f_u(x,1/b^2)f_{\bar{d}}(\tau/x,1/b^2) + f_{\bar{d}}(x,1/b^2)f_u(\tau/x,1/b^2)].\end{aligned} \tag{3.70}$$

This formula applies when $p_{t_W} << M_W$. It is possible to modify this so that it matches smoothly with eqn 3.64.[88] If this is done the result is in remarkable agreement with the transverse momentum of W's observed at CERN.[89]

Jets of hadrons can be produced in hadron-hadron scattering via the scattering of quarks and gluons present inside the hadrons. These quarks and gluons emerge at wide angle and then hadronize into jets of hadrons. The lowest order QCD processes involve $2 \rightarrow 2$ scattering and hence yield a final state of two jets whose transverse momenta balance. The differential cross section for the production of a two jets with rapidities y_1 and y_2 and transverse momentum p_t in the center-of-mass frame of the pp system is given by

$$\begin{aligned}\frac{d\sigma}{dy_1dy_2dp_t} = \frac{2\pi\tau}{\hat{s}}p_t\sum_{i,j}[f_i^a(x_a,M^2)f_j^b(x_b,M^2)\hat{\sigma_{ij}}(\hat{s},\hat{t},\hat{u}) \\ + f_j^a(x_a,M^2)f_i^b(x_b,M^2)\hat{\sigma_{ij}}(\hat{s},\hat{u},\hat{t})]/(1+\delta_{i,j})\end{aligned} \tag{3.71}$$

Here $\hat{s}, \hat{t}$ and $\hat{u}$ are the Mandelstam variables for the $2 \rightarrow 2$ partonic scattering. The various partonic subprocess have the following differential cross sections:-

$$\begin{aligned}\sigma(gg \rightarrow gg) &= \frac{9\alpha_s^2}{2s}[3 - \frac{tu}{s^2} - \frac{su}{t^2} - \frac{st}{u^2}] \\ \sigma(q_iq_j \rightarrow q_iq_j) &= \frac{4\alpha_s^2}{9s}\frac{s^2+u^2}{t^2}\end{aligned}$$

$$
\begin{aligned}
\sigma(q_i\overline{q_i} \to \overline{q_j}q_j) &= \frac{4\alpha_s^2}{9s}[\frac{t^2+u^2}{s^2}] \\
\sigma(gq \to gq) &= \frac{\alpha_s^2(s^2+u^2)}{s}[\frac{1}{t^2} - \frac{4}{9su}] \\
\sigma(gg \to q_i\overline{q_i}) &= \frac{3\alpha_s^2(t^2+u^2)}{8s}[\frac{4}{9tu} - \frac{1}{s^2}] \\
\sigma(q_i\overline{q_i} \to \overline{q_i}q_i) &= \frac{4\alpha_s^2}{9s}[\frac{s^2+u^2}{t^2} + \frac{s^2+t^2}{u^2} - \frac{2u^2}{st}] \\
\sigma(q_i\overline{q_i} \to gg) &= \frac{8\alpha_s^2(t^2+u^2)}{3s}[\frac{4}{9tu} - \frac{1}{s^2}]
\end{aligned}
\tag{3.72}
$$

Figure 40 shows the differential cross section predicted by these formulae and compares it with data from the UA1 and UA2 collaborations.[90,91] It can be seen from this figure that at low values of p_t, the jets are dominantly produced from the fragmentation of gluons. This effect has two causes, the parton cross sections with gluons tend to be larger than those with quarks (see eqn (3.72)), and, at low values of x, gluons are more numerous inside the proton (see figure 38).

Figure 41 shows the total cross section for the production of a pair of jets with total transverse energy greater than $E_{t_{min}}$ and rapidity $|y| < 2.5$. At fixed $E_{t_{min}}$, this cross section rises rapidly with $\sqrt{s}$. This rapid rise is a consequence of the rapid growth in the structure functions at small x which was discussed above (see eqn. (3.58)). The total cross section at $\sqrt{s} = 540GeV$ is of order $50nb$ so that the fraction explicable in terms of perturbative QCD is very small. However, the total cross-section in pp or $p\overline{p}$ collisions is rising like $log^2(s)$ which implies that as s rises a larger fraction of the total cross section is explicable by perturbative QCD. Indeed it has bees suggested that the rise in the total cross section may all due to this larger jet rate.[92]

Three jet events can occur at the next order in α_s. As in the case of e^+e^- annihilation the ratio #(3-jets)/#(2-jets) depends upon the jet definition. Two jets with a very small angle between them may fail to be resolved either because the detector has too poor an angular resolution or because the hadronization spreads them so that they overlap. There are some differences with the e^+e^- case. Firstly, collinear divergences in the three-jet cross section can occur not only when two of the outgoing jets are collinear with each other but also when one of the jets is emitted in the forward direction. Emissions of this type result in jets which are lost in the beam fragments; it is emission of this type which is responsible for the evolution of the structure functions (see eqn 3.52). Secondly, soft emissions which gave rise to a divergence in the e^+e- case are not so important here. This is because the energy of the intial state of the two partons which scatter is not known experimentally and is integrated over in the expression (3.71).

I would now like to discuss some of the errors and uncertainties present in predictions of the rate for QCD processes in hadron-hadron collisions. I will discuss the production of new heavy quarks. A similar discussion applies to most other processes. The relevant QCD processes for the production of a $Q\bar{Q}$ pair are $gg \to Q\bar{Q}$ or $\bar{q}q \to Q\bar{Q}$. The cross-sections are given by[93]

$$\frac{d\sigma}{dt}(gg \to Q\bar{Q}) = \frac{\pi\alpha_s^2(Q^2)}{8s^2}\left\{\frac{6}{s^2}(t-M_Q^2)(u-M_Q^2) + \left[\left(\frac{4}{3}\frac{(t-M_Q^2)(u-M_Q^2)-2M_Q^2(t+M_Q^2)}{(t-M_Q^2)^2}\right.\right.\right.$$
$$\left.\left.\left. + \frac{3(t-M_Q^2)(u-M_Q^2)+M_Q^2(u-t)}{s(t-M_Q^2)}\right) + [t \leftrightarrow u]\right]\right.$$
$$\left. - \frac{M_Q^2(s-4M_Q^2)}{3(t-M_Q^2)(u-M_Q^2)}\right\} \tag{3.73}$$

and

$$\frac{d\sigma}{dt}(q\bar{q} \to q\bar{q}) = \frac{\pi\alpha_s^2(Q^2)}{9s^2}\left[\frac{(t-M_Q^2)^2+(u-M_Q^2)^2+2M_Q^2}{s^2}\right] \tag{3.74}$$

Here s,t and u are the usual Mandelstam variables. The rate for $pp \to Q\bar{Q}+$ *anything* when the quark emerges with transverse momentum $p_\perp$ at angle θ to the beam in the center-of-mass frame of the pp system is given by

$$E\frac{d\sigma}{d^3p} = \frac{1}{\pi}\sum_{ij}\int_{x_{min}}^1 \frac{dx_a}{x_a - x_\perp\left[\frac{\chi+\cos\theta}{2\sin\theta}\right]} x_a x_b f_i(x_a,Q^2) f_j(x_b,Q^2)\frac{d\sigma}{d\hat{t}}(\hat{s},\hat{t},\hat{u}) \tag{3.75}$$

with

$$\hat{s} = x_a x_b s$$
$$\hat{t} = M_Q^2 - x_a x_\perp s\left[\frac{\chi-\cos\theta}{2\sin\theta}\right]$$
$$\hat{u} = M_Q^2 - x_b x_\perp s\left[\frac{\chi+\cos\theta}{2\sin\theta}\right]$$

and

$$x_b = \frac{x_a x_\perp s(\chi-\cos\theta)}{s\sin\theta\left(2x_a - x_\perp\left[\frac{\chi+\cos\theta}{2\sin\theta}\right]\right)} \tag{3.76}$$
$$x_{min} = \frac{x_\perp(\chi+\cos\theta)}{s\sin\theta\left(2 - x_\perp\left[\frac{\chi-\cos\theta}{2\sin\theta}\right]\right)}$$
$$\chi = \left(1 + \frac{4M_Q^2\sin^2\theta}{x_\perp^2 s}\right)^{1/2}$$
$$x_\perp = 2p_\perp/\sqrt{s}$$

In order to use this formula we must; fix the structure functions; determine the scale Q^2 appearing in the structure functions; fix the scale appearing in α_s; and define the quark mass. Let us discuss these problems in turn.

The structure functions are extracted at low Q^2 from the scattering of electrons or neutrinos off hadronic targets. These processes can only measure the quark structure functions directly since the gluons have no electroweak interactions. The gluon distributions must be inferred from the Q^2 dependence of the quark distribution (see Eq. (3.54)). This implies that there is a correlation between $g(x)$ and the value of α_s which controls the Q^2 dependence.

For processes at hadron colliders, the required values of Q^2 are larger than those at which the distribution functions are measured; most electron and neutrino scattering experiments have most of their statistics for $Q^2 < 10\ GeV^2$. The distribution functions are then evolved up to larger Q^2 using QCD. In this evolution some of the uncertainties tend to wash out. This is illustrated in Fig. 38 which compares two sets of structure functions at different Q^2.[94,95]

In the case of $Q\bar{Q}$ production, the rate from gluon-gluon collisions dominates. There are two reasons for this: the gluon distribution is larger than that for quarks at small x (see Fig. 38) and the process $gg \to Q\bar{Q}$ has a larger rate than $q\bar{q} \to Q\bar{Q}$ due to the higher color charge of the gluon. If, however, in $p\bar{p}$ collisions, we produce quarks of very large mass, the appropriate values of x_a and x_b (see Eq. (3.75)) can become large and we are forced into a region where $g(x) < q(x)$ so that the quark antiquark annihilations can dominate. Notice that at these large values of x the distribution functions and hence the cross-sections are small.

Other data from hadron-hadron collisions can be used to check that the gluon distributions are reasonable. For example, jet production occurs via the processes $qq \to qq, gg \to gg, qg \to qg$, etc. If the measured jet cross-sections are in good agreement with the predicted values, we can have confidence that the distribution functions are reasonable. Such a comparison is shown in Fig. 40. Data from the Sp$\bar{p}$S collider[90,91] are compared with a prediction using distribution functions extracted from the CDHS neutrino scattering experiment,[94] which were then extrapolated using QCD.[65] Such good agreement leads us to believe that the distribution functions are reliable at the 30% level.

I will now turn to the question of the scale Q^2 appearing in $\alpha_s(Q^2)$ (Eq. 3.75 and 3.76) and in the distribution functions. Suppose we shift the scale in $\alpha_s(M^2)$

$$\alpha_s(xM^2) = \alpha_s(M^2)\left[1 + \frac{(33-2n_f)}{12\pi}\alpha_s(M^2)\log x + \mathcal{O}(\alpha^2)\right] \qquad (3.77)$$

It is therefore clear that we cannot decide the question of scale without computing the order α_s^3 in Eqs. (3.75) and (3.76). A bad choice of scale is likely to result in large α_s^3 corrections. In the absence of such corrections we can only guess what the

scale should be. Common sense dictates that it should be of order the quark mass M_Q. However, if the quark is being produced at large transverse momenta ($p_\perp$), then something like $\sqrt{M_Q^2 + p_\perp^2}$ is probably appropriate.

To claim that the value of M_Q introduces an ambiguity may seem absurd. But suppose we are calculating the production rate for charm or bottom quarks; we must decide what value to use. The total production cross-section is a very strong function of M_Q, it varies roughly as M_Q^{-4}. What value of the charm quark mass should be used? This question is not easy to answer. The threshold for $c\bar{c}$ production opens when there is sufficient energy in the partonic collisions to produce a $D\bar{D}$ meson pair. This could suggest that one should use $M_Q = M_D$. However, the quark mass which appears in other calculations, such as that for the energy levels of the ψ system, is usually less than this. The uncertainty induced by M_Q becomes irrelevant for quarks heavier than the b.

Figure 42 shows the total cross-section for the production of charmed quark pairs at small values of $\sqrt{s}$. This figure illustrates the longstanding problem of charm production rates. Cross-sections measured at the ISR[96] ($\sqrt{s} \approx 50\ GeV$) usually gave rates which are approximately a factor of 10 larger than QCD expectations. Measurements of $\sqrt{s} \approx 25\ GeV$[97] using protons on a stationary target gave results which were closer to QCD expectations. New results at $\sqrt{s} = 43\ GeV$[98] are also close to the QCD values. The ISR experiments had poor acceptance and it is now difficult to reconcile their large values with those obtained at $\sqrt{s} = 43\ GeV$. It seems fair to conclude that the QCD model works reasonably well[99], and while there may be some need to invoke new mechanisms to explain the rapidity distribution[100] of the produced charmed particles, no drastic modifications are required.

The cross section for heavy quark production at the $Sp\bar{p}S$ colliders is shown in figure 43. If we consider the detection of heavy quarks we can be forced into a kinematical regime where the production cross section is not described by the pair production processes. The mean value of the transverse momenta of the quarks produced by the mechanisms discussed above is of order the quark mass, which can be seen from figure 44. If detection considerations force us to look only at new quarks which are produced at transverse momenta which are much larger than this, then other mechanisms can become more important.[101]

Figure 45 shows a mechanism whereby a pair of quarks are emitted at large transverse momentum which is balanced by the emission of a gluon. This process is more important at large transverse momentum than the pair production processes discussed above in which the transverse momenta of the new particles balance each other. This result is surprising but can be easily understood. The cross-section for $gg \rightarrow gg$ is larger by about a factor of 200 than the corresponding process $gg \rightarrow q\bar{q}$ if both are evaluated at 90 degrees in the center of mass frame (compare the terms in eqn. 3.72). In the former process the gluon can 'decay' into a quark-antiquark

pair at the cost of a factor of order α_s/π. Provided that the transverse momentum of the gluon is much larger than the quark mass, there is no substantial phase space inhibition of this 'decay', and so it can dominate the direct pair production.

Another problem can arise if the quark mass is very small. Integrating eqn. 3.76 over t gives

$$\sigma(gg \to Q\overline{Q}) = \frac{\pi\alpha_s^2}{3\hat{s}}[-(7 + \frac{31m_Q^2}{\hat{s}})\frac{\chi}{4} \\ (1 + \frac{4m_Q^2}{\hat{s}} + \frac{m_Q^4}{\hat{s}^2})log(\frac{1+\chi}{1-\chi})] \qquad (3.78)$$

where $\chi = \sqrt{(1 - 4m_Q^2/\hat{s})}$. In the limit that $m_Q^2/\hat{s}$ is very small this expression contains a term proportional to $log(\hat{s}/m_Q^2)$. If we were to calculate to next order in perturbation theory we would encounter a term of order $\alpha_s^3 log^2(\hat{s}/m_Q^2)$ which is not small compared with the term already computed. The expansion of the cross-section as a series in α_s is no longer reliable. In this case these logarithms must be resummed to all orders in α_s. The resumming is precisely what is accomplished by the Altarelli-Parisi equations. These new quarks start to appear as partons inside the proton. It is important to realise that this does not mean that an extra source of heavy quarks is available from the scattering of one of the partons off a gluon from the other beam.[102] Since the structure functions fall so rapidly with x most of the rate for heavy quark production comes from regions where $log(m_Q^2/\hat{s})$ is not large, so that this problem is not important in practice.

4. The inadequacy of the standard model.

In the previous sections I have discussed some aspects of the standard model. Despite the lack of experimental data which fails to agree with this model, most theorists find it unsatisfactory. One of the troubling features of this model is the origin of the electroweak scale. The origin of the scale of strong interactions, either Λ or the proton mass, can be understood qualitatively as follows. In the context of any unified theory, either a conventional grand unified theory or a more exotic one based on superstrings, all the gauge coupling constants of the standard model are related at some large scale M where the theory is unified. Qualitatively,

$$\alpha_{em}(M^2) \approx \alpha_s(M^2) \qquad (4.1)$$

M is of order the Planck mass ($M_P = 10^{19}\ GeV$), or possibly less ($\sim 10^{15}\ GeV$) in some models. At some scale Q_0, $\alpha_s(Q_0)$ will become large and QCD perturbation theory will no longer be valid. At this scale non-perturbative effects will become important and hadronic bound states will form with mass of order Q_0. Requiring $\alpha(Q_0) = 1$ implies that

$$Q_0^2 \simeq M^2 exp\left[\frac{(33 - 2n_f)}{12\pi}\left[1 - \frac{1}{\alpha(M^2)}\right]\right] \qquad (4.2)$$

It is easy to see that for $\alpha(M^2) \approx 1/40$, $Q_0/M \approx 10^{-15}$ and the large hierarchy of scales between hadron masses and M can be explained. The presence of the exponential in Eq. (4.2) guarantees that the large ratio M/Q_0 will be generated.

A similar argument cannot be used to explain the small ratio M_W/M_P. There is a dimensionful parameter μ in the $SU(2) \times U(1)$ Lagrangian, which is chosen to have a value of order M_W. Consider a radiative correction to this mass term due to the $\lambda(\Phi^+\Phi)$ interaction (see Fig. 46)

$$\delta m^2 = i\lambda \int \frac{d^4k}{(2\pi)^4} \frac{1}{(k^2 - \mu^2)} \tag{4.3}$$

This integral is quadratically divergent: cut it off at scale Λ. Then the value of μ^2 computed at one loop is given by

$$\mu^2_{1loop} = \mu^2 + \lambda\Lambda^2 \tag{4.4}$$

In theories such as those described by M. Green and M. Peskin[103] in their lectures, new physics enters at the Planck mass and cuts off the divergence. In this case Λ is of order 10^{19} GeV. μ^2_{1loop} must be of order M_W^2, so that Eq. (4.4) implies that the bare mass μ must be adjusted to some 18 significant figures. This fine tuning must take place at all orders in perturbation theory. This unnatural fine tuning is usually referred to as the hierarchy problem and is present in theories with quadratic divergences.

This hierarchy problem can be solved in theories where the quadratic divergences are ameliorated on scales of order M_W . Since these divergences are associated with scalar fields,[104] the scalar sector of the theory must be modified.

One strategy is to introduce some new fields which cancel the divergence. Consider the following toy model consisting of a scalar field ϕ and a (two-component) fermion ψ.

$$\mathcal{L} = \partial_\mu\phi^+\partial_\mu\phi - m_s^2\Phi^+\Phi - \bar{\psi}(i\not{\partial} - m_f)\psi + \lambda_1\phi^4 + \lambda_2\bar{\psi}\psi\phi \tag{4.5}$$

In this theory, there are two one-loop diagrams contributing to the one-loop calculation of the scalar mass (see Figs. 46 and 47). The scalar loop gives

$$\delta m^2_{s_1} = i\lambda_1 \int \frac{d^4k}{(2\pi)^4} \frac{1}{(k^2 - m_s)^2} \tag{4.6}$$

and the fermion loop,

$$\delta m^2_{s_2} = \frac{-i\lambda_2^2}{4} \int \frac{d^4k}{(2\pi)^4} \mathrm{Tr}\left(\frac{1}{(k - m_f)(k + m_f)}\right) \tag{4.7}$$

The quadratic divergence is removed if $\lambda_2 = \lambda_1$ with the result

$$\delta m^2 = \lambda_1(m_f^2 - m_s^2) + \text{log divergence}$$

The soft logarithmic divergence is no problem, so the hierarchy problem is solved if $m_f^2 - m_s^2 \approx 0(M_W^2)$. This toy model is a supersymmetric theory in which the supersymmetry is softly broken (via $m_s \neq m_f$). Supersymmetric extensions of the standard model will have this property and so solve the hierarchy problem. Notice that this argument implies that the mass of the new particle predicted by these models must be less than 1 TeV or so. Supersymmetric theories are no help if the the new particles have masses of order the Planck Mass. I shall not discuss the phenomenology of supersymmetric models in these lectures. The reader may consult one of the recent review articles.[105]

Another solution to the hierarchy problem involves the introduction of a new interaction. If the Higgs boson were not elementary but were a bound state of a fermion and an antifermion with binding energy Λ, then the loop integral of Eq. (4.3) will be modified when $k \gtrsim 0(\Lambda)$. If there are no fundamental scalars, only bound states constructed from fermions, the bad divergences associated with elementary scalars will be removed.

The simplest implementation of this idea is in the technicolor theories.[106] I will sketch the basic mechanism here; one of the many review articles can be consulted for more details. Suppose we have a non-abelian gauge theory (called technicolor) with two flavors of fermion call U and D which transform as a doublet with respect to $SU(2)_L$ (cf., QCD with two flavors, up and down). If these fermions are massless, the underlying theory has a chiral symmetry $SU(2)_L \times SU(2)_R \times U(1)$. When the theory confines the chiral symmetry may break spontaneously via the formation of condensates $\left\langle \bar{U}U \right\rangle, \left\langle \bar{D}D \right\rangle \neq 0$. The symmetry will break to $SU(2) \times U(1)$ resulting in the appearance of three Goldstone bosons (these are analogous to the pions of QCD which would be massless in the absence of bare quark masses). Since the U and D form a doublet of $SU(2)_L$ then the W boson can couple to $U\bar{D}$ and hence to the "pion". The graph of Fig. 48 will generate a self energy for the W viz.,

$$\Pi_{\mu\nu} = \frac{g_2^2}{4}(k^2 g_{\mu\nu} - k_\mu k_\nu)\Pi(k^2) \tag{4.8}$$

where $\Pi(k^2)$ represents the $U\bar{D}$ bound state.

If there are no Higgs fields then the W is massless and its propagator (calculated to lowest order in g_2) is

$$\frac{g^{\mu\nu} - k^\mu k^\nu / k^2}{k^2} \tag{4.9}$$

The effect of $\Pi^{\mu\nu}$ is to modify the propagator thus:

$$\frac{g^{\mu\nu} - k^\mu k^\nu / k^2}{k^2\left[1 + \frac{g_2^2}{4}\Pi(k^2)\right]} \tag{4.10}$$

Since the lowest lying $U\bar{D}$ bound state is massless $\Pi(k^2) = f_\pi/k^2$ as $k^2 \to 0$. Hence (4.10) has no pole at $k^2 = 0$ but instead acquires a pole at $M_W^2 = \frac{g_2^2}{4} f_\pi^2$. The "pion" is eaten and becomes the extra polarization state of the massive W boson. If this mechanism is to yield the correct value for M_W, then we need $f_\pi \approx 250\ GeV$. The neutral pions cause mixing between the "W_3" (i.e., the $I_3 = 0$ member of the $SU(2)_L$ gauge boson multiplet) and B, the gauge boson of $U(1)_y$. The couplings of "π^0" to B and W_3 are determined by the weak charges of the U and D quarks. The resulting mass matrix has the following form:

$$\frac{f_\pi^2}{4} \begin{pmatrix} g_2^2 & g_2 g_1 \\ g_2 g_1 & g_1^2 \end{pmatrix} \tag{4.11}$$

This has one zero eigenvalue corresponding to the photon and one non-zero with mass

$$M_Z^2 = \left(\frac{g_1^2 + g_2^2}{4} \right) f_\pi^2 = \frac{M_W^2 (g_1^2 + g_2^2)}{g_2^2} \tag{4.12}$$

Notice that this corresponds to $\rho = 1$ (see Eq.(1.27)). This theory possesses a custodial $SU(2)$ symmetry since there is a chiral symmetry $SU(2)_L \times SU(2)_R \times U(1)$ which breaks to $SU(2) \times U(1)$ in the binding.

Such a theory can be expected to have more states than are present in the Weinberg-Salam model. For example, there will be spin-1 bound states $U\bar{D}, D\bar{U}, U\bar{U} + D\bar{D}, U\bar{U} - D\bar{D}$ analogous to the ρ and ω mesons in QCD. These will have mass of order a few times f_π and will decay to WW, WZ and ZZ (recall that $\rho \to 2\pi$ in QCD and that the "π" in this technicolor theory has been absorbed into the W and Z). One should also get technibaryons made from UUU, etc.

This simple technicolor theory which I have described cannot explain quark and lepton masses. The electron mass arises in the Weinberg-Salam model from the coupling

$$\lambda \Phi \psi_L \psi_R \tag{4.13}$$

which generates $m_e = \lambda \langle \Phi \rangle$. The analogous term in a technicolor theory would be

$$\bar{U}_L U_R \bar{\psi}_L \psi_R \tag{4.14}$$

Such a term is non-renormalizable and is not allowed. The problem is solved by introducing yet another set of interactions which have massive gauge bosons. These bosons mediate interactions between the quarks and techniquarks. The interaction (4.14) then arises as the low energy limit of this theory,[107,108] in the same way that the Fermi-interaction arises as a low energy limit of the Weinberg-Salam model. Such extended technicolor theories have a rich phenomenology which is discussed in detail in review articles to which the reader is referred.[106]

I shall discuss one other variant of the standard model — the idea that quarks and leptons may be composite. This idea is rather unfashionable.[109] It implies that there

must be another fundamental scale in physics, that on which the forces responsible for the binding of quarks and leptons are strong. This would be one other scale for theorists to explain. However, experimentalists should be aware that this option exists. Historically it has been the correct route, the chain being molecules, atoms, nuclei, quarks. It is also a natural extension of technicolor models where only the scalars are composite.

Fortunately, it is possible to analyze the phenomenological consequences of compositeness without reference to a specific model. This is done by placing phenomenological constraints on the possible effective operators[110] which involve quarks and leptons and which an arise as a result of the interactions which are responsible for the binding.

The various new particles predicted by these variants of the standard model can be searched for at the new colliders. Rather than go through a detailed analysis of all the options I shall make some general comments. Any new particle with electroweak interactions can be produced in pairs from the decay of a Z produced at LEP or the SLC. The signal to noise ratio is likely to be good since the production is democratic. It will be difficult to miss such new particles with mass less than 40 GeV. Conversely, if a new particle has strong interactions only, it cannot be produced directly. This makes e^+e^- machines a very poor place to look for the gluino (a particle predicted by supersymmetric models, it is the partner of the gluon and has spin 1/2).

In a hadron collider the situation is more complicated. First consider particles without strong interactions. It may be possible to produce such particles singly from the annihilation of quark-antiquark pairs in the same manner as the Z and W. Figure 49 shows the production cross-section for a new Z boson in $p\overline{p}$ interactions. I have assumed that the couplings are the same as those for a standard model Z. It can be seen that the Tevatron will be sensitive to masses of order 250 GeV provided that new Z decays into a clean channel (e.g. e^+e^-) with a branching ratio of at least a few percent.

If a particle has only electroweak interactions and must be produced in pairs the situation is worse. Not only is the phase space restricted but an additional power of the weak coupling appears in cross-section. As an example, figure 50 show the rate for the production of a pair of charged heavy leptons. The production rate which is given by quark-antiquark annihilation via a virtual photon or Z, is very small. For a light lepton the dominant source is likely to be the production and decay of a Z. In this case the rate is given by the production rate of a Z (6 nb at $\sqrt{s} = 2$ TeV), multiplied by the branching ratio for the decay $Z \rightarrow L^+L^-$. The UA1 collaboration has been able to place a limit of order 40 GeV on the mass of a new heavy lepton produced in association with a massless neutrino from the decay of a W.[111] It should be remarked that these comments concerning particles without strong interactions only apply to low luminosity hadron machines. The proposed SSC will be able to

produce such particles because of its much larger luminosity.

A particle with strong interactions is produced copiously in a hadron collider since it can be made in pairs via gluon-gluon collisions. Typical rates have already been shown (see figure 43). The UA1 collaboration has been able to set limits on gluinos (the supersymmetric partner of a gluon) of mass less than 70 GEV from their failure to observe exotic events.[112] We can expect the Tevatron to be sensitive to masses of order 150 GeV for these particles.

In an *ep* collider new particles with strong and electroweak interactions are produced via the collision of a gluon from the proton and a photon radiated off the electron line. An example is shown in figure 51 which shows the rate for the production of a pair of heavy quarks. The decay signature is the same as in hadron-hadron collisions, i.e. the semileptonic decay to a b quark, which will give rise to jets and isolated leptons, or to the b quark and a W if the mass is large enough. The background may be less severe that in a hadron collider, nevertheless it is clear that HERA is not likely to be competitive with the Tevatron. There are some special cases where *ep* collisions may have an advantage. Consider the production of a squark (the supersymmetric partner of a quark) and a selectron. This can proceed via the graph shown in figure 52, where we can exchange the photino, $\tilde{\gamma}$, or a Zino (the partner of the Z). If we assume that the exchanged particle is a massless photino (the partner of the photon), the rate is shown in figure 53. In order to compare notice that masses of less than 40 GeV can be seen at the SLC or LEP. In addition squark of mass less than 70 GeV have been ruled out by UA1 (subject to some caveats concerning the decay modes).[112] The Tevatron can reach 140 GeV or so. New particle searches at HERA will be very hard indeed. However if something new is seen at the Tevatron or SLC, HERA could be a vital tool in sorting out the origin of the new effect.

Models of composite leptons and quarks have different signatures from other exotic models. This is because the new particles predicted by these theories will have masses of order the composite scale, whereas there will be modifications of the interactions between quarks and leptons which will be visible before the new particles can be produced. In the case of composite electrons, one expects that there will be a four electron operator of the form[110]

$$\begin{aligned} g^{*2}/2\Lambda_*^2 \quad & \left[\eta_{LL}\bar{e}\gamma^u\frac{(1-\gamma_5)}{2}e\bar{e}\gamma^u\frac{(1-\gamma_5)}{2}e\right. \\ & \eta_{RR}\bar{e}\gamma^u\frac{(1+\gamma_5)}{2}e\bar{e}\gamma^u\frac{(1+\gamma_5)}{2}e \\ & \left.2\eta_{LR}\bar{e}\gamma^u\frac{(1-\gamma_5)}{2}e\bar{e}\gamma^u\frac{(1-\gamma_5)}{2}e\right] \end{aligned} \tag{4.15}$$

This term will interfere with the usual one-photon exchange process and cause a

modification of the Bhabha scattering cross-section $e^+e^- \to e^+e^-$, *viz.*,

$$\frac{d\sigma}{d\Omega} = \frac{\pi\alpha^2}{4s}[4A_0 + A_+(1+\cos\theta)^2 + A_-(1-\cos\theta)^2] \tag{4.16}$$

$$A_0 = \left(\frac{s}{t}\right)^2 \left|1 + \frac{g_R g_L}{e^2}\ \frac{t}{t_z} + \frac{\eta_{RL} t}{\alpha\Lambda_*^2}\right|^2, \quad A_- = \left|1 + \frac{g_R g_L}{e^2}\ \frac{s}{s_z} + \frac{\eta_{RL} s}{\alpha\Lambda_*^2}\right|^2$$

$$A_+ = \frac{1}{2}\left|1 + \frac{s}{t} + \frac{g_R^2}{e^2}\left(\frac{s}{s_z} + \frac{s}{t_z}\right) + \frac{2\eta_{RR} s}{\alpha\Lambda_*^2}\right|^2 + \frac{1}{2}\left|1 + \frac{s}{t} + \frac{g_L^2}{e^2}\left(\frac{s}{s_z} + \frac{s}{t_z}\right) + \frac{2\eta_{LL} s}{\alpha\Lambda_*^2}\right|^2$$

Here $t = -s(1-\cos\theta)/2$, $s_z = s - M_z^2 + i\Gamma_z M_z$, $t_z - t - M_z^2 - iM_z M_z$, $g_R = e\tan\theta_w$ and $g_L = -e\cot 2\theta_w$. In this formula I have set $g^{*2} = 4\pi$, a reasonable value for a strongly coupled theory. Current data can be used to set a limit of $\Lambda_* \lesssim 2.5\ TeV$.[113]

In the case of quark compositeness an effect will be seen in the production of jets in a hadron collider since one of the relevant partonic processes is quark-quark scattering. The presence of a four-quark operator of the form (4.15) with a quark replacing an electron will yield a modification of the predicted jet cross-section in hadronic collisions. If we take $\eta_{LR} = \eta_{RR} = 0$ then this interaction leads to a modification of the cross-section for quark-quark scattering

$$\begin{aligned}
\frac{d\sigma}{dt}(q_i q_i \to q_i q_i) &= \frac{4\alpha_s^2}{9s^2}\left[\frac{u^2+s^2}{t^2} + \frac{s^2+t^2}{u^2} - \frac{2}{3}\ \frac{u^2}{st}\right] \\
&\quad + \frac{8\eta_{LL}\alpha_s}{9\Lambda_*^2}\left(\frac{s^2}{t} + \frac{s^2}{u}\right) \\
&\quad + \frac{\eta_{LL}^2}{\Lambda_*^4}\left(u^2 + t^2 + \frac{2s^2}{3}\right) \qquad (4.17) \\
\frac{d\sigma}{dt}(q_i q_j \to q_i q_j) &= \frac{4}{9}\ \frac{\pi\alpha_s^2}{s^2}\left[\frac{u^2+s^2}{t^2} + \frac{9}{4\alpha_s^2}\ \frac{\eta_{LL}^2 u^2}{\Lambda^{*4}}\right]
\end{aligned}$$

Again I have taken $g^{*2} = 4\pi$. It is to be remarked that these effects are not visible in quark-quark scattering until a higher value of s than was the case for Bhabha scattering. This is simply because the dominant contribution to the jet cross-sections arises from gluon-gluon and gluon-quark scattering which are not modified since the gluon is not composite. The effects of compositeness are not visible until s/Λ_*^2 is sufficiently large for the composite effects to raise the quark-quark scattering rates above those for gluon-gluon and gluon-quark. The effect is shown in Fig. 54. Current data from the $Sp\bar{p}S$ collider place a limit of order 450 GeV.[114]

If quarks and leptons share constituents then operators of the type

$$\eta_0 \frac{g_*^2}{4\pi}\bar{q}\gamma^u\frac{(1-\gamma_5)}{2}q\bar{e}\gamma^u\frac{(1-\gamma_5)}{2}e \tag{4.18}$$

The effect of such a term can be seen in two different ways. First, it will affect the production rate for lepton pairs in a hadron-hadron collision. This is controlled by the process $q\bar{q} \to e^+e^-$ for which the cross-section has the form

$$\frac{d\sigma}{dt}(q_i\bar{q}_i \to l^+l^-) = \frac{\pi\alpha^2}{s^2}\left[A_i(s)\left[\frac{u}{s}\right]^2 + B_i(s)\left[\frac{t}{s}\right]^2\right] \tag{4.19}$$

where the quark flavors are i = up, down. The coefficients A_i and B_i may be written as

$$\begin{aligned} A_i(s) &= \left|Q_i - \frac{L_iL_i}{4x_W(1-x_W)}\,\frac{s}{s-M_Z^2+iM_Z\Gamma_Z} - \frac{\eta_0 s}{\alpha\Lambda^{*2}}\right|^2 \\ &+ \left|Q_i - \frac{R_iR_i}{4x_W(1-x_W)}\,\frac{s}{s-M_Z^2+iM_Z\Gamma_Z}\right|^2 \\ B_i(s) &= \left|Q_i - \frac{R_iL_i}{4x_W(1-x_W)}\,\frac{s}{s-M_Z^2+iM_Z\Gamma_Z}\right|^2 \\ &+ \left|Q_i - \frac{L_iR_i}{4x_W(1-x_W)}\,\frac{s}{s-M_Z^2+iM_Z\Gamma_Z}\right|^2 \end{aligned} \tag{4.20}$$

where the chiral couplings of the neutral weak current are, as usual, $L_i = \tau_3 - 2Q_ix_W$ and $R_i = -2Q_ixW$. Here the weak mixing parameter is $x_W = \sin^2\theta_W$ and τ_3 is twice the weak-isospin projection of fermion i.

The cross-sections $d\sigma/dMdy|_{y=0}$ for the reaction

$$p\bar{p} \to l^+l^- + \text{anything}$$

are shown in Fig 55. A contribution of the type (4.18) will also shown up in deep inelastic scattering where it will cause a modification of the proton structure function $F_2(x,Q^2)$. This is discussed in the lectures by Gunter Wolf.[115] The values of Λ which can be probed at HERA are similar to those reached using the Drell-Yan mechanism at the Tevatron collider.

Acknowledgments

The work was supported by the Director, Office of Energy Research, Office of High Energy Physics, Division of High Energy Physics of the U.S. Department of Energy under Contract DE–AC03–76SF00098.

REFERENCES

1 S. Glashow, *Nucl. Phys.* 22:579 (1961);
S. Weinberg, *Phys. Rev. Lett.* 19:1264 (1967);
A. Salam, *in*: "Elementary Particle Theory," W. Svartholm, ed., Almquist and Wiksell, Stockholm (1968).

2 L. Di Lella, lectures at this school.

3 E. Eichten, Lectures at the Yale University TASI summer school,Ed by F. Gursey, World Scientific Publishing Company (1986).

4 Physics at LEP, J. Ellis and R. Peccei, eds., CERN 86-02 (1986).

5 Proceedings of the SSC Workshop, SLAC-PUB-267 (1982).

6 G. 't Hooft and M. Veltman, *Nucl. Phys. B* 44:189 (1972);
C.G. Bollini, J.J. Giambiagi and A. Gonzáles Domínguez, *Nuovo Cim.* 31:551 (1964);
J. Ashmore, *Nuovo Cim. Lett.* 4:289 (1972);
G.N. Cicuta and E. Montaldi, *Nuovo Cim. Lett.* 4:329 (1972).

7 W.A. Bardeen et al., *Phys. Rev. D* 18:3998 (1978).

8 See, for example, J.D. Bjorken and S.D. Drell, "Relativistic Quantum Mechanics," McGraw-Hill (1964).

9 E.R. Williams and P.T. Olsen, *Phys. Rev. Lett.* 62:1575 (1979).

10 W. Marciano, *Phys. Rev. D* 20:276 (1979).

11 A. Sirlin, *Phys. Rev. D* 22:971 (1980).

12 W. Marciano and A. Sirlin, *Phys. Rev. D* 29:945 (1984).

13 Ch. Llewellyn Smith and J. Wheaten, *Phys. Lett. B* 105:486 (1981).

14 G. Arnison et al., *Phys. Lett. B* 166:484 (1986);
J. Appel et al., *Z. Physik C* 30:1 (1986).

15 L. S. Durkin and P. Langacker, *Phys. Lett. B* 166:436 (1986).

16 L. DiLella, *in* "Proceedings of the 1985 International Symposium on Lepton and Photon Interactions at High Energies," Kyoto, Japan (1985).

17 L. A. Ahrens et al., Univ. of Penn. preprint E-734-85-1 (1985).

18 C. Prescott et al., *Phys. Lett. B* 84:524 (1979);
J.E. et al., *Rev. Mod. Phys.* 53:211 (1981).

19 F. Bergsma et al., *Phys. Lett. B* 147:481 (1984);
L.A. Ahrens et al., *Phys. Rev. Lett.* 54:18 (1985).

20 M.A. Bouchiat et al., *Phys. Lett. B* 134:465 (1984);
E.W. Fortson and L.L. Lewis, *Phys. Rep.* 113:289 (1984).

21 H. Abramowicz et. al, *Phys. Rev. Lett.* 57:298 (1986);
J.V. Allaby et al., CERN preprint CERN-EP-86/94 (1986).

22 W. Marciano and A. Sirlin, *Nucl. Phys. B* 189:442 (1981).

23 M.S. Chanowitz, M. Furman and I. Hinchliffe, *Nucl. Phys. B* 153:402 (1979).

24 M. Veltman, *Phys. Lett. B* 70:253 (1977).

25 T. Appelquist and J. Carrazone, *Phys. Rev. D* 11:2856 (1975).

26 S. Weinberg, *Phys. Rev. D* 19:1277 (1979);
L. Susskind, *Phys. Rev. D* 20:2619 (1979).

27 G. Barbiellini et al., in Ref. 4.

28 B. Pifer et al., D0 Design Report.

29 B.W. Lynn, M. Peskin and R.G. Stuart, in Ref. 4.

30 D. Blockus et al., "Proposal for Polarization at the SSC."

31 B.W. Lynn and M. Cvetic, SLAC-PUB-3900 (1986);
F. Gilman and P. Franzini, SLAC-PUB-3932 (1986).

32 F. Wilczek, Lectures at 1983 Erice Summer School. Ed A. Zichichi.

33 S. Weinberg, *Trans. N. Y. Academ. Sci.* 38:185 (1977).

34 D. B. Kaplan and A. Manohar, *Phys. Rev. Lett.* 56:2004 (1986).

35 R. Peccei and H. Quinn, *Phys. Rev. Lett.*

36 P. Sikivie, Lectures at the 1986 Les Houches Summer School on *Architecture of fundamental interactions*, Ed, R Stora and P. Ramond, North Holland 1987.

37 L. Maiani, in *Proc. 1977 Int. Symp. on Lepton and Photon Interactions at High Energies*, DESY, Hamburg (1977).

38 For a Review see L. Wolfenstein, *Ann. Rev. Nucl. and Part. Sci.* 36:137 (1986).

39 R. H. Bernstein *et al., Phys. Rev. Lett.* 54:1631 (1985). Talk given at the 1987 DPF meeting, Salt Lake City.

40 M. K. Gaillard and B. W. Lee, *Phys. Rev. Lett.* 33:108 (1974). G. Altarelli and L. Maiani *Phys. Lett.* 52B:351 (1974).

41 M. Shifman *et al., JETP Lett.* 22:55 (1975).

42 F.J Gilman and M. Wise, *Phys. Rev.* D27:1128 (1980).

43 J. M. Gerard *et al., Nucl. Phys.* B253:93 (1985).

44 G. Athanasiu and F. Gilman, *Phys. Lett.* 153B:274 (1985). P. A. S. De Sousa Gerbert, *Nucl. Phys.* B272:581 (1986).

45 S. Sharpe. SLAC-Pub 4147 (1986). C. Bernard *et al.,* UCLA/86/TEP/48 (1986).

46 D. Cline. Talk at the Meeting on New Physics, U. Wisconsin, May 1986.

47 J. W. Cronin *et al.,* In Proc. of 1984 Snowmass Summer Study of the Design and of the SSC, Ed R. Donaldson and J. Morfin.

48 E. W. Kolb and J. Turner, *Ann. Rev. Nucl. and Part. Sci.,* 33:645 (1983).

49 S. Coleman and E. Weinberg, *Phys. Rev. D* 7:1888 (1973).

50 S. Weinberg *Phys. Rev. Lett.* 36:294 (1976);
A. Linde, *JETP Lett.* 23:64 (1976).

51 A. Guth and E. Weinberg, *Phys. Rev. Lett.* 65:1131 (1980).

52 R. Flores and M. Sher, *Ann. Phys.* 168:95 (1983).

53 C. Quigg, D.W. Lee and H. Thacker, *Phys. Rev. D* 16:1519 (1977).

54 M. Veltman, *Acta Phys. Polon. B* 8:475 (1977).

55 J.D. Bjorken, *in*: "Proceedings of the 1976 SLAC Summer Institute," M. Zipf, ed.

56 R.N. Cahn, M.S. Chanowitz and N. Fleishon, *Phys. Lett. B* 82:113 (1979).

57 B.L. Ioffe and V.A. Khoze, Leningrad report LINP-274 (1976).

58 F. Wilczek, *Phys. Rev. Lett.* 39:1304 (1977).

59 M. Vysotsky, *Phys. Lett. B* 97:159 (1980).

60 H.M. Georgi et al., *Phys. Rev. Lett.* 40:692 (1978).

61 R.N. Cahn and S. Dawson, *Phys. Lett. B* 136:196 (1986);
S. Petcov and D.R.T. Jones, *Phys. Lett. B* 84:660 (1979).

62 M. Chanowitz and M.K. Gaillard, *Phys. Lett. B* 142:85 (1986).

63 Z. Kunszt, *Nucl. Phys. B* 247:339 (1984).

64 J.F. Gunion et al., *Phys. Rev. Lett.* 54:1226 (1985).

65 E. Eichten et al., *Rev. Mod. Phys.* 56:579 (1986).

66 J.F. Gunion and M. Soldate, *Phys. Rev. D* 34:826 (1986).

67 J. Ellis, M.K. Gaillard and D.V. Nanopoulos, *Nucl. Phys. B* 106:292 (1976).

68 G. Kane University of Michigan preprint UM TH 86-16 (1986), F. Gilman, J. Gunion and P. Wiesman, In preparation.

69 D. Burke, Lectures at this school.

70 F. Halzen and K. Mursula, *Phys. Rev. Lett.*, 51:857 (1983).

71 G. Altarelli, *Phys. Rep.* 81:1 (1982).

72 A. H. Mueller Lectures at the 1985 TASI (Yale University), published by World Scientific Publishing (Singapore).

73 M. Dine and J. Saperstein *Phys. Rev. Lett.* 43:688 (1979), W Celmaster and R J. Gonsalves *Phys. Rev. Lett.* 44:560 (1979).

74 G. Sterman and S. Weinberg, *Phys. Rev. Lett.*, 39:1436 (1977).

75 S. L. Wu, *Phys. Rep.*, 107:59 (1983).

76 T. Gottschalk, CALT-68-1413 (1987). F. Paige, in *Proc. of DPF meeting,* Eugene, OR, Ed. R. Hwa (1986)

77 K. Ellis, D. A. Ross and T. A. Terrano, *Phys. Rev. Lett.*,45:1226 (1980).

78 A. H. Mueller, *Phys. Lett.*, 104B:161 (1981). Yu. Dokshitzer, *et al.*, *Phys. Lett.* 115B:242 (1982). A. Bassetto, *et al.*, *Phys. Rep.*, 100:201 (1983).

79 G. Marchesini and B. Webber, *Nucl. Phys.*, B238:501 (1984).

80 G. Altarelli and G. Parisi, *Nucl. Phys.* B126:298 (1977).

81 L. V. Gribov, E. M. Levin and M. G. Ryskin, *Phys. Rep.*, 100c:1 (1983).

82 J. Collins in *Proc of the 1984 Summer Study on the Design and Utilization the SSC,* Ed. J. Morfin and R. Donaldson.

83 G. Altarelli, R. K. Ellis and G. Martinelli, *Nucl. Phys.* B143 521 (1978).

84 A. H. Mueller, *Phys. Rev.*, D18:3705 (1978). J. Collins, D. Soper and G. Sterman, *Nucl. Phys.*,B223:81 (1983), *Phys. Lett.*, 109B:388 (1983). R. K. Ellis, *et al.*, *Nucl. Phys.*, B152:285 (1979).

85 G. Altarelli *et al.*, *Z. Phys.*, C27:617 (1985).

86 F. Halzen and W. Scott, *Phys. Rev.*, D18:3378 (1978).

87 G. Parisi and R. Petronzio, *Nucl. Phys.*, B154:427 (1979). G. Curci, *et al.*, *Nucl. Phys.*, B159:451 (1979). Yu. Dokshitzer *et al. Phys. Rep.*, 58:269 (1980).

88 G. Altarelli *et al.*, *Nucl. Phys.*, B246:12 (1984).

89 G. Arnison *et al.*, *Phys. Lett.*, 139B115 (1984). P. Bagnaia *et al.*, *Phys. Lett.*, 139B:105 (1984).

90 P. Bagnaia et al., *Z. Physik* C20:117 (1983),

91 G. Arnison et al., *Phys. Lett.* 123B:115 (1983),

92 T. K. Gaisser and F. Halzen, *Ann. New York Acad.*, 461 (1986).

93 B. L. Combridge, *Nucl. Phys.* B151:429 (1977).

94 F. Bergsma et al., *Phys. Lett.* 123B:269 (1983).

95 H. Abramowicz et al., *Z. Physik* C13:199 (1982), C17:283 (1983).

96 D. Drijard et al., *Phys. Lett.* 85B:425 (1979).

97 R. Ammer et al., *Phys. Lett.* 135B:237 (1984).

98 R. Ammer et al., CERN EP/86-122 (1986).

99 J.R. Cuddell and F. Halzen, *Phys.Lett.* 175B:227 (1986).

100 G. VanDalen and A. Kernan, *Phys. Rep.* 106:297 (1984).

101 F. Herzog and Z. Kunszt, *Phys. Lett.* 157B:430 (1985).

102 J. C. Collins and D. Soper, *Nucl. Phys.*, B263:37 (1986).

103 M. Green and M. Peskin, lectures at this school.

104 K.G Wilson, *Phys. Rev.* D3:1818 (1973).

105 See for example J. Ellis, CERN–TH–4255/85 Lectures presented at the 28th Scottish Universities Summer School in Physics, Edinburgh. Scotland. or H. Haber and G. L. Kane *Phys. Rep.* 117:75 1985.

106 E. Farhi and L. Susskind, *Phys. Rep.* 74:277 (1981).

107 E. Eichten and K. Lane, *Phys. Lett.* 90:125 (1980).

108 E. Farhi and L. Susskind, *Phys. Rev.* D20:3404 (1979).

109 R.D. Peccei, DESY 86-010 (1986).

110 E. Eichten, K. D. Lane and M. Peskin, *Phys. Rev. Lett.* 50:811 (1982).

111 C. Albajar, *et al.,* CERN-EP/86-82, *Phys. Lett.*, to appear.

112 A. Honma, *et al.,* Proc. of 23^{rd} International Conferance on High Energy Physics, Berkeley CA. (1986).

113 W. Bartel *et al., Z. Physik,* C19:197 (1983).

114 P. Bagnaia *et al., Phys. Lett.,* 129B:130 (1983).

115 G. Wolf, Lectures at the NATO advanced study institute, St Croix, June 1986, Plenum, Press Ed. T. Ferbel.

	Tevatron	*Tristan*	*SLC*	*LEP*	*HERA*
particles	$p\bar{p}$	e^+e^-	e^+e^-	e^+e^-	ep
max center of mass energy TEV	2.0	0.06	0.10	0.12	.318
Luminosity $10^{30} cm^{-2} sec^{-1}$	1	20	6	16	15

Table 1: Some of the characteristics of colliders which will be operational in the late 1980's. LEP will alternately have a center–of–mass energy of 200 Gev.

$Wf\bar{f}$	$\frac{g_2}{2\sqrt{2}} W_\mu \bar{f}\gamma^\mu(1-\gamma_5)f$
$Z\bar{f}f$	$\frac{e}{2\sin\theta_W \cos\theta_W} Z_\mu \bar{f}\gamma^\mu(v_f - a_f\gamma_5)f$
	$v_f = T_3 - 4Q\sin^2\theta_W$
	$a_f = T_3$
HWW	$g_2 M_W H W^+_\mu W^-_\mu$
HZZ	$\frac{g_2}{2\cos\theta_W} M_z Z_\mu Z_\mu$
$Hf\bar{f}$	$\frac{g_2 m_f}{2M_W} H\bar{f}f$

Table 2: Couplings of physical particles in the Weinberg-Salam model (unitary gauge). f is a fermion of charge Q_f and weak isospin T_3 (= + 1 for u, c, t quarks and neutrinos, -1 otherwise).

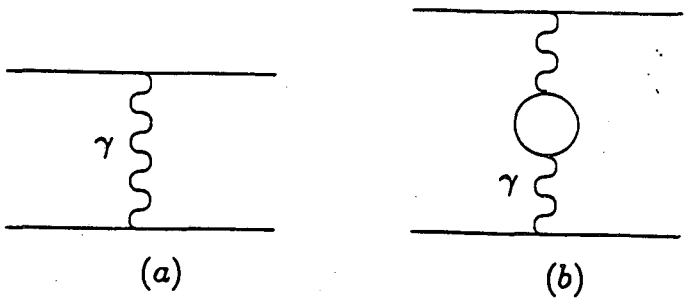

Figure 1: (a) Feynman diagram showing a contribution to the scattering of two charged particles in QED; (b) A higher order contribution.

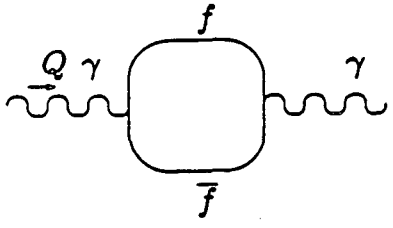

Figure 2: A contribution to the photon self energy at one loop due to a charged fermion of mass m_e.

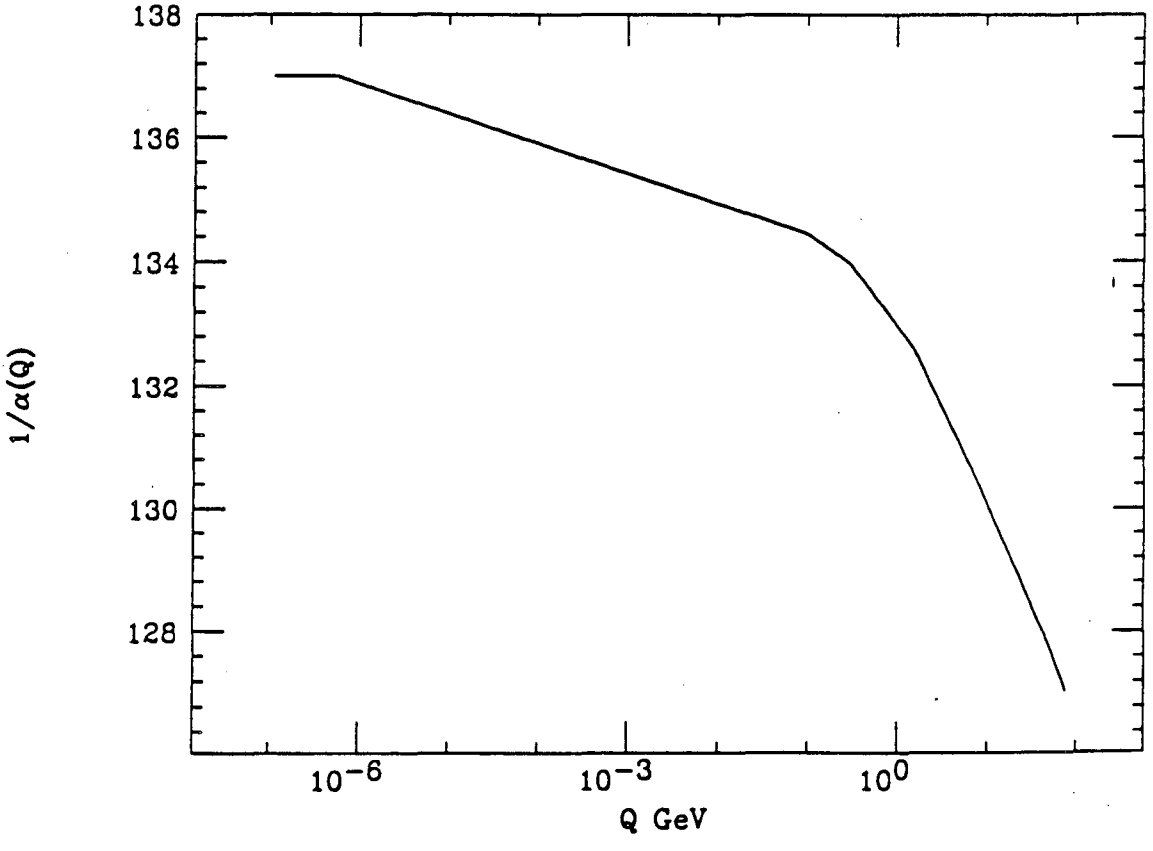

Figure 3: The behavior of $\alpha_{em}(Q)$ with Q, which shows the increase of $\alpha_{em}(Q)$ due to the known quarks and leptons.

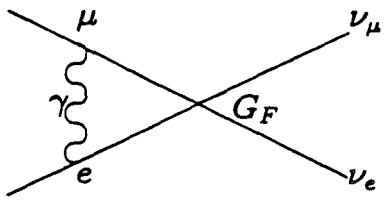

Figure 4: Feynman diagram showing a QED correction to the muon lifetime.

Process	M_Z	$\sin^2\theta_W$	Ref.
$e^+e^- \to \mu^+\mu^-$	84 $\pm$4.8	0.17 $\pm$0.02	16
$\nu p \to \nu p$ $\bar{\nu} p \to \bar{\nu} p$	91.8$\pm$2.8	0.23 $\pm$0.02	17
ed asymmetry	93.3$\pm$2.1	0.220$\pm$0.014	18
$\nu_\mu e \to \nu_\mu e$	91.8$\pm$2.8	0.23 $\pm$0.02	19
Parity violation in atoms	98.5$\pm$7.9	0.19 $\pm$0.04	20
$\bar{\nu} N \to \mu X, \bar{\nu} X$ $\nu N \to \mu X, \nu X$	92.4$\pm$0.6	0.226$\pm$0.004	21

Table 3: Values of M_Z (or $\sin^2\theta_W$) extracted from various experiments.

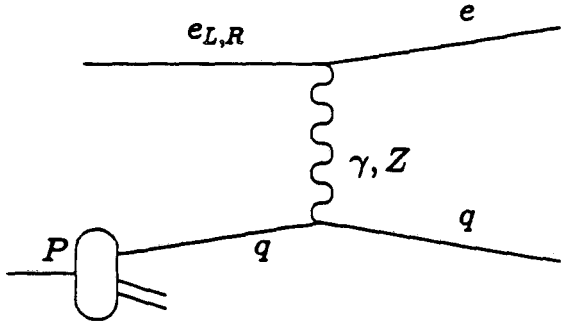

Figure 5: Diagram relevant for the scattering of polarized electrons from a nuclear target.

.	UA1	UA2	Values[15] obtained using Table 2
$M_W(GeV)$	$83.5^{+1.1}_{-1.0} \pm 2.7$	$81.2 \pm 1.1 \pm 1.3$	81.4 ± 0.6 (79.8 without radiative corr.)
$M_Z(GeV)$	$93.0 \pm 1.4 \pm 3$	$92.5 \pm 1.3 \pm 1.5$	92.5 ± 0.5 (90.2 without radiative corr.)

Table 4: Values of M_W and M_Z measured by the UA1 and UA2 collaborations[14].

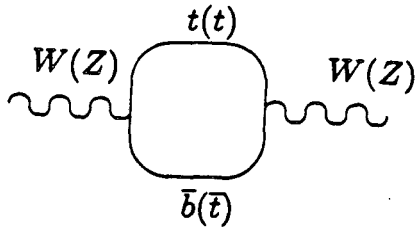

Figure 6: Feynman diagram showing contributions to the W and Z self energies from the t and b quarks.

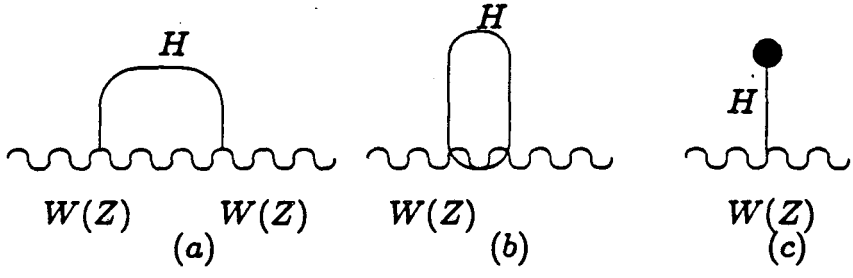

Figure 7: Feynman diagrams showing contributions to the W and Z self energies from the Higgs boson.

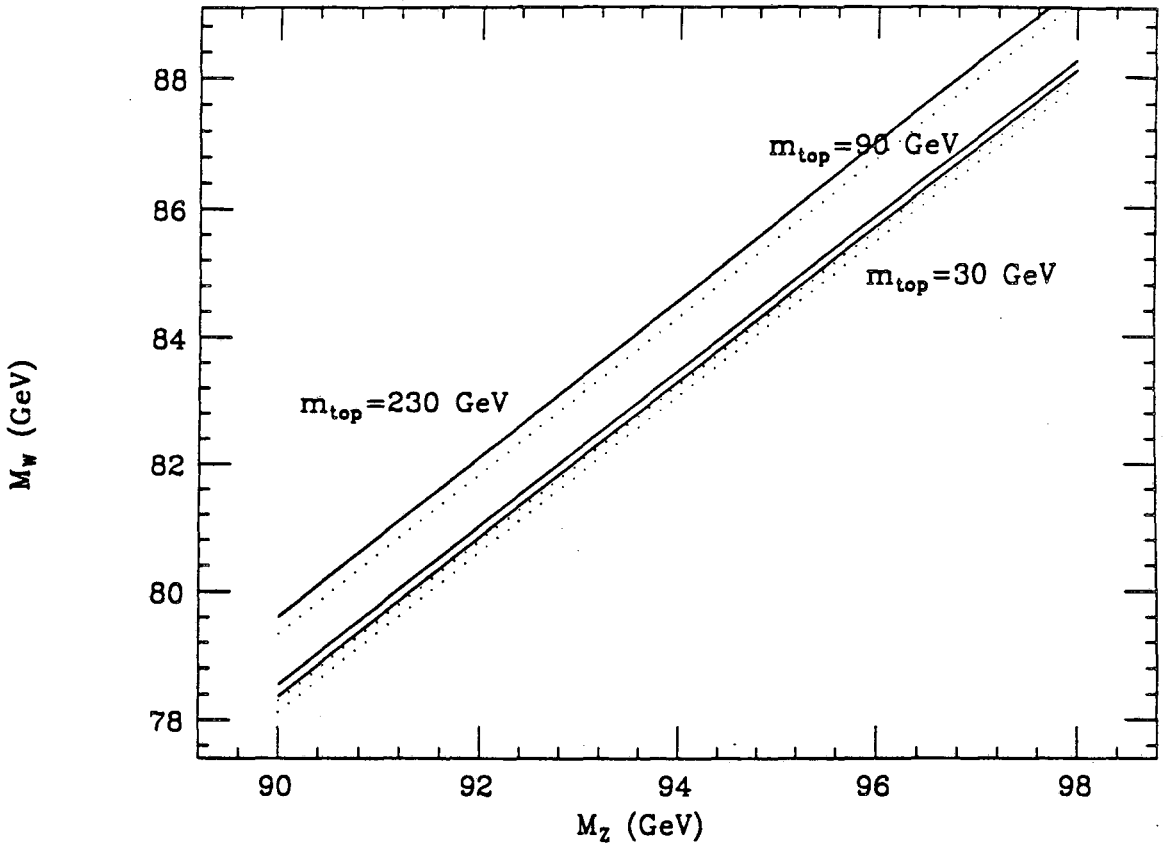

Figure 8: The dependence of M_W upon M_Z for several choices of m_t The solid lines are for $m_H = 10GeV$ and the dotted for $m_H = 1000GeV$.

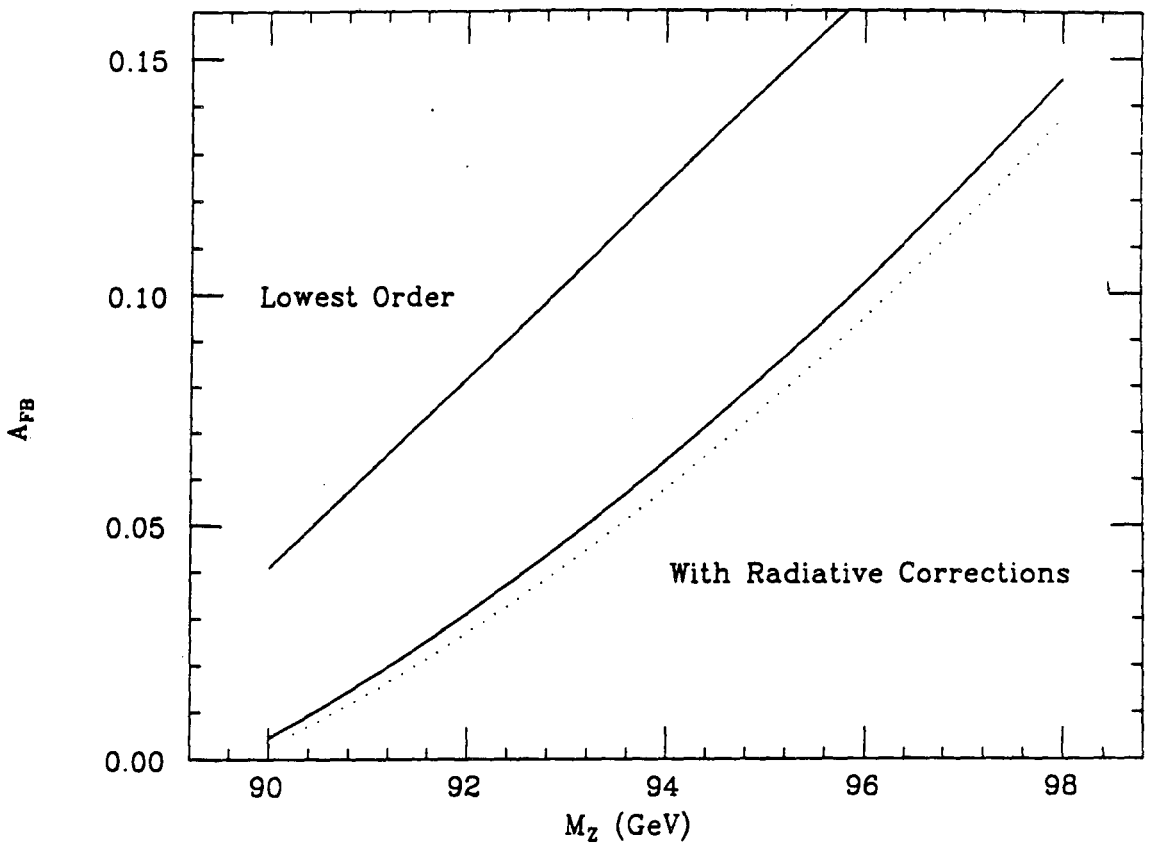

Figure 9: The dependence of A_{FB} for the process $e^+e^- \rightarrow Z \rightarrow \mu^+\mu^-$ for unpolarized e^+e^- beams as a function of M_Z for a top quark mass of 30 GeV. The solid lines are for $m_H = 10GeV$ and the dotted for $m_H = 1000GeV$.

$\Delta P/P$	$N = 10^4$	$N = 10^5$	$N = 10^6$
5%	0.025	0.013	0.010
3%	0.023	0.009	0.006
1%	0.022	0.007	0.003

Table 5: The error estimated on the left-right asymmetry as a function of the number of produced Z^0's (N) and the accuracy of the measurement of the electron polarization $(\Delta P/P)$[30].

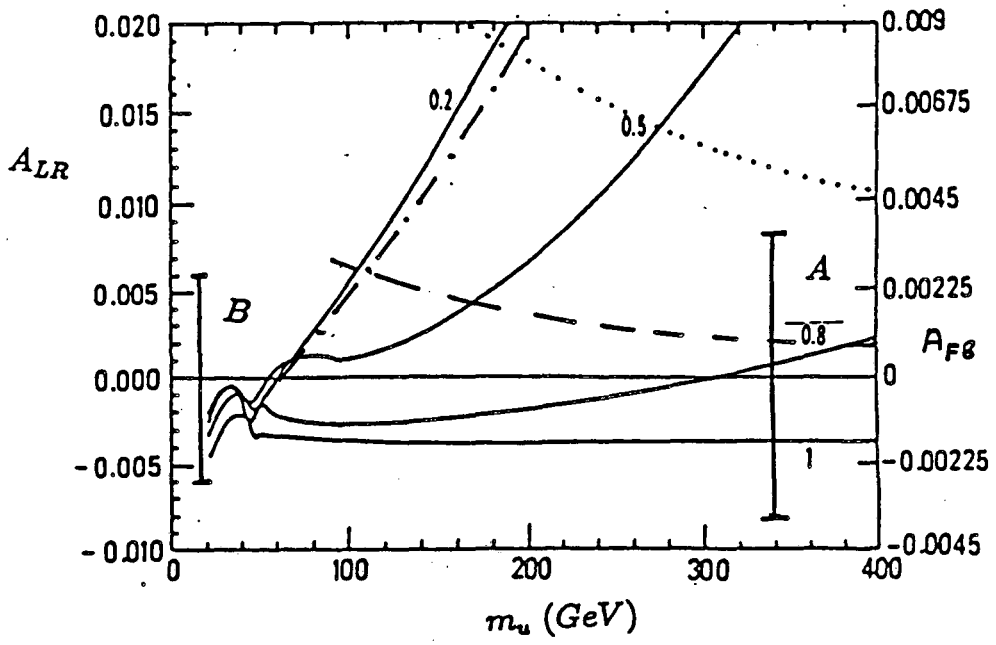

Figure 10: The contribution to A_{FB} and to A_{LR} from the presence of an additional quark doublet as a function of m_u, the mass of the charge 2/3 member of the doublet. The curves are labelled by the ratio m_u/m_d, where m_d is the mass of the charge 1/3 member. The region above the dot-dashed line can be probed directly since m_d is low enough for the Z to decay to $d\bar{d}$. If M_W is within 300(100)MeV of it predicted value, the region above the dotted (dashed) line is excluded. The error bar A applies to A_{FB} and B to A_{LR} (see text).

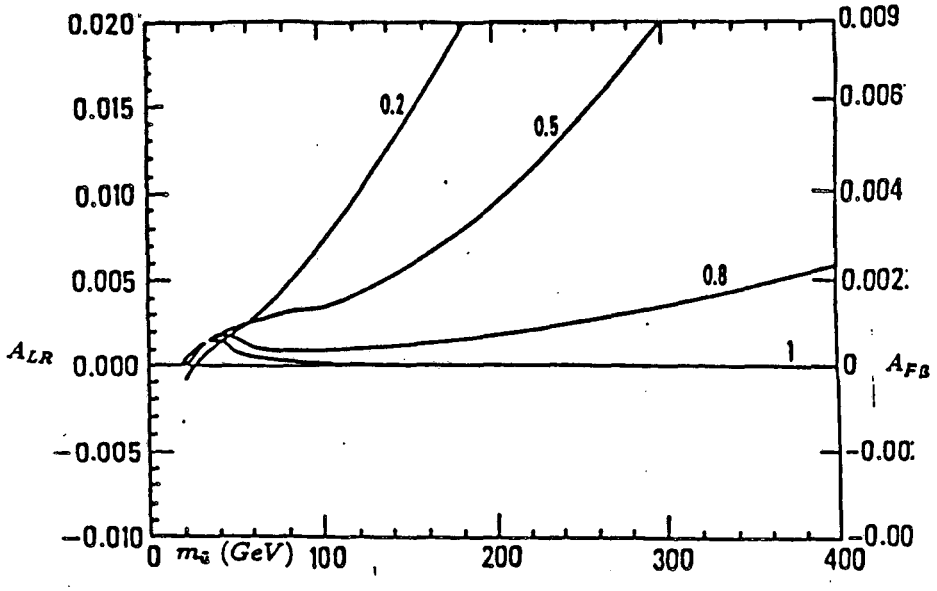

Figure 11: The contribution to A_{FB} from a squark doublet as a function of the up squark mass for fixed ratios of the up to down squark masses.

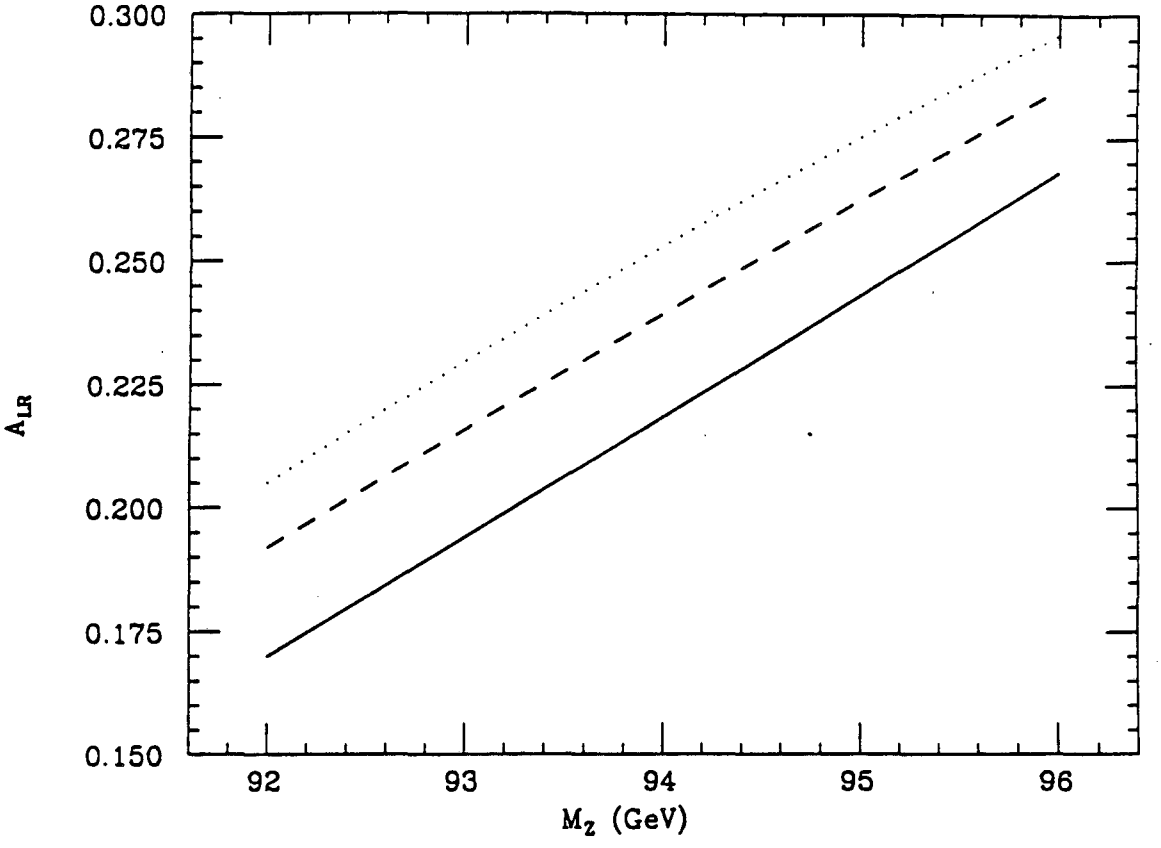

Figure 12: The quantity A_{LR} as a function of M_Z. The solid line has $m_t = 30\ GeV$ and $m_H = 100\ GeV$. The dashed line has $m_t = 180\ GeV$ and $m_H = 100\ GeV$. The dotted line has $m_t = 30\ GeV$ and a modified Higgs sector such that $\rho = 1.01$.

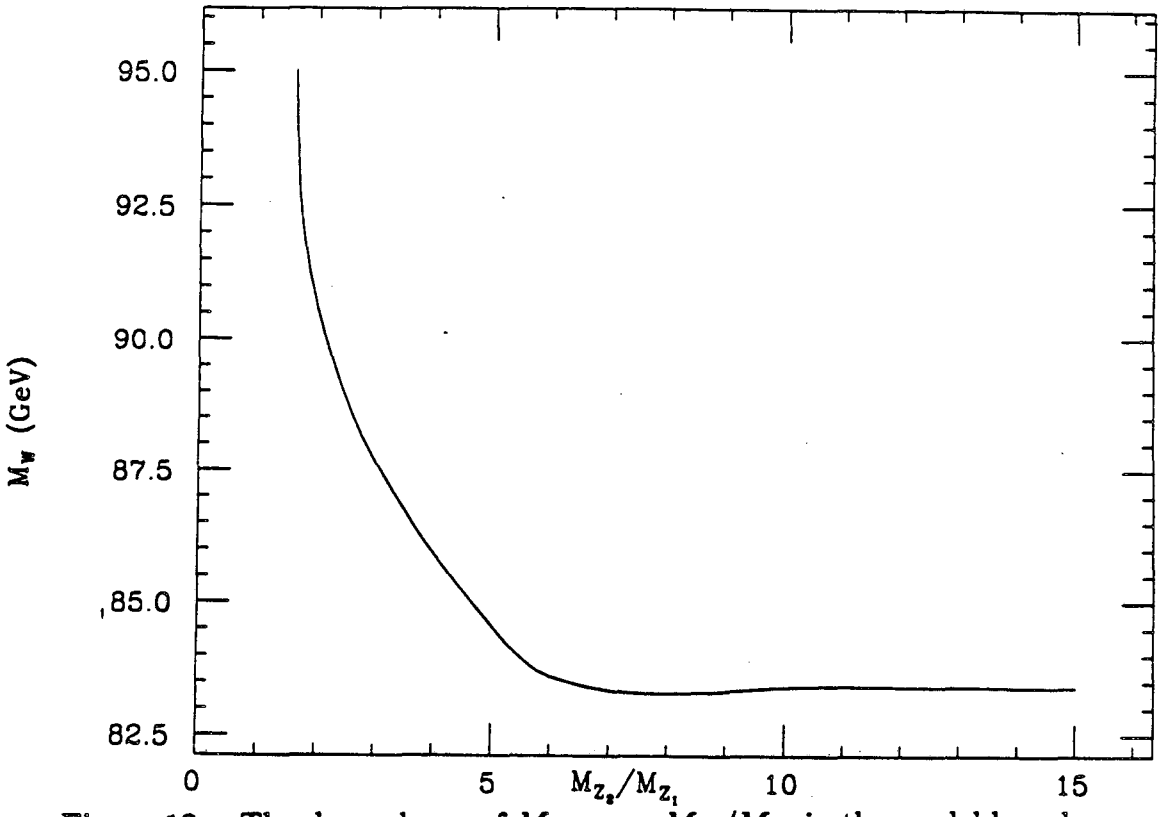

Figure 13: The dependence of M_W upon M_{Z_2}/M_{Z_1} in the model based on $SU(2) \times U(1)_y \times U(1)_{y'}$ for $M_{Z_1} = 94\ GeV$ and $\rho_{y'} = 1/3$.

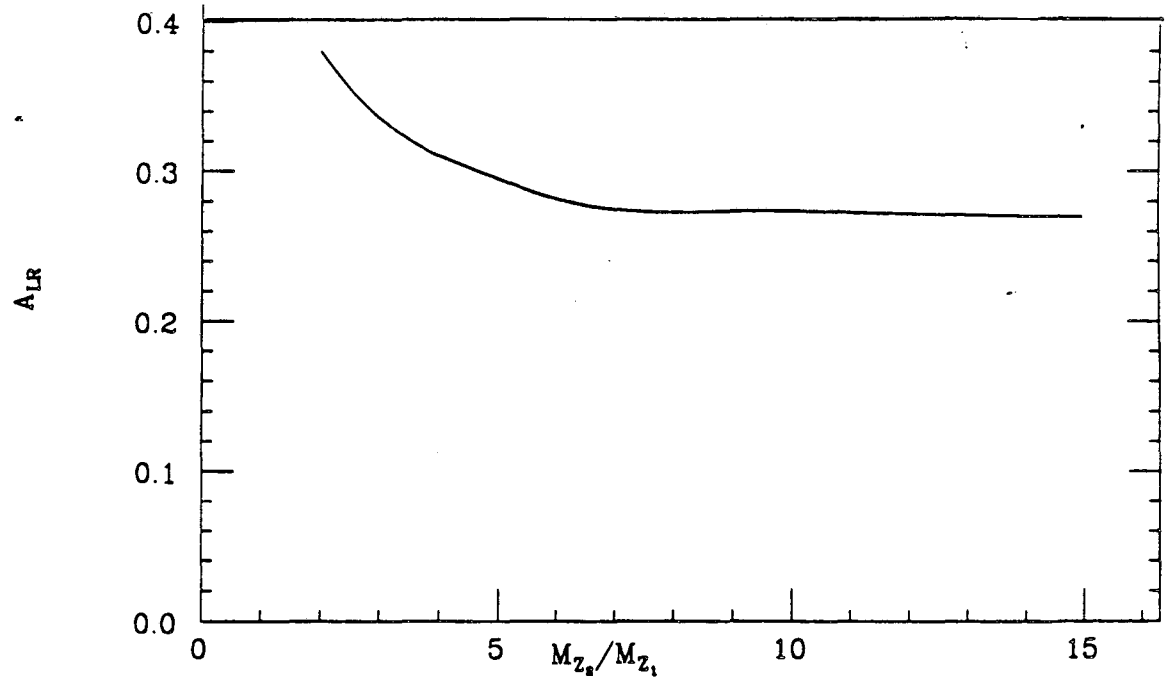

Figure 14: The left-right asymmetry A_{LR} as a function of M_{Z_2} for $\rho_{y'} = 1/3$ in the $SU(2) \times U(1)_y \times U(1)_{y'}$ model. The asymmetry is evaluated at $\sqrt{s} = M_{Z_1}$ which is assumed to be 94 GeV.

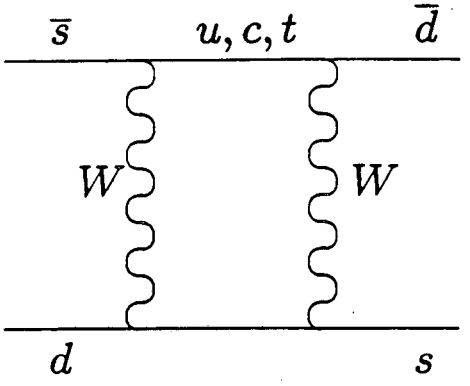

Figure 15: Feynman diagram showing the second order weak contribution to the mixing of K_0 and $\overline{K_0}$.

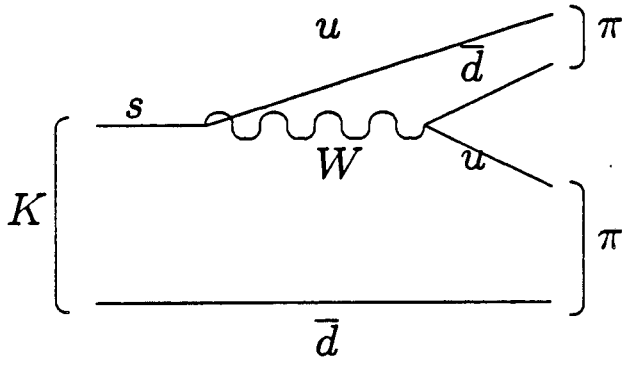

Figure 16: Feynman diagram showing the decay $K \rightarrow 2\pi$ via the spectator diagram.

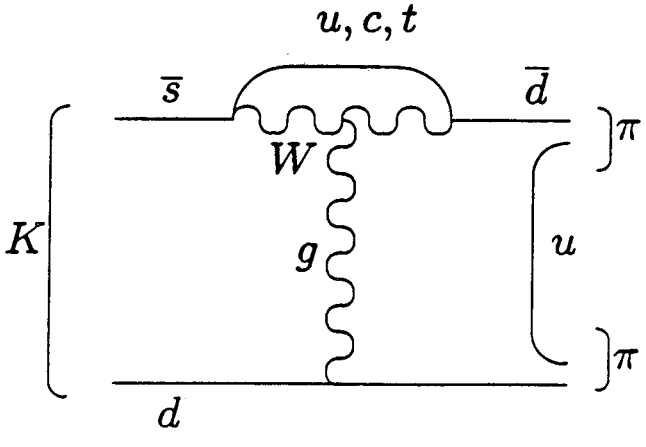

Figure 17: Feynman diagram showing the decay $K \rightarrow 2\pi$ via the Penguin diagram.

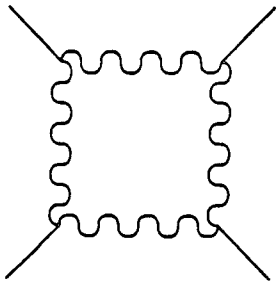

Figure 18: Feynman diagram showing a contribution to the effective potential for the Higgs field due to interactions of the Higgs with W bosons.

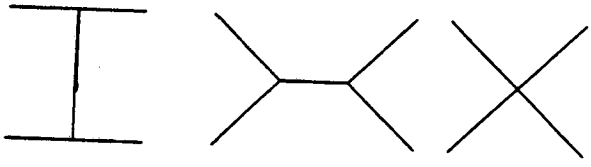

Figure 19: Feynman diagram for the process $HH \rightarrow HH$ which dominate in the limit $m_H >> m_W$.

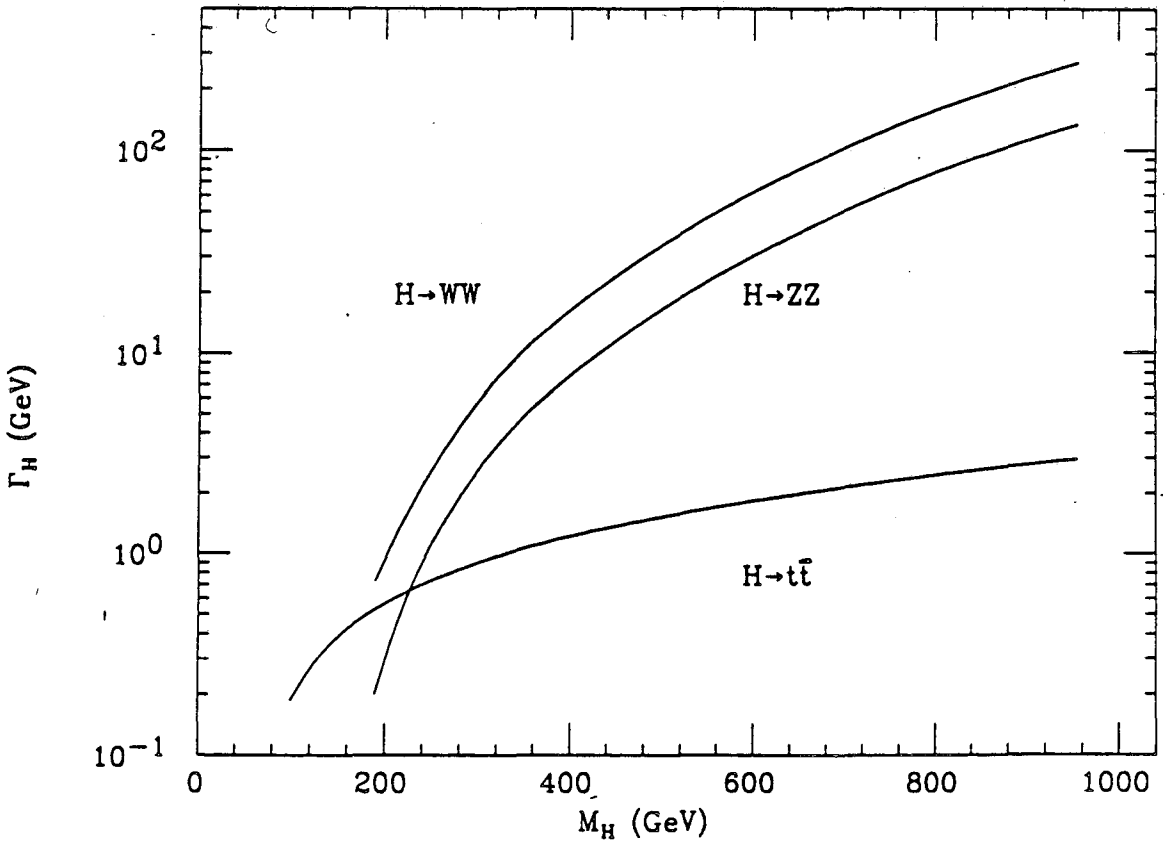

Figure 20: The partial widths $H \rightarrow t\bar{t}$ (solid lines), W^+W^- (dashed line) and ZZ (dotted line) as a function of m_H. The top quark mass is taken to be 40 GeV.

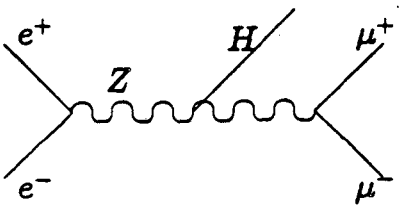

Figure 21: Feynman diagram for the process $e^+e^- \to Z \to H + \mu^+\mu^-$.

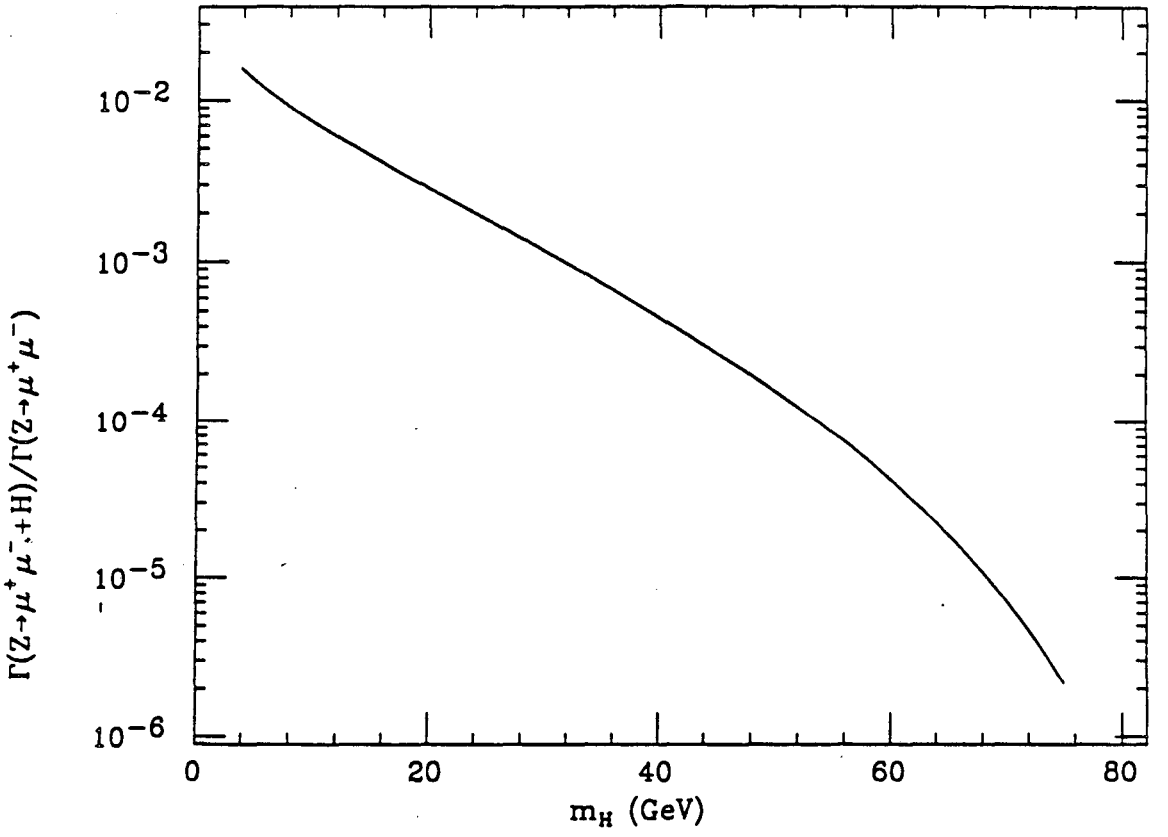

Figure 22: The ratio of widths $\Gamma(Z \to H\mu^+\mu^-)/\Gamma(Z \to \mu^+\mu^-)$ as a function of the Higgs mass.

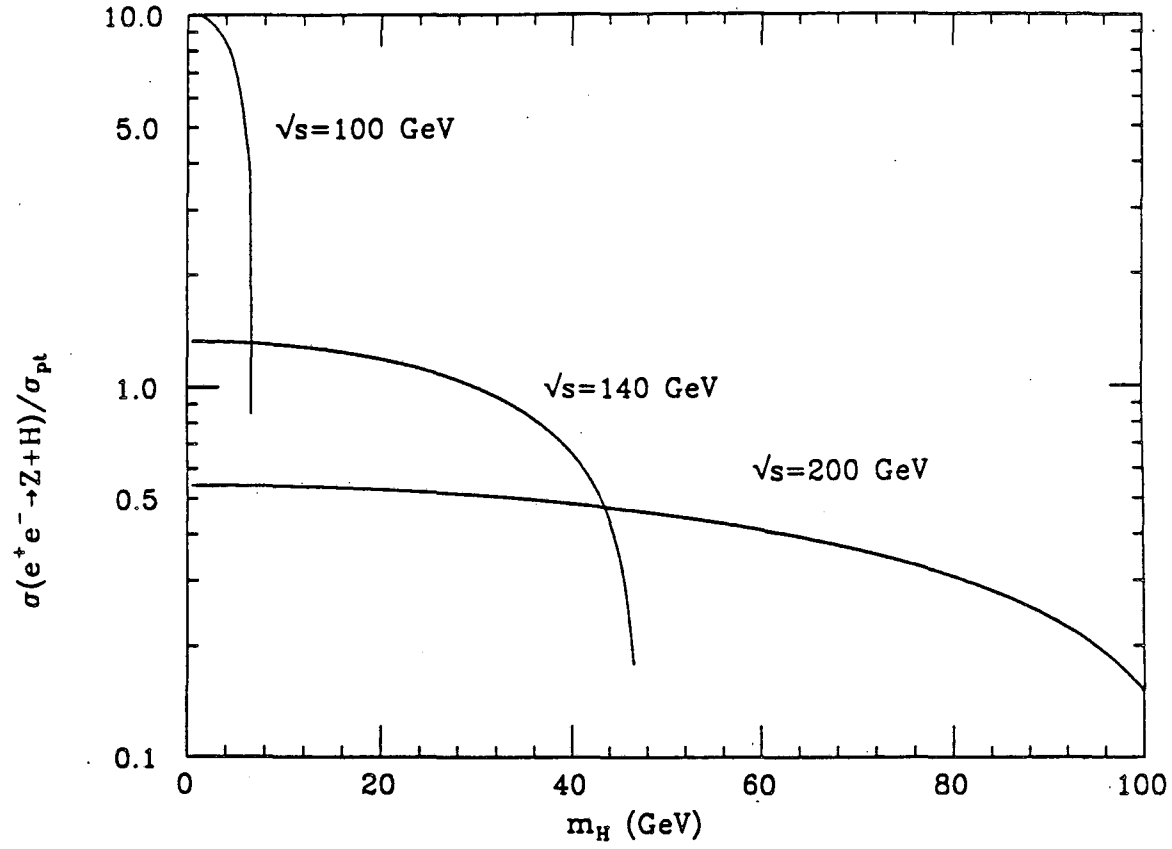

Figure 23: The cross-section for the process $e^+e^- \to Z + H$ as a function of m_H for various values of $\sqrt{s}$.

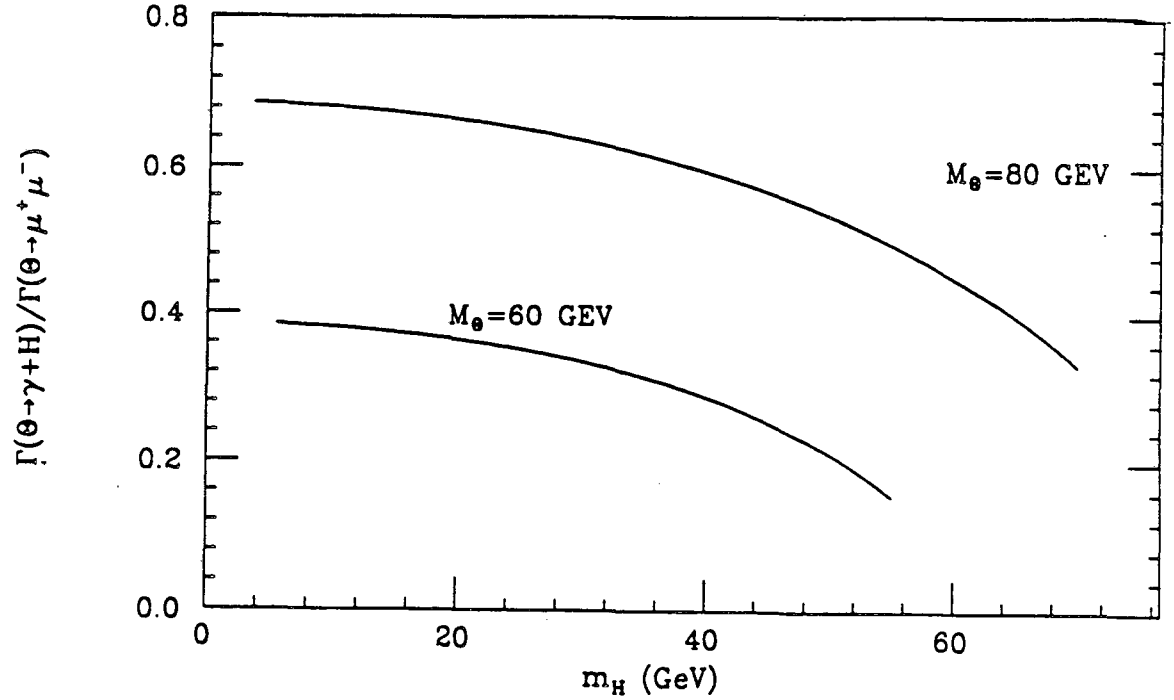

Figure 24: The ratio of decay widths $\Gamma(\theta \to H\gamma)/\Gamma(\theta \to \mu^+\mu^-)$ for the decay of the 1^{--} bound state (θ) of $t\bar{t}$.

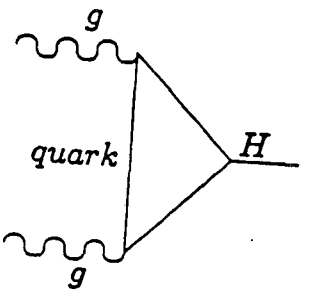

Figure 25: Feynman diagram showing the production of a Higgs boson via gluon-gluon fusion.

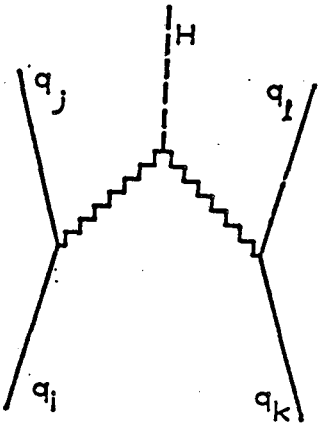

Figure 26: Feynman diagram showing the process $qq \rightarrow H + qq$.

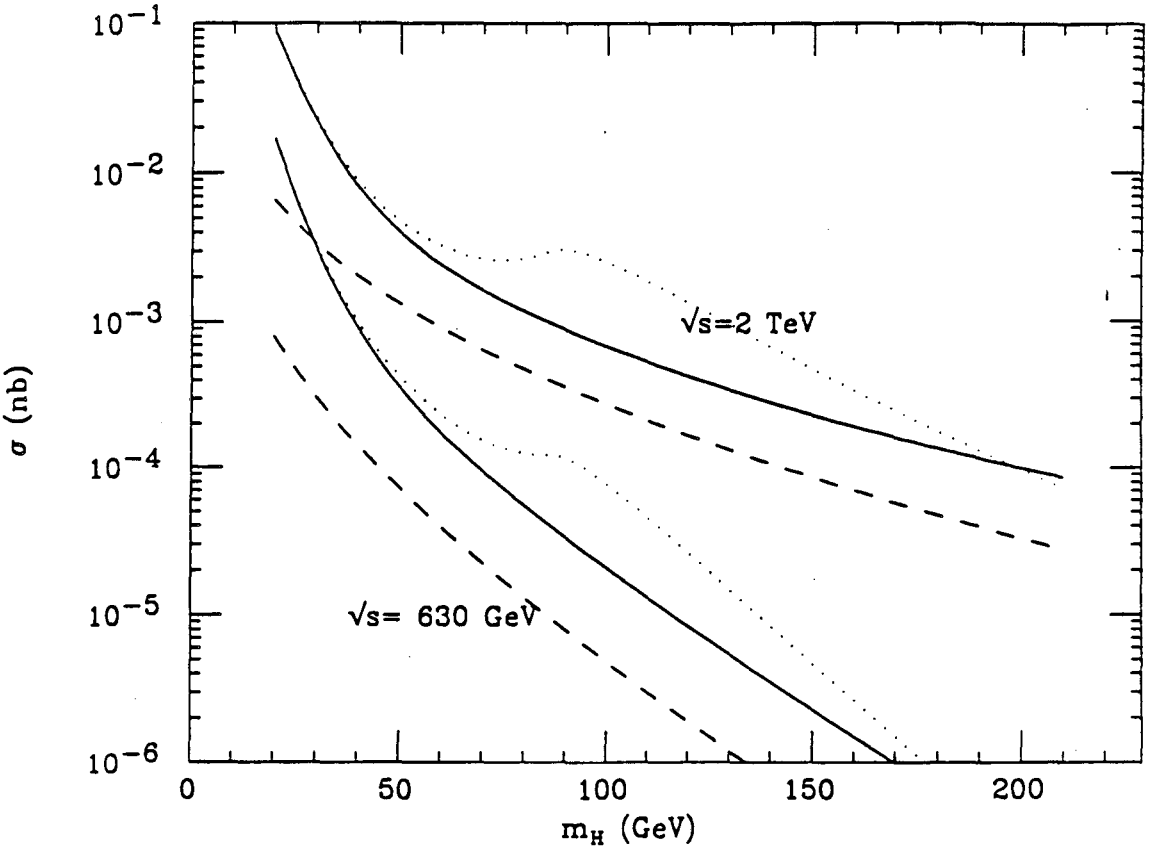

Figure 27: The cross-section $p\bar{p} \rightarrow H + X$ as a function of Higgs mass. The solid (dotted) lines correspond to the gluon fusion process of figure 25 with a top quark mass of 150 (40) GeV , and the dashed to the WW fusion process of figure 26.

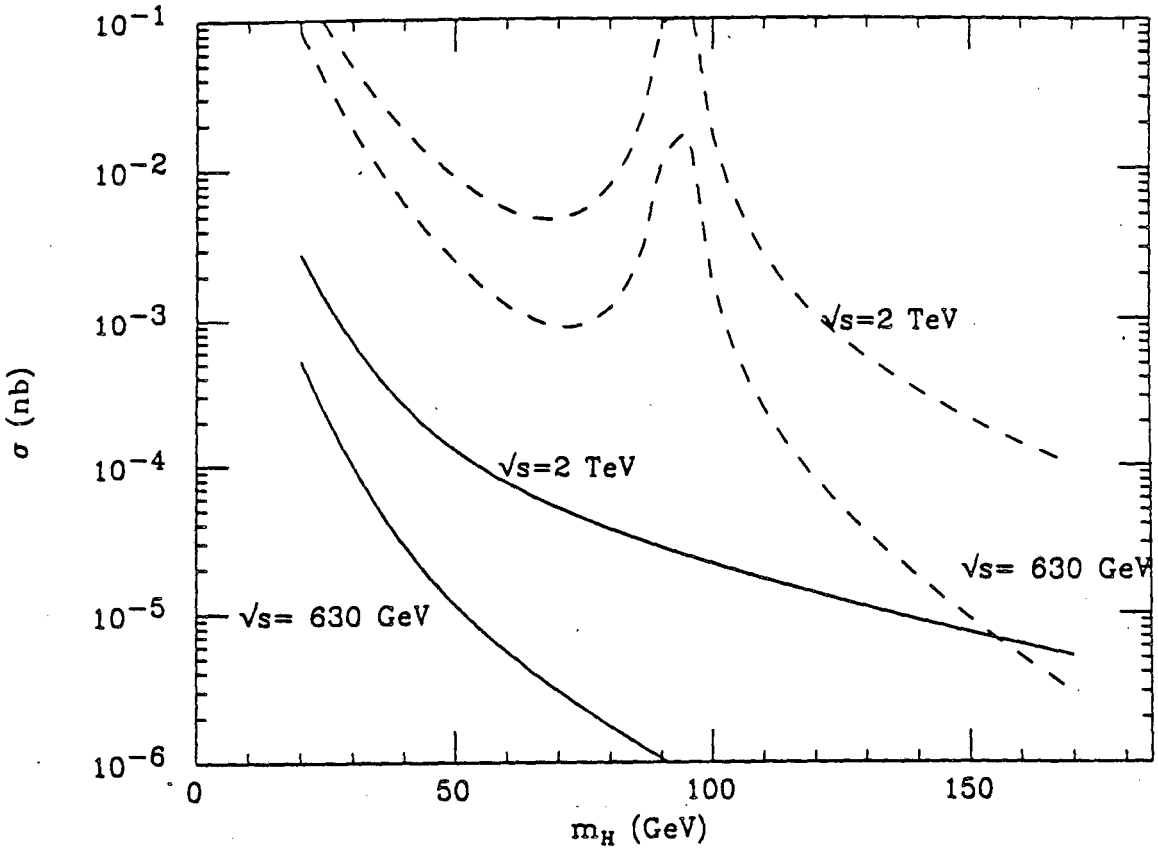

Figure 28: A comparison of the signal and background for the process $p\bar{p} \rightarrow H + X \rightarrow \tau^+\tau^- + X$. It is assumed that $m_H < 2m_t$. The background is calculated from the Drell-Yan process (see Sect. 3) being $d\sigma/dM \ \ \Delta M$. The resolution in the invariant mass of the tau pair (ΔM) is taken to be 10 GeV.

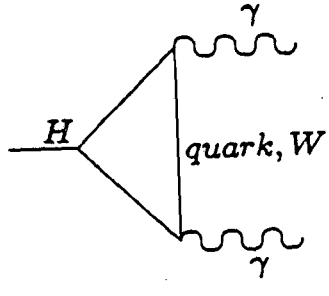

Figure 29: Feynman diagram for the process $H \rightarrow \gamma\gamma$.

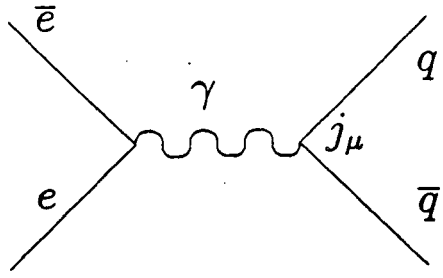

Figure 30: Feynman graph for $e^+e^- \rightarrow$ hadrons.

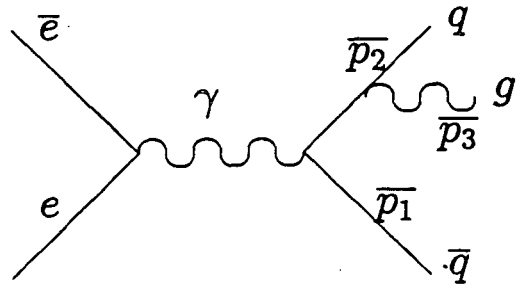

Figure 31: Feynman diagram showing a contribution to the three jet final state described by eqn. 3.23.

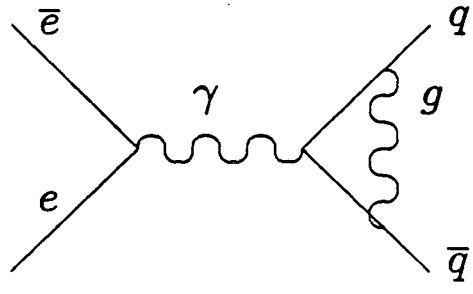

Figure 32: Feynman diagram showing a virtual correction to the total cross section in e^+e^- annihilation.

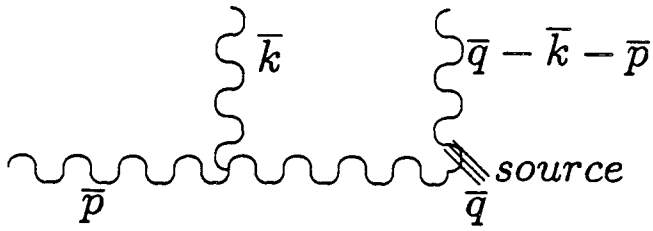

Figure 33: Diagram showing the evolution of a gluon shower at order α_s. See eqn. 3.28.

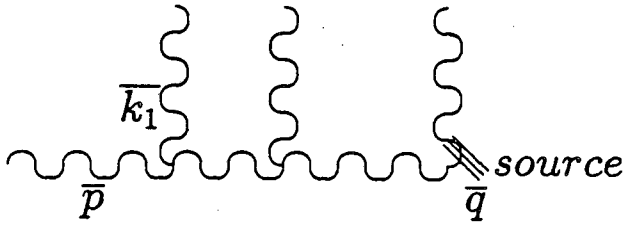

Figure 34: Diagram showing the evolution of a gluon shower at order α_s^2. See eqn. 3.32.

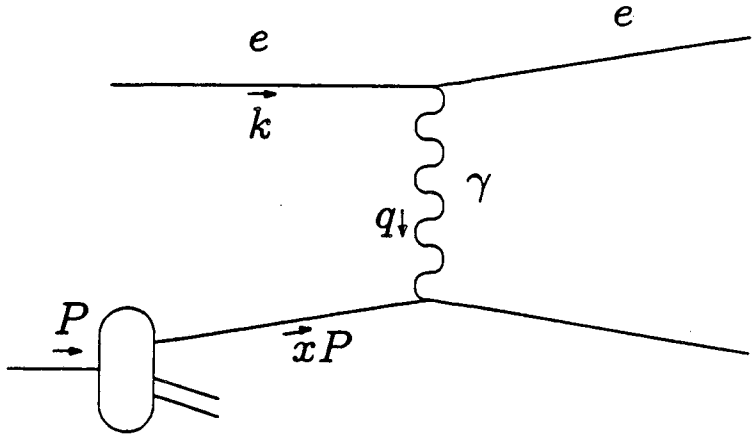

Figure 35: Diagram illustrating the variables in deep inelastic scattering (see Eq. (3.44)): electron + proton $\rightarrow$ electron + anything.

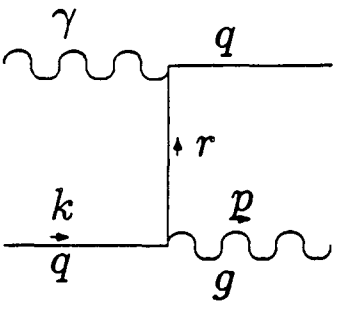

Figure 36: Diagram contributing to the process $q + \gamma \to X$ at order α_s.

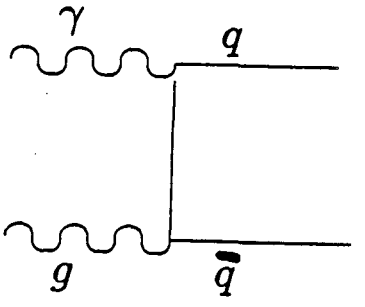

Figure 37: Diagram showing $g + \gamma \to q + \bar{q}$.

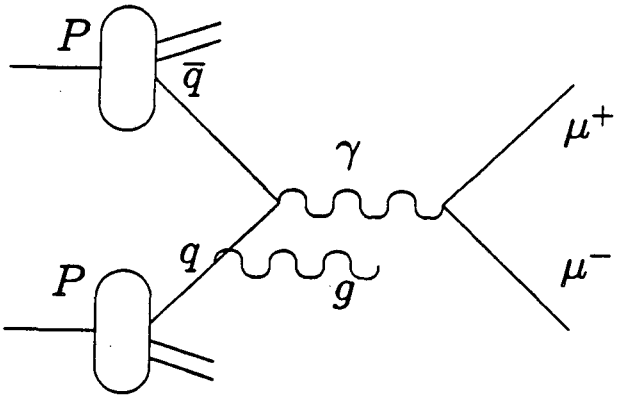

Figure 39: Feynman graph illustrating an order α_s contribution to the Drell-Yan process (see Eq. (3.61)).

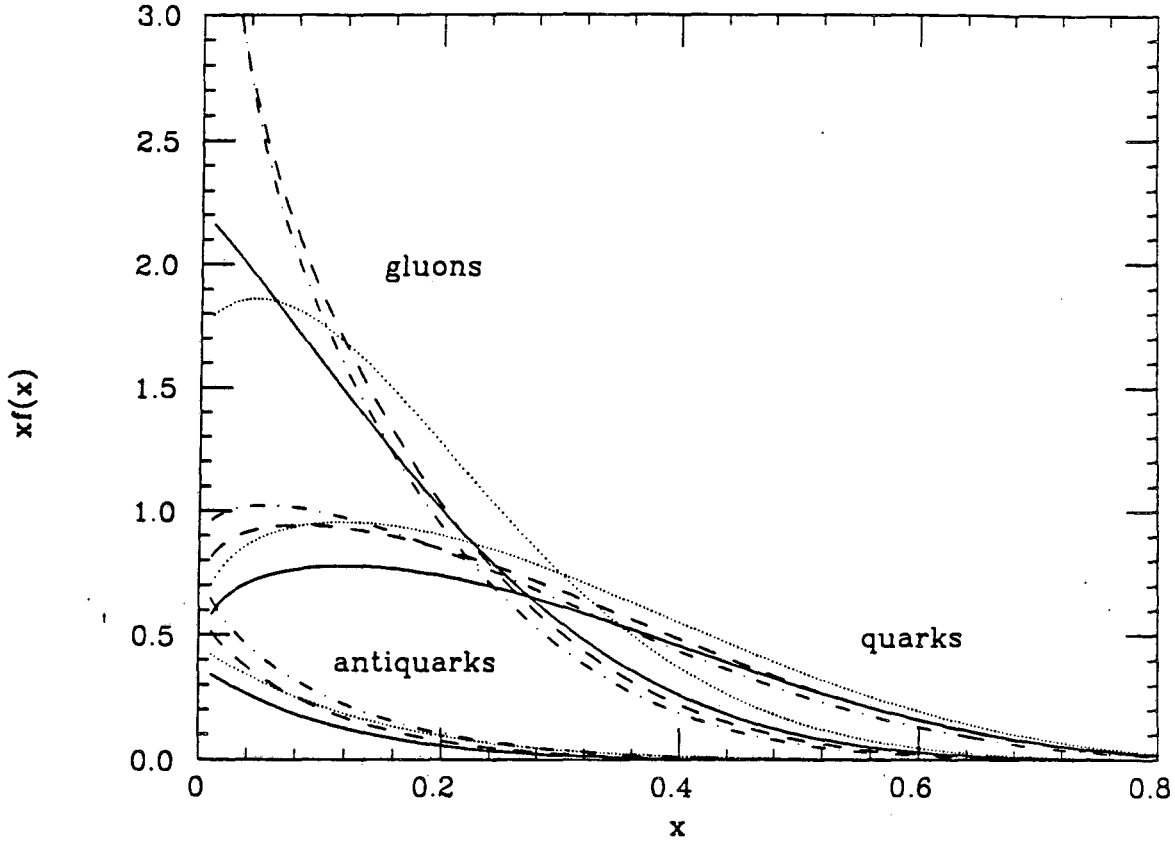

Figure 38: Diagram showing the behavior of the quark and gluon distributions as functions of x for various Q^2. Plotted is $xf(x)$ for gluons, quarks and antiquarks (summed over quark flavors). The solid (dotted) lines correspond to the structure functions of ref. 94 (95) at $Q^2 = 5\ GeV^2$. The dashed (dot-dashed) lines correspond to the structure functions of ref. 94 (95) at $Q^2 = 25\ GeV^2$. The evolution with Q^2 is given by perturbative QCD[65].

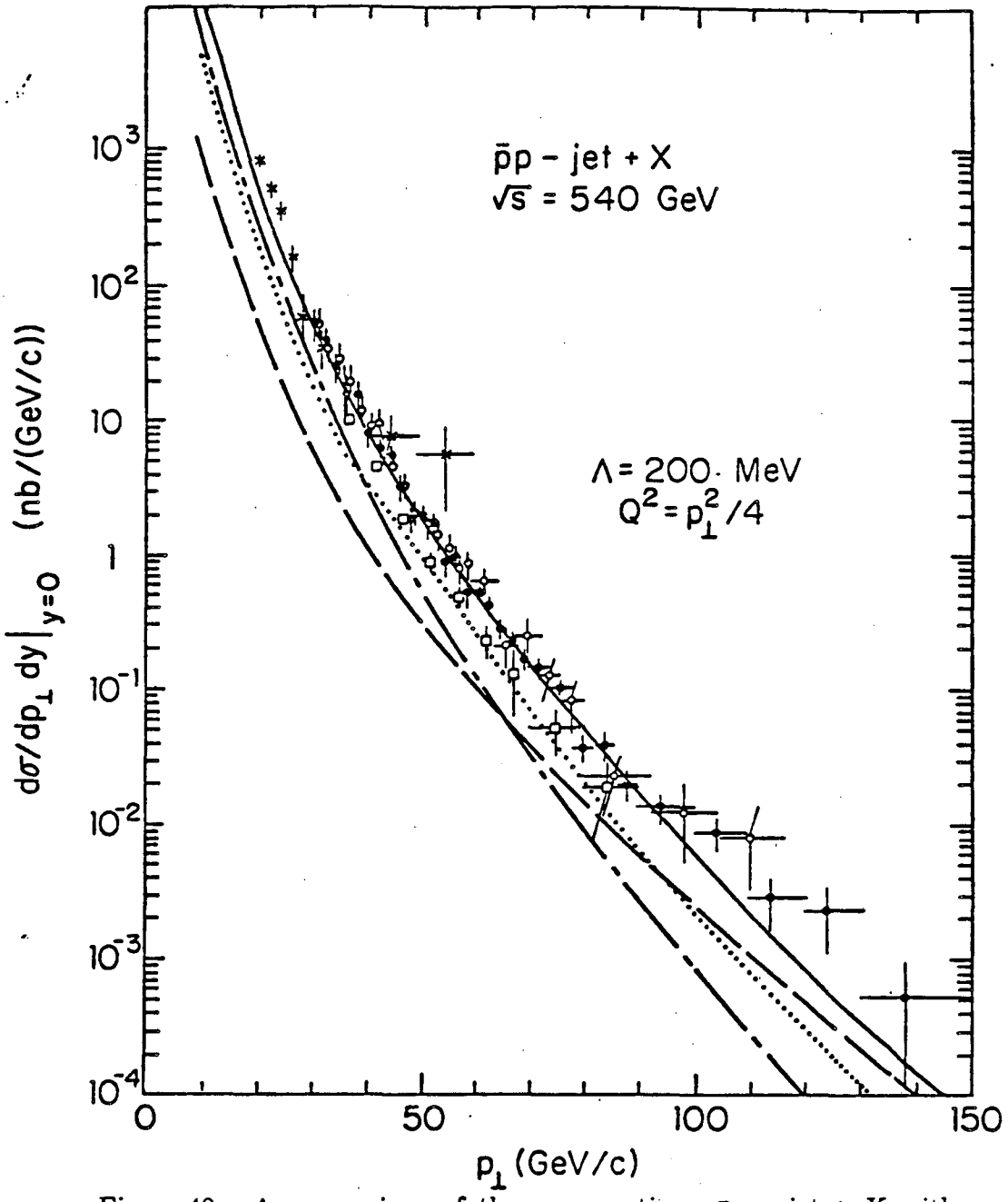

Figure 40: A comparison of the cross-section $p\bar{p} \rightarrow$ jet $+ X$ with a calculation using perturbative QCD for the subprocess $qq \rightarrow qq, gg \rightarrow gg$, etc. The structure functions are those of Ref. 95 evolved in Q^2 up to the relevant scale ($Q = p_\perp/2$).The data are from the UA1[90] and UA2[91] collaborations. The contributions of the differant partonic final states are shown seperately: gg (dot-dashed line), gq (dotted line) and qq (dashed line).

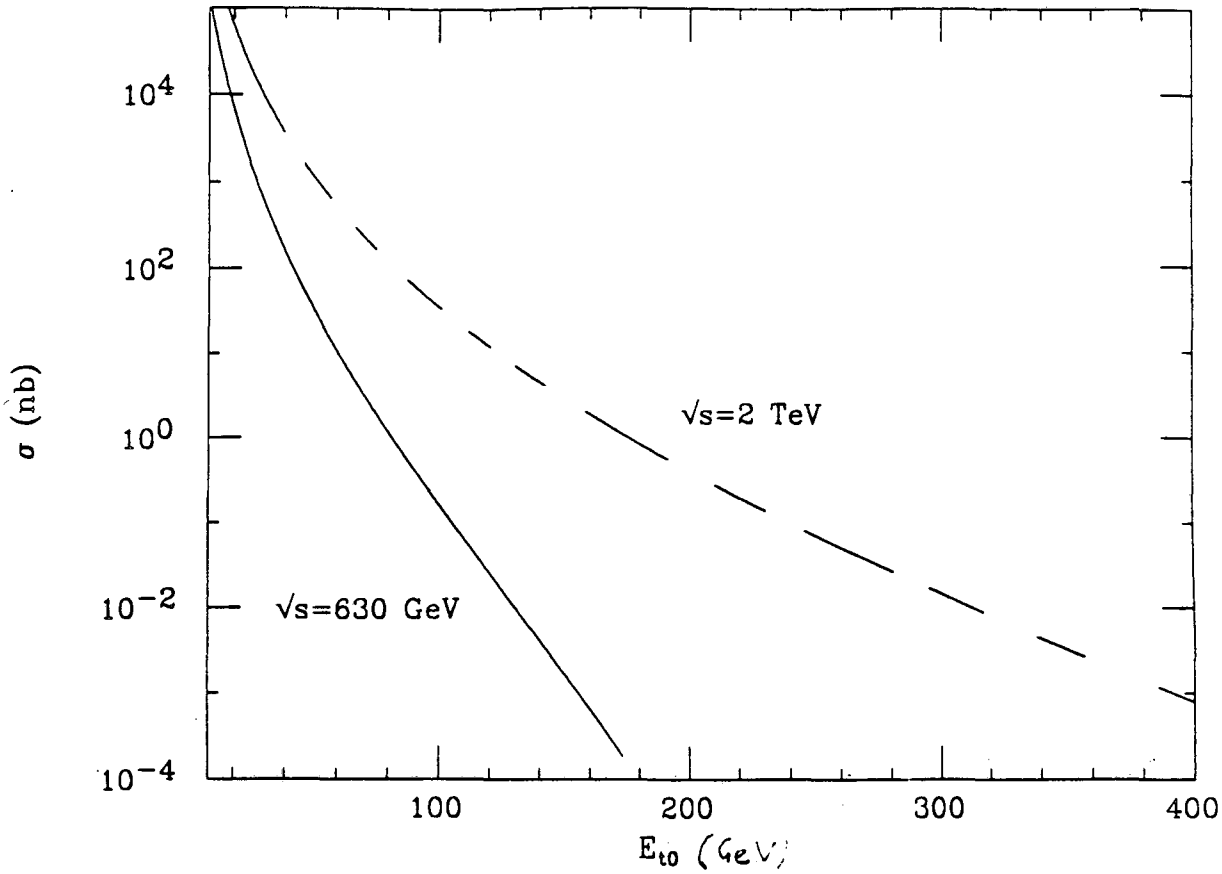

Figure 41: The cross-section for the production of a pair of jets, such that the total transverse energy is greater than E_{t_0} in $p\bar{p}$ collisions. Both jets are required to have rapidity $|y| < 2.5$.

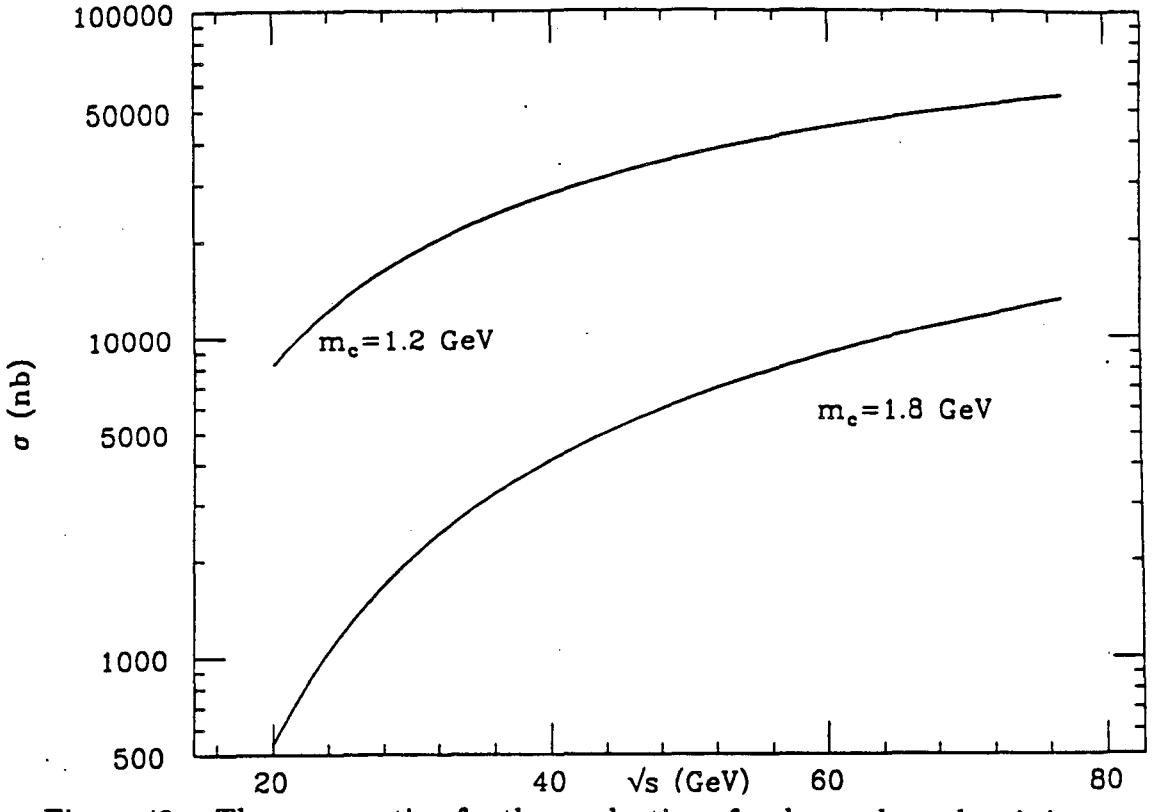

Figure 42: The cross section for the production of a charmed quark pair in proton-proton collisions as a function of $\sqrt{s}$.

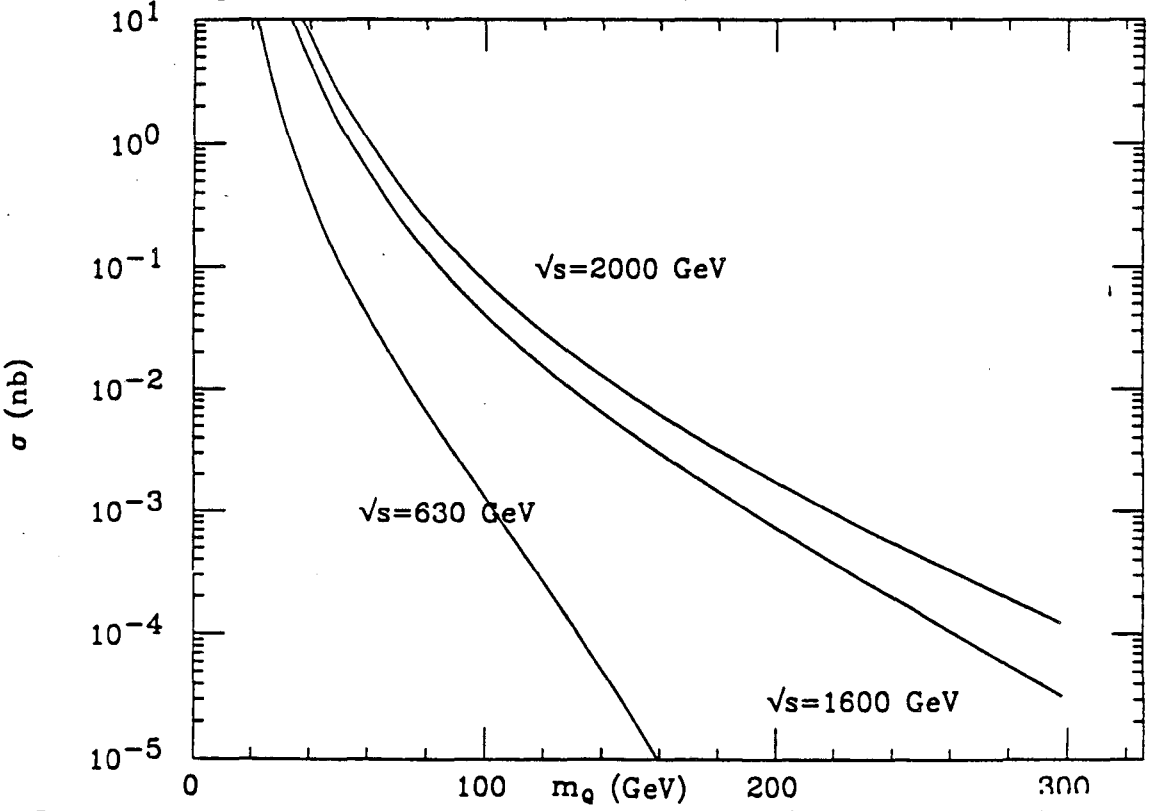

Figure 43: The cross section for the production of a heavy quark pair in proton antiproton collisions as a function of the heavy quark mass.

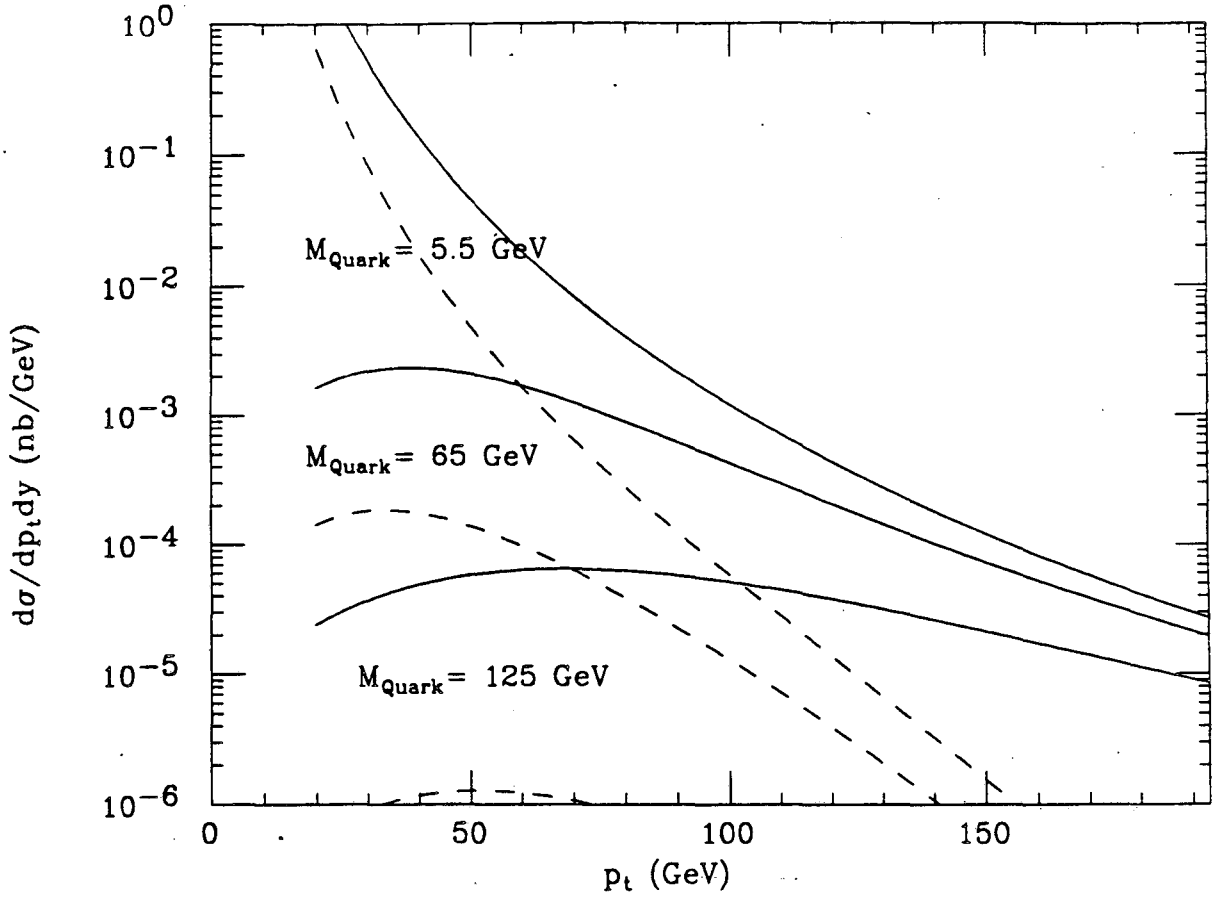

Figure 44: The transverse momentum distribution $d\sigma/dp_t dy$ at $y = 0$ of a heavy quark produced by the process of eqns. 3.73 and 3.74. The solid (dashed) lines are for $\sqrt{s}$= 2 TeV (630 GeV).

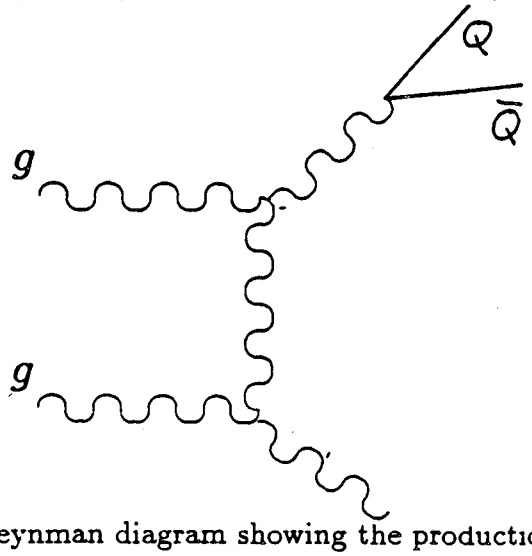

Figure 45: Feynman diagram showing the production of a pair of heavy quarks in gluon-gluon collisions. The transverse momentum of the pair is balanced by that of the recoiling gluon.

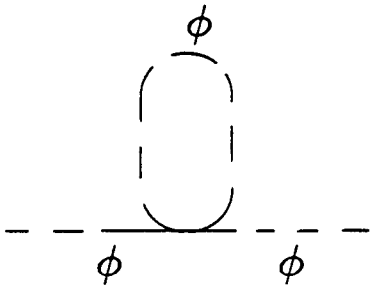

Figure 46: Feynman diagram showing a contribution to the Higgs mass renormalization in the Weinberg-Salam model.

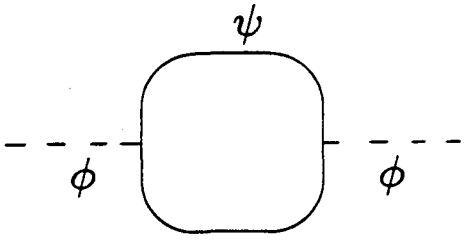

Figure 47: Feynman diagram showing contributions to the mass renormalization of the scalar field ϕ (dashed lines) from its self interactions and those with the fermion ψ (solid lines) in the toy model of equation 4.5.

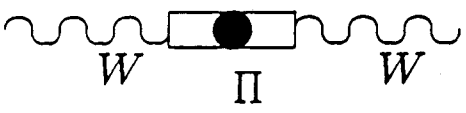

Figure 48: Diagram illustrating the generation of a mass for the W boson from its coupling to the Goldstone boson in a technicolor theory. See eqn. 4.8.

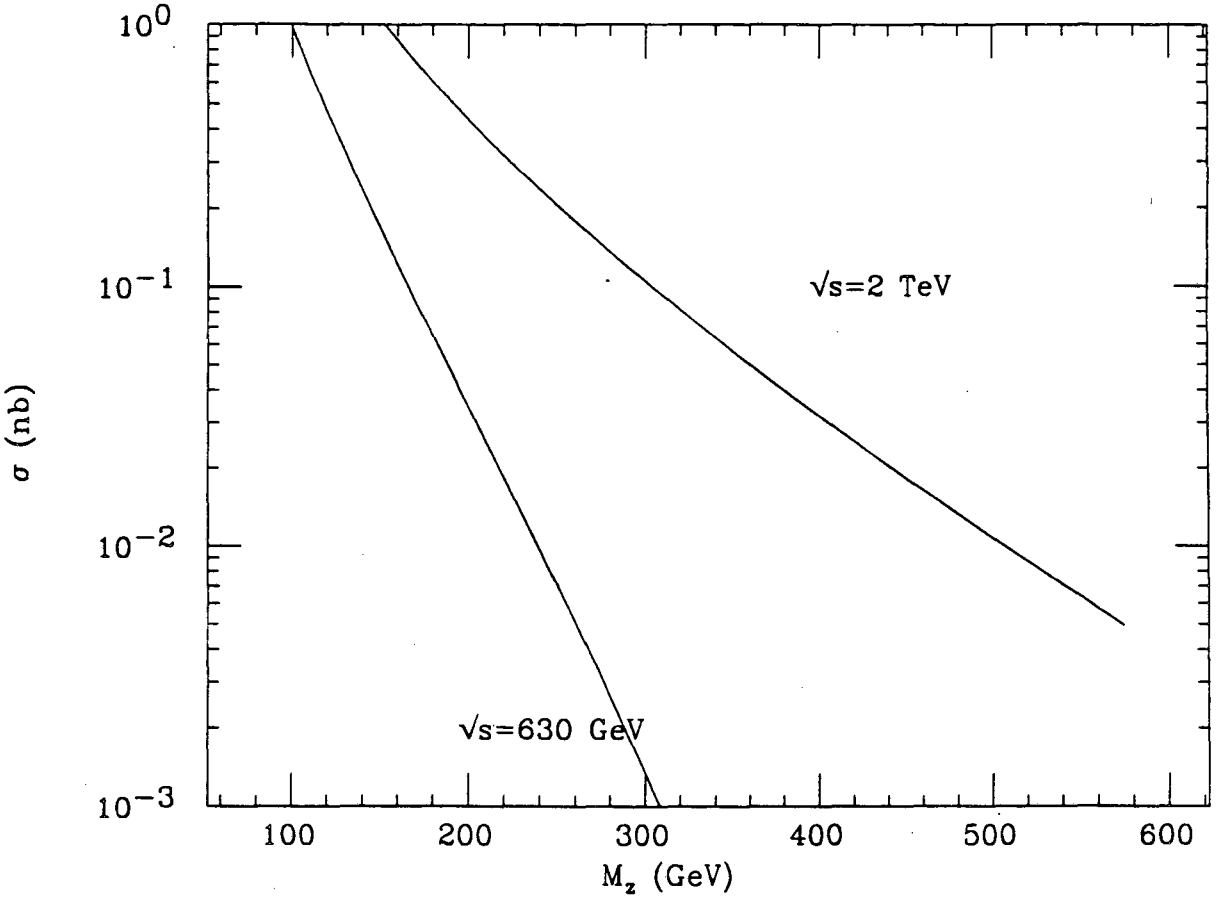

Figure 49: The total cross section for the production of a new Z, boson in $p\bar{p}$ collisions. The new Z is assumed to have the same couplings to quarks as the standard model Z.

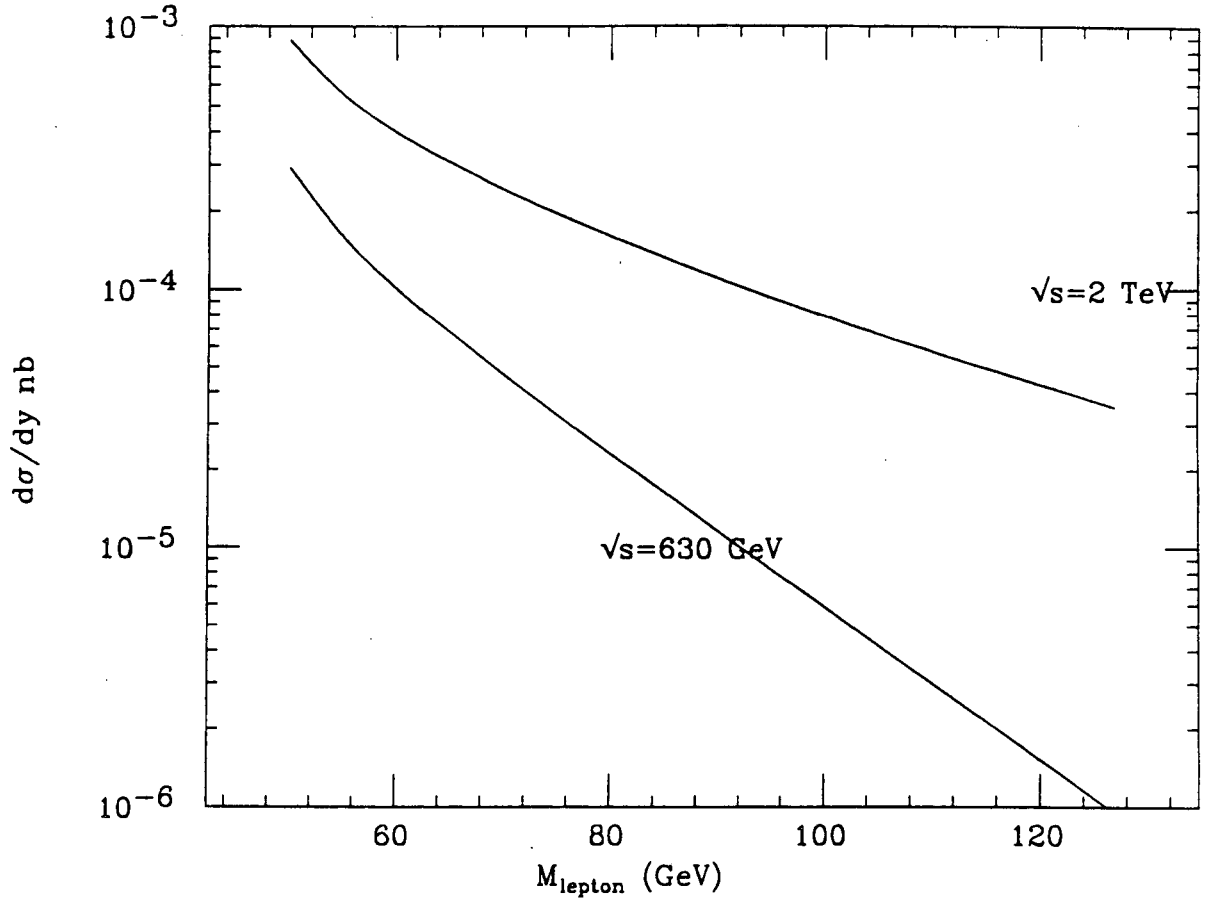

Figure 50: The cross-section $d\sigma/dy$ for the production of a pair of heavy leptons of rapidity $y = 0$ in $p\bar{p}$ collisions as a function of the heavy lepton mass.

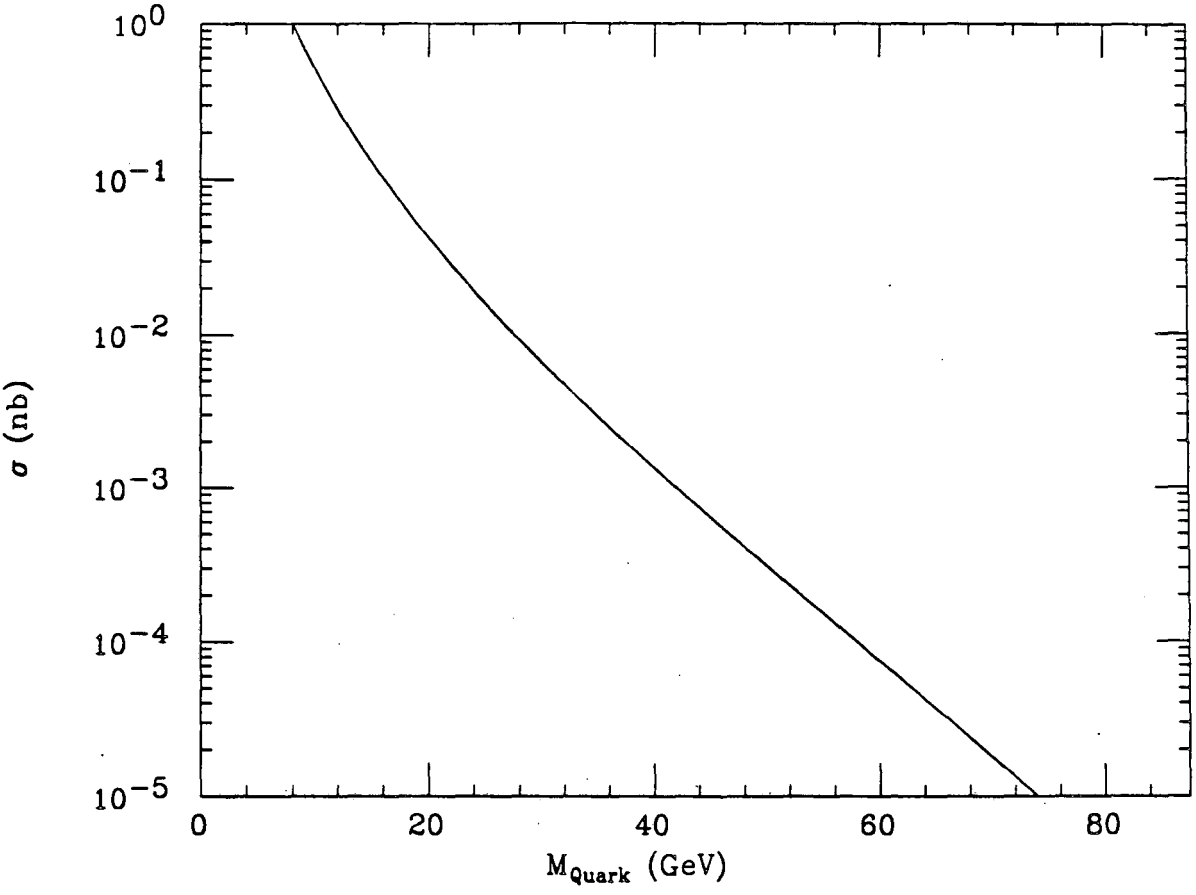

Figure 51: The cross section for the production of a pair of heavy quarks in *ep* collisions at $\sqrt{s} = 318GeV$ as a function of the quark mass.

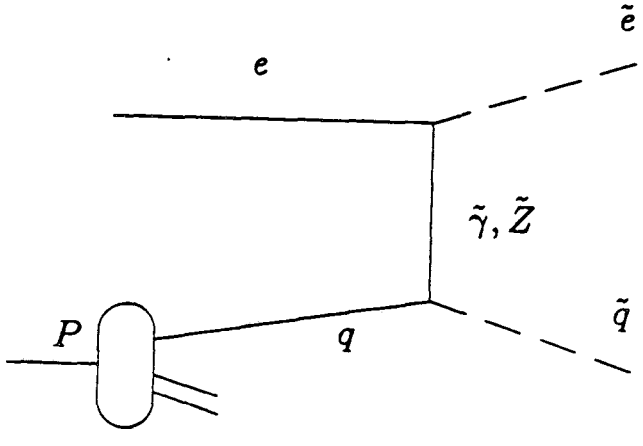

Figure 52: Feynman diagram showing the associated production of a squark and a selectron in *ep* collisions.

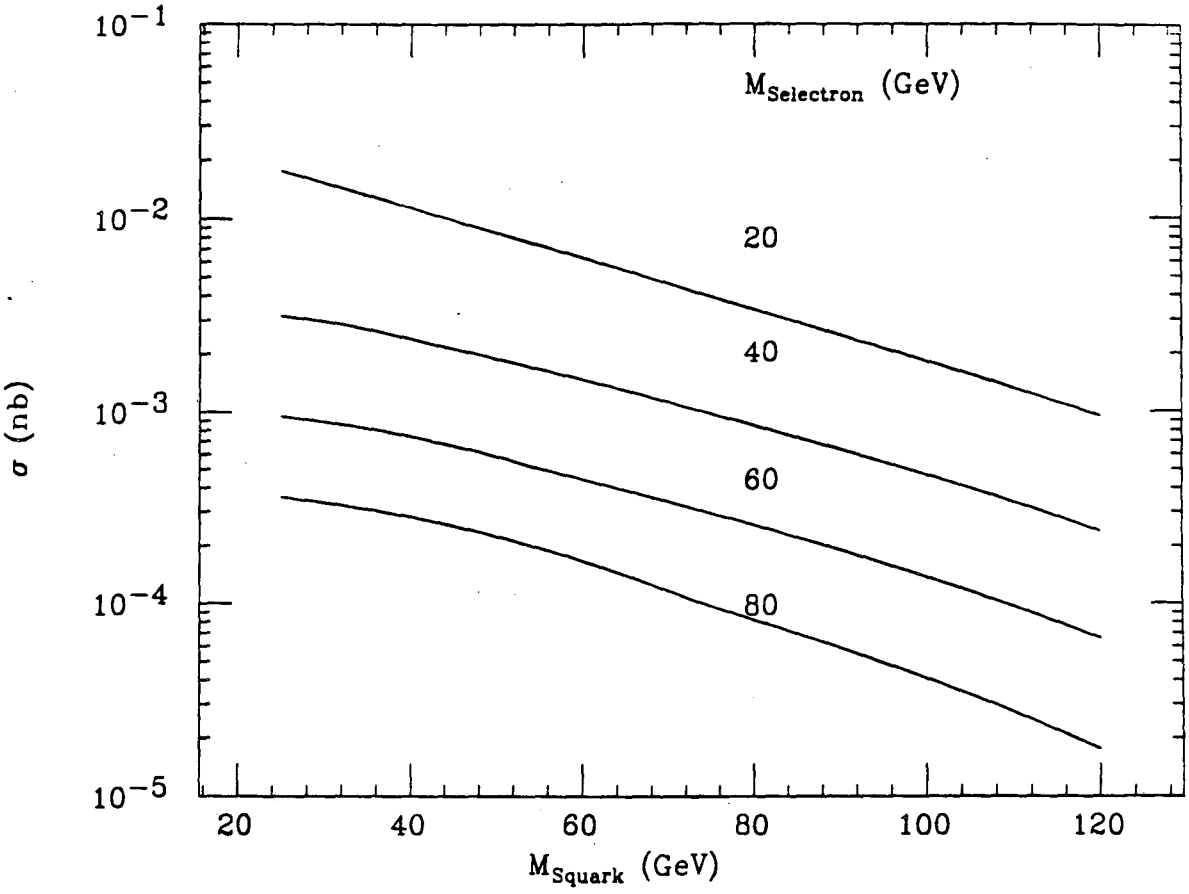

Figure 53: The cross section for the associated production of a squark and a selectron in ep collisions at $\sqrt{s} = 318$ GeV as a function of the squark mass at fixed selectron mass. The exchanged particle in figure 53 is assumed to be a photino of small mass and the up and down squarks are taken to be degenerate.

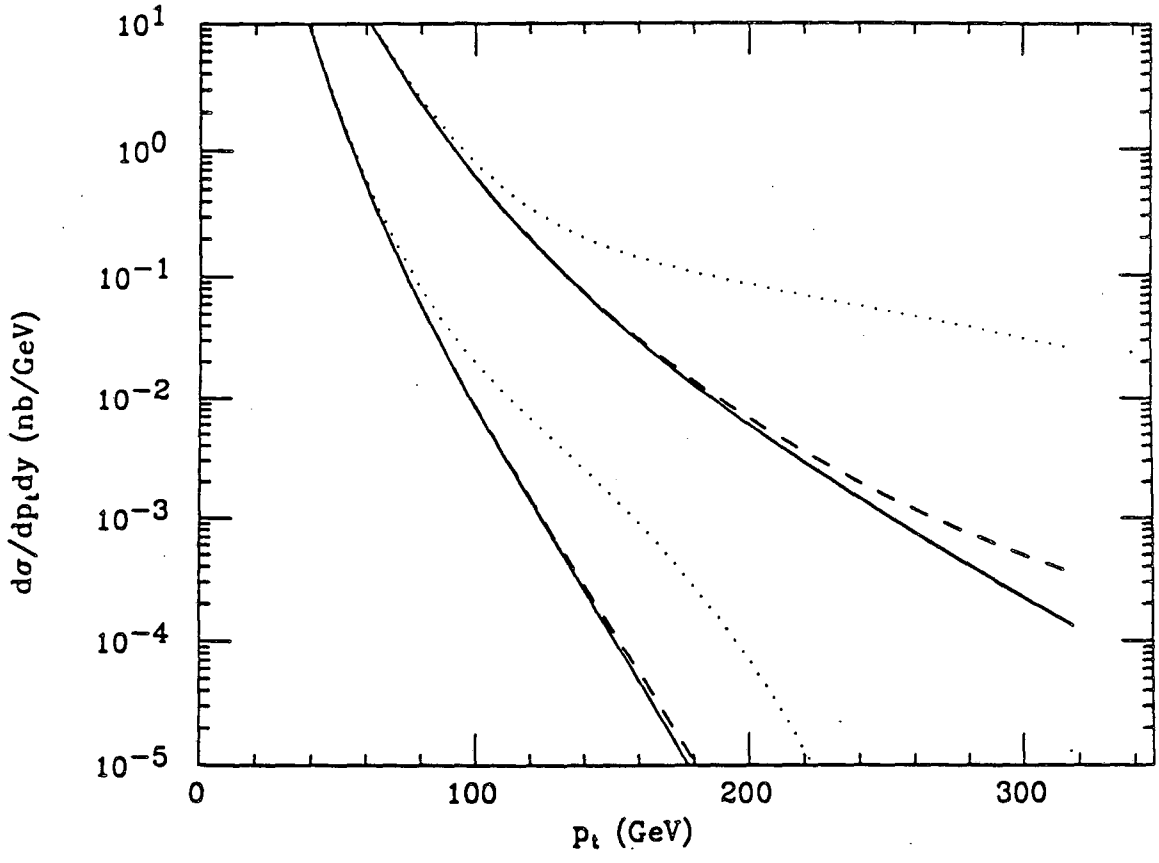

Figure 54: The cross section $d\sigma/dp_t dy$ for the production of jets of hadrons transverse momentum p_t and rapidity $y = 0$ in $p\bar{p}$ collisions. The curves include the effects of compositeness given by Eqn. 4.17 with $\eta_{LL} = 1$ and $\Lambda^* = 300$ GeV (dotted lines), 1000 GeV (dashed lines) and 5000 GeV (solid lines). The curves are for proton-antiproton interactions as $\sqrt{s} = 630$ GeV (lower lines) and 2000 TeV.

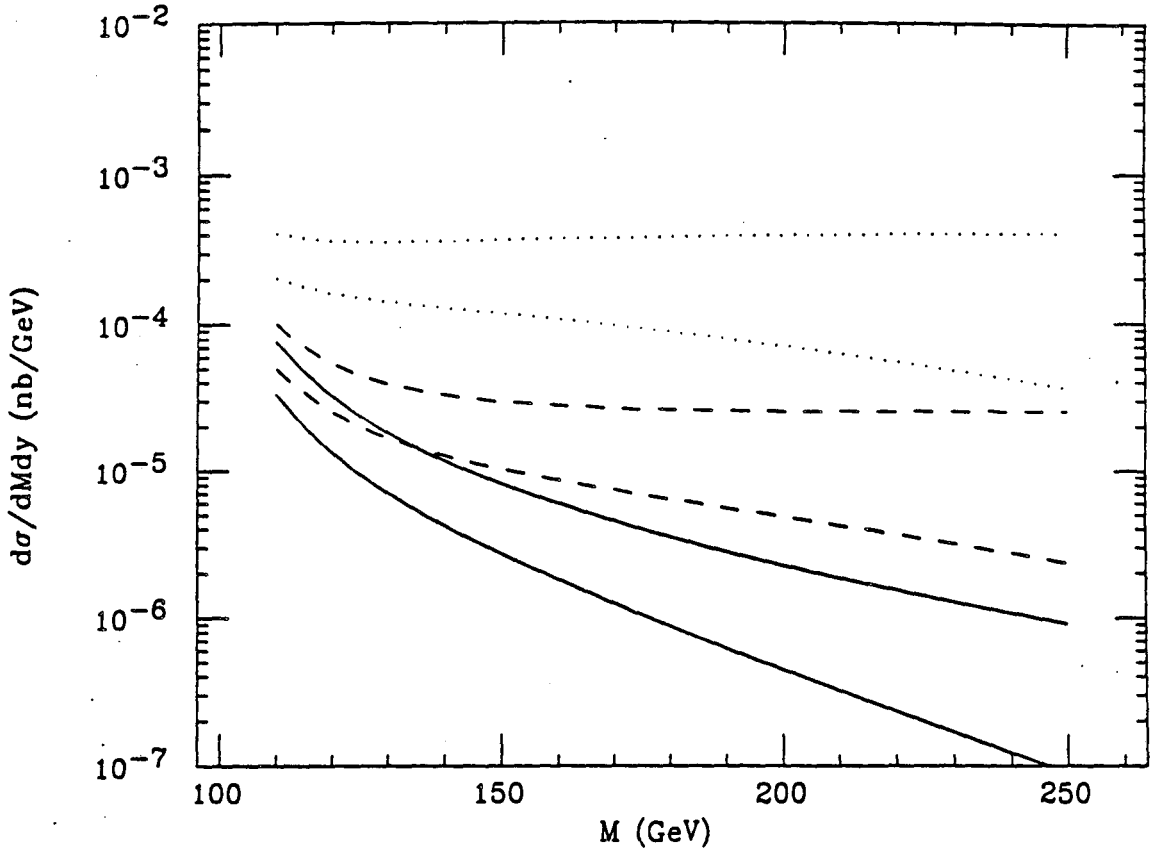

Figure 55: The cross section $d\sigma/dMdy$ for the production of a Drell-Yan pair of mass M and rapidity $y = 0$. The curves include the effects of compositeness given by Eqn. 4.20 with $\eta = 1$ and $\Lambda^* = 500$ GeV (dotted lines), 1000 GeV (dashed lines) and 5000 GeV (solid lines). The curves are for proton-antiproton interactions as $\sqrt{s} = 630$ GeV (lower lines) and 2000 TeV.

LAWRENCE BERKELEY LABORATORY
TECHNICAL INFORMATION DEPARTMENT
UNIVERSITY OF CALIFORNIA
BERKELEY, CALIFORNIA 94720